AN ABSTRACT OF THE THESIS OF

LEONARD J. SCHUSSEL for the degree of DOCTOR OF PHILOSOPHY in CHEMISTRY presented on MAY 26, 1987 .

Title: SYNTHESIS AND OXIDATION OF METAL-THIOLATE COMPOUNDS WHICH MIMIC THE ACTIVE SITE FUNCTION OF THIOLATE DIOXYGENASE ENZYMES

Abstract approved: Redacted for Privacy
Dr. James H. Krueger

Part I describes the synthesis of bis(fac-S)((tris)2-amino-ethanethiolatoiron(III))iron(III) chloride. The compound was first discovered during an attempt to prepare a ternary complex of iron, thiolate and pi-acid ligand. The compound is a reasonably air-stable iron(III)-thiolate that contains a linear tri-iron cluster with each iron bridged to the adjacent iron by three thiolate sulfurs. The elemental analysis of a microcrystalline sample corresponds to $[Fe(Fe(SCH_2CH_2NH_2)_3)_2]Cl_3 \cdot 3H_2O \cdot CH_3OH$. Large crystals showed little or no x-ray diffraction. Data collected for one crystal resulted in a structure solution (R = 0.098) for the Fe_3 cluster in one-electron reduced form as a dichloride.

UV-visible spectroscopy shows a peak at 490 nm which is due to an Fe^{III}-SR charge transfer. The cluster reacts slowly with oxygen when dissolved in solution, causing a decomposition of the compound to iron rust and disulfide. Cyclic voltammetry shows a reversible redox couple between the +3 and +2 charged cluster on a short

timescale (-310 mV, -240 mV vs. SCE), followed by dissociation of the reduced cluster after several scans.

The infrared spectrum of the cluster has a characteristic pattern in the region between 1800-400 cm^{-1}. Magnetic susceptibility measurements give μ_{eff} = 2.6 Bohr Magnetons, which corresponds to each of the three irons being in the low spin ferric state with coupling of spins (S = 1/2). Mossbauer spectroscopy supports this conclusion, giving two major doublets with relative intensity 1.7:1, ΔE_Q = 1.78, δ = +0.24 and ΔE_Q = 1.55, δ = +0.34. Oxidation with H_2O_2 and MCPBA did not produce sulfenates; however, added thiolates did react with the cluster.

Part II of this work describes the stereochemistry of the products of the H_2O_2 oxidation of potassium trans-N-bis (penicillaminato-N,S,O)cobaltate(III). Two optical isomers were found for the disulfenate (R,S and S,S), while only one isomer (S) was isolated by column chromatography for the monosulfenate. The second isomer (R) was produced in dilute solution and shown to exist by circular dichroism spectroscopy. Differences in the product distribution under light and dark conditions are noted.

Synthesis and Oxidation of Metal-Thiolate Compounds Which Mimic the Active Site Function of Thiolate Dioxygenase Enzymes

by

Leonard J. Schussel

A THESIS

submitted to

Oregon State University

in partial fulfillment of
the requirements for the
degree of

Doctor of Philosophy

Completed May 26, 1987

Commencement June, 1988

APPROVED:

Redacted for Privacy

Professor of Chemistry
in charge of major

Redacted for Privacy

Chairman of Department of Chemistry

Redacted for Privacy

Dean of Graduate School

Date thesis is presented May 26, 1987

Typed by Leonard J. Schussel for Leonard J. Schussel

Dedication

I dedicate this work to my parents, Sandy and Saul Schussel; to the memory of my grandparents, Mary and Herman Schussel and Celia Feldman; to my wife Louise and the ever-faithful Cobalt, who never let me forget his morning walk in the park.

Acknowledgements

I would like to express gratitude to each of the following people for his time, effort and aid. Dr. John Yoke for the use of his laboratory equipment, the Schlenk glassware, Gouy Balance and rotory evaporator; Dr. Hollis Wickman for help in collecting the Mossbauer data and interpreting the results; Dr. Doug Keszler and Scott Hein for running the Texsan program which calculated the solution for the crystal structure; Dr. Clara Shoemaker for the cobalt crystal structure; Jeff Fahey for assistance in running the cyclic voltammetry; Dr. W. Curtis Johnson for the use of the spectro-polarimeter for determination of the circular dichroism; Dr. Gerald

and Mary Kay Gleicher for moral support and Thankgiving dinners; and the Chemistry Department for everlasting support as a teaching assistant.

Also much thanks to Dr. James H. Krueger for spending many hours interpreting my interpretations of the results into terms that could be compiled into a thesis. I would also like to thank the N.L. Tartar Reasearch Committee for two summers worth of support. In addition, I should recognize all the other second floor inorganic graduate students, who have formed a single research group within a vast range of topics; Smokey, Steve, Oravan, Dave, Gyu Shik.

I would like to recognize all my friends at OSU who have been around through the good times and bad. Anthony, Jason, Darroch, Brooks, Danno, Crazy Paul and Kathy, Dean and Joy, Duncan, Dovina and Jimmy, Tim and Sarah, Margie and Paul, Sara, Scott and Claudia, James, Ron, Jay, Joe, Art, Lamar, Jeff, Jeff, Jeff, Stacey, Dan, Todd and Terri, Sharron, Jim, Eric and Jane, Cary and Jane, Bob Russell, and many, many more.

TABLE OF CONTENTS

LIST OF FIGURES

LIST OF TABLES

Synthesis and Oxidation of Metal-Thiolate Compounds Which Mimic the Active Site Function of Thiolate Dioxygenase Enzymes

General Introduction.

Inorganic chemists are in a position to make a major contribution toward understanding the mechanisms of metalloprotein reactions. The field of bioinorganic mimicracy involves the preparation and characterization of low molecular weight compounds which are designed to imitate the structure, electronic and magnetic properties, and chemistry of the metal ions at the active sites of protein and enzyme systems.

In this thesis, the biomimetic approach is applied to the study of the iron-containing enzymes cysteine dioxygenase and cysteamine dioxygenase. One of the roles of iron in biological systems is to mediate oxidation-reduction reactions. The major redox processes involve electron transfer and hydrogen atom abstraction. The thiolate dioxygenases use a third, less frequently found pathway, oxygen atom incorporation. These enzymes catalyze the O_2 oxidation of a substrate thiol to its corresponding sulfinate, a process that starts the metabolism of excess sulfur in the body toward the eventual waste product, the sulfate anion. (Figure 1)

The 'normal' chemical reactivity of thiolate sulfur is modified by coordination to a metal. The thiolate dioxygenase enzymes use a ferric ion to oxidize a substrate thiolate to the corresponding sulfur-oxygen bonded species. The formation of this type of product is unusual, because the oxidation of thiolate usually gives

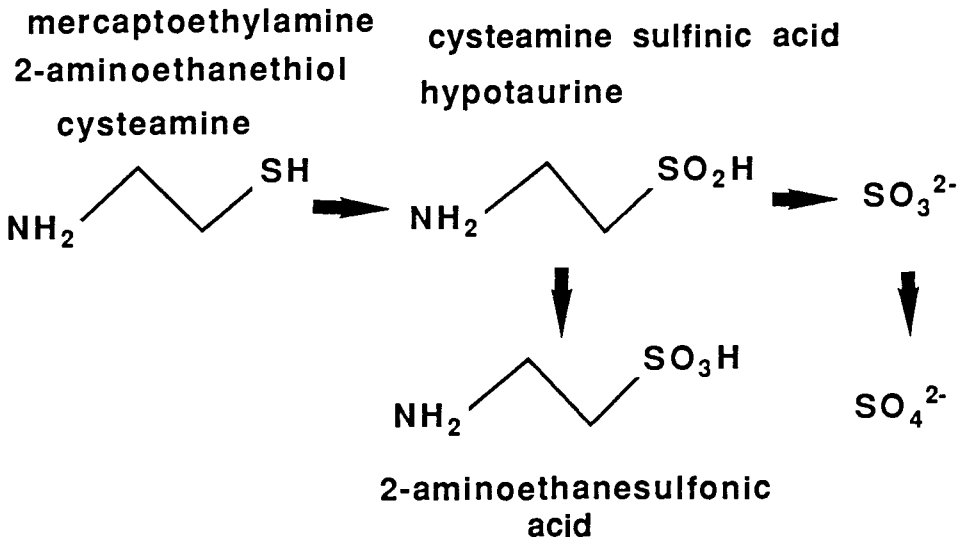

Figure 1. Metabolic Oxidation Products of Cysteamine

disulfide; the sulfur-sulfur bond is kinetically favored. The specific role of the metal in this diversion from 'in vitro' chemistry is of interest.

Previous work in this laboratory has been to study the oxidation of cobalt-bound thiolates.[1] These non-labile systems provide a direct route to an air-stable coordinated sulfenate species. Part II extends this study by examining the stereochemistry of the H_2O_2 oxidation products of a bisthiolatocobalt(III) complex.

Parallel studies on iron(II) systems have been limited. Complications arise due to the extreme oxygen sensitivity of ferrous thiolates. Air oxidation of the iron to the ferric state is usually accompanied by the oxidation of the thiolate to disulfide, with concommitant reduction of the metal. An internal means has to be developed to prevent this oxidation chemistry. We have prepared a compound in which this difficulty is minimized. The formation and characterization of this complex are described in Part I.

Oxidation Chemistry of Sulfur. The organic chemistry of thiolate sulfur (RSH) is well characterized and can be found in most organic chemistry books. Thiols will react with mild oxidizing agents to produce disulfides, a net one electron oxidation of each sulfur atom. This reaction will occur with molecular oxygen in the presence of catalytic amounts of a divalent transition metal.

$$4\ RSH + O_2 \xrightarrow{M^{2+}} 2\ RSSR + 2\ H_2O \qquad (1)$$

The reaction is easily reversed with a reducing agent.

A stronger oxidizing agent such as $KMnO_4$ will oxidize the sulfur to a sulfonic acid RSO_3H.

$$RSH + 2MnO_4^- + 2H^+ \longrightarrow RSO_3H + 2MnO_2 + H_2O \qquad (2)$$

Intermediate oxidation states within the 6 electron range between +4 and -2 difficult to produce in the free state. Sulfenic acids (RSOH) are known to exist, but are unstable and highly reactive. Sulfenic acids will disproportionate to produce a disulfide and a sulfinic acid, or react with thiolates to produce disulfides and water.

$$3\ RSOH \longrightarrow RSSR + RSO_2H + H_2O \qquad (3)$$

$$RSOH + RSH \longrightarrow RSSR + H_2O \qquad (4)$$

Sulfinic acids (RSO_2H) are more stable than sulfenic acids, but have a tendency to oxidize furthur to sulfonic acids when left in solution. They are key intermediates in the biological oxidation of sulfur containing compounds.

When the thiolate is coordinated to a metal center, the chemical reactivity is modified to allow the oxidation to proceed directly to these intermediate species. The coordination to the metal prevents the oxidation reactions given in (3) and (4).

Hydrogen peroxide is used to oxidize the cobalt(III)-bound thiolate function to either sulfenate or sulfinate. The initial mole ratio dictates the stoichiometry, the product dependent upon the amount of peroxide.

$$H_2O_2 + CoSR \longrightarrow CoS(O)R + H_2O \qquad (5)$$

$$H_2O_2 + CoS(O)R \longrightarrow CoS(O)_2R + H_2O \qquad (6)$$

The oxidation of metal bound thiolates does not necessarily lead to sulfur-oxygen bonded products. If alkylation is desired, an alkyl halide such as methyl iodide can be used to generate a coordinated thioether.

$$CH_3I + CoSR \longrightarrow CoS(CH_3)R^+ + I^- \qquad (7)$$

A sulfenyl iodide will produce a coordinated disulfide and an aminating agent such as hydroxylamine-O-sulfonic acid will react to form a sulfenamide.

$$(R'S)_2I + CoSR \longrightarrow CoS(SR')R^+ + R'SH + I^- \qquad (8)$$

$$H_2NOSO_3H + CoSR \longrightarrow CoS(NH_2)R^+ + HSO_4^- \qquad (9)$$

The coordination of a thiolate to a metal center renders the sulfur prochiral. Oxidation of a bound thiolate can occur at either of the lone pairs, which are in different environments. Both the R and S configurations are possible for the sulfenate, sulfenamide and thioether. The difference in the reactivity between the two lone pairs is indicative of the spatial environment of each pair.

Sulfide (S^{2-}) can be added to a metal thiolate mixture to create a multinuclear cluster, in which the sulfide bridges between metal ions. An example would be the $Fe_4S_4(SR)_4$ cubane type iron-sulfur protein models.[2]

Several thiolates are present in metabolic systems. Cysteine is one of the twenty primary amino acids that constitute protein chains. Its decarboxylated analogue, cysteamine is also present in biological systems. Penicillamine, β,β-dimethylcysteine, is used as a therapeutic agent to chelate excess copper ions present due to the body dysfunction known as Wilson's disease.[3] Both cysteamine and cysteine undergo oxidation to a sulfinic acid by the function of an enzyme which is specific for the individual thiolate.

$$HSCH_2CH_2NH_2 \longrightarrow HO_2SCH_2CH_2NH_2 \quad (10)$$

cysteamine — hypotaurine

$$HSCH_2CH(COOH)NH_2 \longrightarrow HO_2SCH_2CH(COOH)NH_2 \quad (11)$$

cysteine — cysteine sulfinic acid

$$HSC(CH_3)_2CH(COOH)NH_2 \longrightarrow HO_2SC(CH_3)_2CH(COOH)NH_2 \quad (12)$$

penicillamine — penicillamine sulfinic acid

In biological systems, specific enzymes function to enable the oxidation of these thiolates to the corresponding sulfinates, by altering the reactivity of the thiolate via coordination to a metal center.

Chemistry of Thiolate Dioxygenase and Related Enzymes. Thiol dioxygenases are mammalian enzymes that function to oxidize thiolate sulfur to sulfinate. In the metabolic process, the substrate thiolate is held at the enzyme active site by the folding of the proteins that constitute the enzyme[4]. The active site, which is buried within the protein shell, is made available by a conformational change in the

tertiary structure of the protein.

Ferric iron is present at the active site of cysteamine dioxygenase.[5] This enzyme also contains zinc and copper sites, which are not involved in the oxidation of the thiolates. The enzyme can function by one of two distinct reaction pathways; the mechanism is dependent upon the enzyme/substrate ratio. If there is an excess of thiolate present, the enzyme functions via an oxidasic pathway. By this route the thiolate is oxidized to disulfide. However, when only a small amount of thiolate is present, the iron functions to catalyze an oxygenasic pathway which adds molecular oxygen to the thiolate to form the metal-bound sulfinate.[6] Once the sulfinate has been formed, the protein unfolds and releases the highly reactive sulfinic acid, where it is transaminated and desulfinated by other enzymes. Cysteine dioxygenase is believed to react in a similar manner.

Cavallini, et al., have studied the function of the cysteamine dioxygenase enzyme.[7] Isolated from horse kidney, this enzyme converts cysteamine to hypotaurine at a non-heme iron active site. The purified enzyme has a molecular weight of 83,000, has two subunits, and contains one iron atom per molecule. It is specific for cysteamine; other thiolates are not affected. The enzyme activity is dependent upon several cofactors being present, with an absolute dependence on ferrous iron.

The nature of the iron active site through the catalytic cycle of the isolated enzyme was probed using Electron Paramagnetic Resonance Spectroscopy (EPR).[5] In EPR, the transition energy is given by the

equation $\Delta E=gBH$ where B is the electron Bohr magneton and H is the magnetic field strength. Thus the g term is directly correlated to the chemical structure.[8]

The EPR studies of cysteamine dioxygenase give an initial g factor of 4.3, which is a typical value for a high spin ferric ion in a field of low symmetry. The iron atom in the enzyme activates the substrate thiolate upon coordination. As the cysteamine is introduced under anaerobic conditions, a significant change in the shape of the EPR signal is observed. The signal is sharper and more symmetric, implying that the substrate is bound directly to the ferric center. Admittance of O_2 causes the signal to broaden slowly, resulting in a gradual restoration of the original form. The sulfinate is the only compound produced.

The introduction of sulfide into the enzyme system causes an additional peak (g=7.25) which disappears upon admittance of O_2. S^{2-} binds differently from the substrate and causes some iron reduction, which gives rise to the second EPR peak. The addition of more cysteamine at this point will further modify the g=4.3 peak. The addition of other thiolates such as cysteine or reduced glutathione have no effect on the EPR spectrum.[9] The summation of this EPR evidence demonstrates that the iron functions as the active site of the enzyme.

The iron is located between the two subunits of the enzyme.[10] The active site was also probed by using a dissociating agent in conjunction with a chelating ligand. Treatment with urea or dithiothreitol denatures the enzyme by breaking disulfide bonds,

which enables the unfolding of the protein structure.[11] Addition of 1,10-phenanthroline as a specific chelating agent for iron inhibits all enzymatic activity. This provides a secondary confirmation that the iron plays a central role in the enzymatic activity.

L-Cysteine (L≡R) is converted to L-cysteine sulfinic acid by a different enzyme, cysteine dioxygenase, which has been studied by Singer.[12] This cytoplasmic enzyme obtained from mammalian liver requires both a ferrous ion and a reduced pyridine nucleotide cofactor. A third, unidentified heat sensitive cofactor is believed to form an adduct with cysteine to enhance the rate of oxidation. An isotopic substitution of oxygen $^{18}O_2$ and water $H_2{}^{18}O$ was used to demonstrate that both sulfinate oxygen atoms arise from molecular oxygen rather than water. (This has also been demonstrated for the cysteamine dioxygenase enzyme and is the key experiment for the identification of a dioxygenase.) Hydroxylamine is required to prevent further metabolic oxidation of the product, cysteine sulfinic acid. Cysteine dioxygenase is sensitive to oxygen in the air and will decompose during storage, preventing EPR studies similar to those made of the cysteamine dioxygenase enzyme.

Several other sulfhydryl-containing dioxygenase enzymes are known to catalyze the O_2 oxidation of aromatic rings. A ternary complex has been proposed to explain the mechanism for iron enzymes, such as protocatechuate 3,4 dioxygenase and metapyrocatechase.[13] The three components are the enzyme, molecular oxygen and the aromatic substrate. Although dioxygen is not directly coordinated to the iron center, these enzymes activate both the substrate and the oxygen to

allow the oxidation to occur at the active site. The actual mechanisms for these reactions are unknown, but the iron appears to remain high spin ferric during the whole process. Resonance Raman spectroscopy failed to detect evidence for an O_2-Fe^{2+} bond.[14]

Dioxygenases are not the only biological iron-thiolate systems. Ferrous iron plays a significant role in the inhibition of uroporphyrinogen decarboxylase.[15] This enzyme is responsible for the removal of carboxylate functional groups from porphyrinogens. When the enzyme does not function properly, non-metabolizable porphryns accumulate causing skin lesions. The resulting disease, porphria citanea tarda, is associated with alcoholism. As iron accumulates in the liver, it reacts with sulfhydryl residues at the enzyme active site to cause a 50% inhibition of enzymatic activity under anaerobic conditions. Addition of oxygen stimulates a metal oxidation-reduction sequence (Fe^{2+}/Fe^{3+}), which generates active oxygen species such as the superoxide radical anion. This results in 20% further loss of enzymatic activity. A free radical inhibitor can reverse this trend. Addition of cysteine will also prevent the inhibition of the enzyme.

There are many questions concerning the mechanism of these iron-thiolate enzymes. The isolated enzymes tend to be extremely air-sensitive and difficult to handle. This has prevented the complete description of the structure at the active sites. The development of a chemical model system may lead to a better theoretical basis for understanding the factors that influence the oxidation of thiolates.

Part I: Synthesis and Characterization of Bis(fac-S)((tris)2-amino-ethanethiolatoiron(III))iron(III) Chloride.

Historical (1) Iron-Sulfur Complexes. There are several laboratories that specialize in iron-sulfur biological mimicry. Holm and coworkers have developed an extensive array of compounds within the $Fe(SR)_4$, $Fe_2S_2(SR)_4$ and $Fe_4S_4(SR)_4$ genre, which serve as analogues for rubredoxin and ferredoxin. These are electron transfer systems common to both plants and animals. Millar and Koch have also developed several different tetrahedral $Fe(SR)_4$ models for rubredoxin, in both oxidized and reduced forms. Lippard's group has worked with multidentate chelates, as a means of duplicating biological function without the inherent intractibility of the actual biological systems. Collman and others have used model protoporphyrins with axially coordinated thiolate ligands to reproduce the functional chemistry of cytochrome P450, a monohydroxylase enzyme. While none of these groups has specifically developed models for the thiolate dioxygenase enzymes, each group has laid down some of the groundwork toward the development of tractable iron-thiolate systems. A brief review of iron-sulfur model systems is relevant to the analysis of our chemical model.

Iron-sulfur coordination compounds with biologically relevant ligands have been fairly elusive until recently. The major difficulties were caused by the facile oxidation of mercaptide and sulfide ligands by iron(III) salts, the tendency for iron(II) thiolates to polymerize, and the extreme oxygen sensitivity of the

compounds prepared.[16] The development of modern, inert atmosphere techniques and the improvement of crystal data collection methods have allowed the study of previously intractable systems.

Early work in iron-thiolate systems suffered from the lack of structural solutions, due to the difficulties associated with crystal growth. Murray and Newman prepared complexes of cysteine and thioglycolic acid, $HSCH_2COOH$, which they surmised to be polymeric based on infrared and physical data.[17] The structure proposed for a

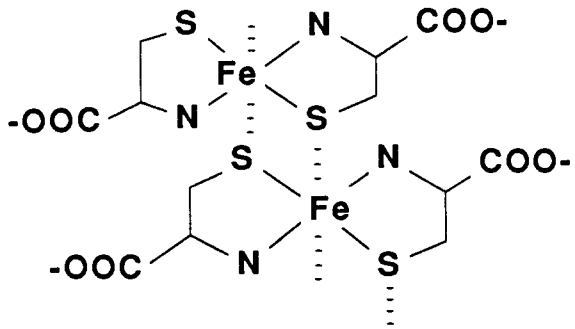

$Fe(CyS)_2$

1:2 ferrous cysteinate contains two N,S bound cysteines in a polymer stack with the sulfur atoms bridging between iron atoms in an axial formation. This system sets a precedent for multinuclear, bridged iron-thiolate species.

Panossian studied ferrous cysteinates, preparing 1:1 and 1:2 complexes which were characterized by infrared spectroscopy and elemental analyses.[18] Bell studied the aqueous chemistry of iron-penicillamine and iron-cysteamine-N-acetic acid compounds by standard absorbance methods, but could not specify the compositions of any distinct molecular species.[19]

Ethanedithiolato complexes were first reported by Holm's group in

1975 and have been of interest recently.[20] Snow and Ibers provide crystal details for the iron(III) system containing 1,2 ethanedithiol.[21] For this complex, $[Fe_2(edt)_4]^{2-}$, there

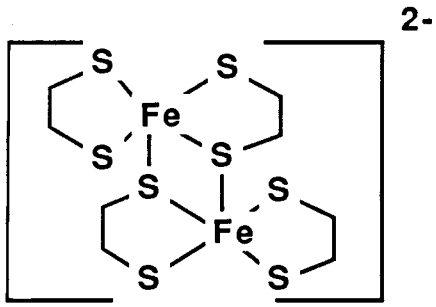

$Fe_2(edt)_4^{2-}$

are two bridging thiolates which extend back to each iron, and two non-bridging thiolates, uniquely owned by the different iron atoms. Each ligand is bidentate and each iron is five-coordinate with trigonal bipyramidal geometry. The Fe···Fe distance is about 3.4Å. The compound is extremely air sensitive.

Lippard and Hu also have prepared a crystalline complex featuring thiolate bridges between iron atoms.[22,23] They used a tetradentate chelate with thiolate ends to produce a high spin iron(II) compound.

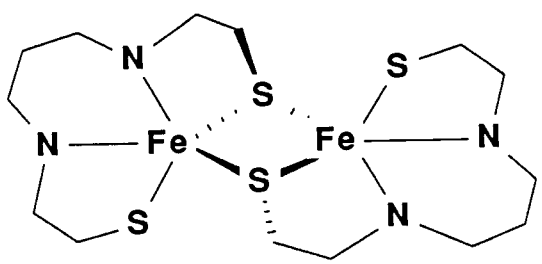

$(FeL)_2$

The dimer is cleaved by reaction with CO. They claim to have the

first transition metal complex with saturated nitrogen and thiolate functional groups. The macrochelate provides steric constraints which dictate the geometry of the compound. Variations in the chelate ring size affect both the magnetic and spectral properties of related compounds.[24]

Hagen and Holm have reported both the syn- and anti- forms of $[Fe_2(SEt)_6]^{2-}$, where the bridged ligand can be oriented

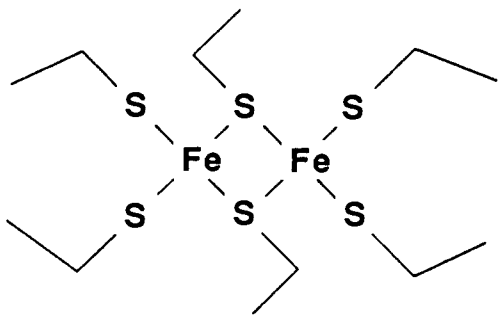

$Fe_2(SEt)_6^{2-}$

in similar or opposite spatial sites.[25] The complex is centrosymmetric with the $Fe_2(\mu\text{-}SEt)_2$ unit being planar for the anti configuration. The $S_b\text{-}S_b$ distance of 3.7Å is 0.7Å longer than the Fe···Fe separation of 3.0Å. This compound is very similar to the rubredoxin analogue $[FeS_2(S_2\text{-}o\text{-}xyl)_2]^{2-/3-}$.[26,49]

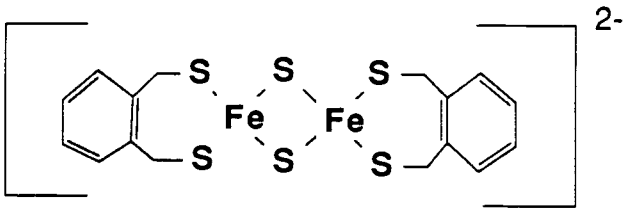

$Fe_2S_2(S_2\text{-}o\text{-}xyl)_2^{2-}$

$[Fe_2S_2(S_2\text{-o-xyl})_2]^{3-}$ has a distinct UV-Vis spectrum that features charge transfer bands at 380, 490 and 560 nm, plus a d-d band at 745 nm. $[Fe(S_2C_4O_2)_2]^{2-}$ also demonstrates similar spectroscopic properties.[27]

Millar and Koch have synthesized several crystalline solids which have the $Fe(SR)_4$ unit, where R is a severely hindered thiolate such as 2,3,5,6-tetramethylbenzenethiol.[28,29] Both aromatic and aliphatic thiolates have been used to construct these oxygen sensitive rubredoxin analogues. Previous attempts had failed due to oligomerization or autoreduction to Fe(II) and disulfide, but success with hindered thiolates led to successful syntheses of some less-hindered systems. For example in $[Fe(SPh)_4]^{2-}$, one

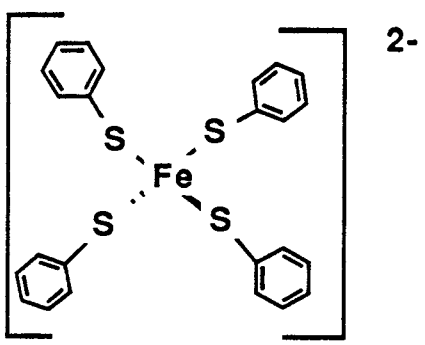

$Fe(SPh)_4^{2-}$

thiolate is pushed out of its idealized geometry by the steric constraint in packing four bulky ligands tetrahedrally about the iron atom.

The question of high vs. low spin iron is also relevant for the cluster characterization. Most of the iron-thiolate complexes discussed have been high spin, yet biological systems can operate with a change in the spin state. Collman has developed a

tetraphenylporphyrin (TPP) complex in which benzenethiol is coordinated axially to iron. The compound functions as a working model for cytochrome P450.[30] The P450 electron transfer system is known to have a deprotonated cysteinyl thiolate as the fifth ligand and either a histidine, lysine, cysteine, or methionine at the sixth coordination site. The crystal structure of the model was resolved into two components, a low spin six coordinate compound with both thiol and thiolate axial ligands, and a high spin five coordinate complex with the thiol unbound, but still present in the lattice.[31]

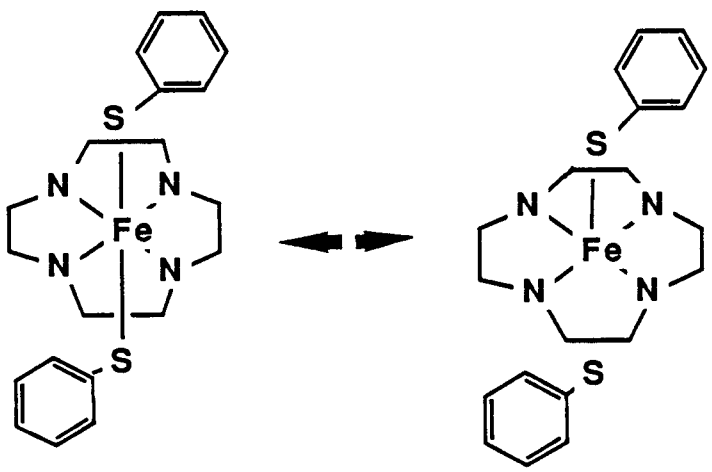

Koch, Holm and coworkers developed similar systems which are five coordinate only, and can be pushed into any of three spin states (S=1/2, 3/2, 5/2) by changing the axial ligand.[32,33] The thiolate complexes were formed by oxidative addition, whereas the non-thiolates generally required a substitution method.

Walters reports the synthesis of a linear trinuclear triiron cluster containing bridged benzenethiolates.[34] This hexacarbonyl compound, $Fe_3(\mu\text{-}S\phi)_6(CO)_6$, is stable under a CO atmosphere, but

decomposes readily in solvents or air. The Mossbauer spectrum of the compound is consistent with the formulation of two low-spin iron(II) units flanking a high spin iron(II) central metal. Magnetic moment measurement gives 5.62 μ_B at 294 K by the Evans method, and the cyclic voltammetry reveals an irreversible oxidation wave at +0.48 V vs $Ag^+/AgCl$.

(2) Cysteamine Complexes. There has not been any reported work done on iron-cysteamine compounds, presumably because of the air sensitivity of unhindered iron-thiolates. Several other metals have been used to form cysteamine chelate complexes. Busch and Jicha prepared a series of papers on the bridging abilities of the cysteamine ligand.[35] They found that square planar Ni^{2+} and Pd^{2+} metal centers would use bridging sulfur atoms to form heterometallic trinuclear cluster complexes. Several linear cluster complexes of tris(2-aminoethanethiolato)cobalt(III) were

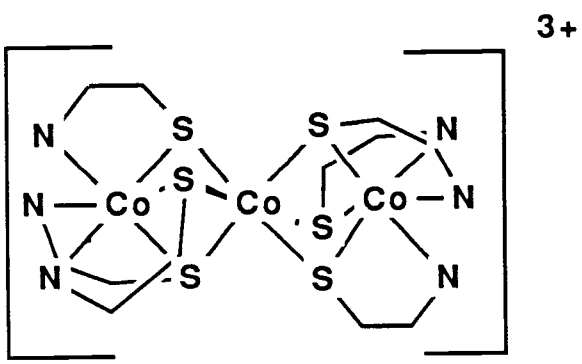

$Co(Co(CySte)_3)_2^{3+}$

synthesized, each containing a different central metal ion, $M[CoL_3]_2^{2+}$. The tris cobalt ligand acts as a tridentate donor, with the sulfur atoms in a fac-S orientation.

Butler and Blinn also have synthesized CoL_3 compounds of several transition metal ions: Ni^{2+}, Fe^{3+}, Co^{3+}, Zn^{2+}, Cd^{2+} and Pb^{2+}.[36] They were able to demonstrate the oxidation of Ni and Pb compounds to the sulfenato form using H_2O_2 as the oxidant, and concluded that only redox active metals had oxidizable thiolates.[37] Schlapfer and Nakamoto assigned the metal-nitrogen and metal-sulfur IR bands for these two cysteamine complexes, but did not consider the possibility of bridging thiolates within these assignments.[38]

DeSimone, et al., reported the UV, ESR and Mossbauer spectra of the low spin trinuclear ferric centered CoL_3 complex.[39] Heeg provided the crystal structure for the tricobalt system and discussed a possible mechanism for oxidation of the ligands to disulfide.[40]

Willis, et al., assigned the infrared spectrum of $MoO_2[NH_2CH_2CH_2S]_2$ and found only a mononuclear species.[41] In this work, some IR changes were induced by bridging the thiolate sulfurs with an ethylene unit, which created new constraints on the bonding modes of the atoms in the coordination sphere.

Synthetic Objectives. Iron is ubiquitous in biological systems because of the redox couple between the two readily accessible oxidation states. The labile nature provides for facile maneuverability of the substrate to and from the iron atom, when several coordination positions are occupied by strongly bonded protein donor groups. Iron atoms participate at active sites in numerous metalloproteins, which are both structurally and functionally diverse. They play roles in iron storage and transport (transferrin), oxidation and reduction (oxygenases), and provide many

other necessary functions. In hemoglobin, iron serves as the specific binding center for the dioxygen molecule. Certain iron-sulfur proteins, rubredoxins and ferredoxins, serve as one electron donors or acceptors in several cytochromes.

Iron-thiolate compounds are difficult to handle. They tend to be air-sensitive and require special techniques, such as glove boxes, vacuum lines, and Schlenk glassware to ensure inert handling throughout the entire study. As previously mentioned, ferrous iron serves as an catalyst for the oxidation of thiolate to disulfide. A small amount of O_2 in the system can ruin an entire synthesis.

Past work in this laboratory has demonstrated that the sulfenate and sulfinate moieties can be produced at a cobalt metal center.[1] The resolution of sulfenates of a bis(thiolato)cobalt ion is detailed in the second section of this work. A similar model system for the dioxygenase enzymes should be developed based on an iron metal center. The model is intended to mimic the active site oxidation of thiolate to sulfinate at an iron center, while avoiding the technical difficulties introduced by trying to duplicate the large protein content of the bio-system. A model complex that has the chemical modifications necessary for duplication of the oxidative function of the enzymes is desired. The chemical goal is to develop a low molecular weight molecule with a central iron atom in an octahedral environment.

The iron compound originally envisioned would contain two different types of ligands: a thiolate to simulate the substrate of the enzyme system and an electron withdrawing ligand to provide

internal stabilization from immediate redox chemistry. Since rigorously inert conditions are expensive to maintain, a secondary goal was to develop a compound that is air-stable, so that the post-synthesis characterization of the system does not require inert conditions.

The initial premise of the iron research was that an iron-thiolate complex could be formed by manipulating the electron density distribution at the central iron of a coordination complex. Pi-acid ligands have low-lying vacant orbitals of the correct symmetry to form pi-bonds by accepting electrons from filled metal d-orbitals. This backbonding stabilizes the metal electrons by distributing them over ligand orbitals, reducing any excess negative charge on the metal. This in effect lowers the reactivity of the metal toward oxidation/reduction chemistry.

By using a multidentate chelate ligand with pi-acid ends, electron density should be removed from the iron-sulfur bond. The complexes desired were similar to those of Hu and Lippard, except that the thiolate ligand would be a separate entity from the tetradentate chelate ligand.[22,23] The thiolate sulfur would be less nucleophilic and therefore less likely to be oxidized to a disulfide. Molecular models were built to determine which ligands would provide a sterically feasible molecule for the addition of the thiolate substrate. By tying up four of the six coordination sites of the iron octahedron with sulfur and nitrogen donor atoms, the biological protein network of the enzyme could be simulated at a fraction of the molecular weight of the actual enzyme.

The first iron syntheses were attempted using the tetradentate chelates 1,6-bis(2'-pyridyl)-2,5-dithiahexane (1,6) and 1,8-bis(2'-pyridyl)-3,6-dithiaoctane (1,8).(Figure 2) The thioethers provide a non-oxidizable sulfur ligation while the pyridine rings withdraw electron density. According to the model, the pyridyl rings of the molecule lie in separate planes which are parallel to each other. A stable (1,6)Fe(SR) complex was predicted, but the reactions with cysteamine and cysteine displaced the chelate ligands from the coordination sphere.(Figure 3)

The next change was to make the system more simple. By first adding the thiolates to iron in a 2:1 ratio under inert conditions and then adding a bidentate pi-acid ligand, a ternary compound might be formed. The compound would have a mixed ligand system with two thiolates and four nitrogen atoms (two pyridyl, two amine) in the iron coordination sphere, an FeS_2N_4 chromophore. The initial results with bipyridine were promising; the red compound that was produced appeared to contain both types of ligand. Inert anion exchange chromatography was attempted in order to separate a single, pure compound. However, two compounds were separated by the column. A purple complex eluted through the column without retention, while the red compound remained adhered as a -1 charge type. The red compound was removed from the column using 0.1 $\underline{M}$ NEt_4Cl. It was isolated and then recrystallized from hot acetonitrile. The elemental analysis demonstrated a total lack of sulfur in the compound. It was later found that the red compound was tris(bipyridyl)iron(II) chloride, a thermodynamically stable compound.

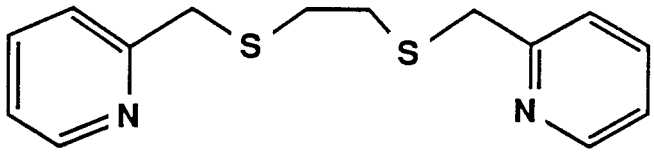

1,6-Bis(2'-pyridyl)-2,5-dithiahexane

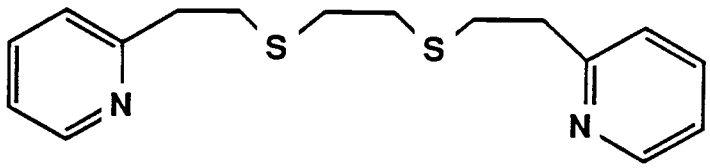

1,8-Bis(2'-pyridyl)-3,6-dithiaoctane

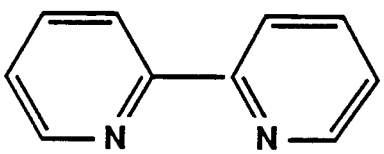

bipyridine

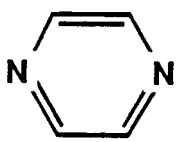

pyrazine

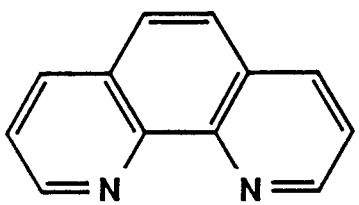

1,10 phenanthroline

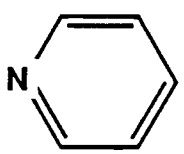

pyridine

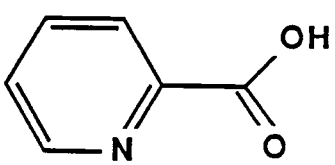

picolinic acid

Figure 2. Tetradentate Chelates and Pi-acids Used in Early Attempts at Synthesis of an Iron-Thiolate Model for Dioxygenase Enzymes.

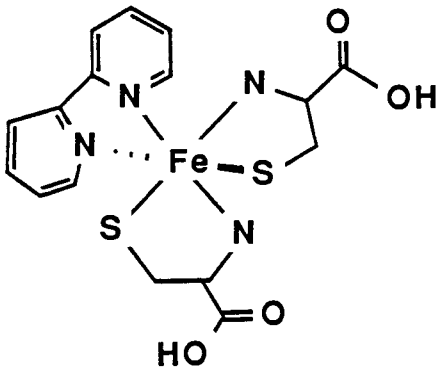

bpyFe(CyS)$_2$

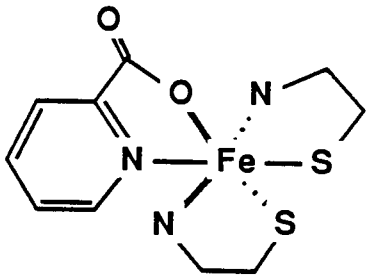

picFe(CySte)$_2$

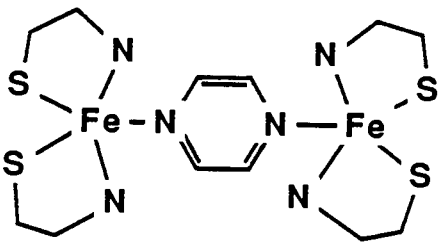

pyz(Fe(CySte)$_2$)$_2$

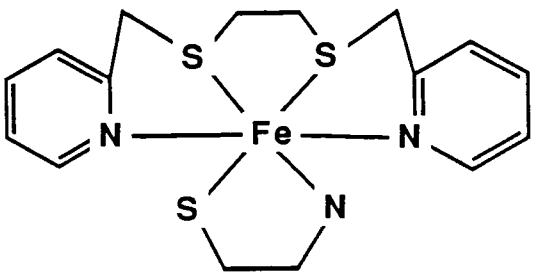

(1,6)FeCySte

Figure 3. Some of the Target Molecules for Ternary Iron-Thiolates.

Several other pi-acids were used in attempts to prepare a ternary complex; bidentate ligands such as 1,10 phenanthroline and picolinic acid produced red 'tris' species while the monodentate pi-acids pyridine and pyrazine did not cause the color change, implying that these ligands did not coordinate to the iron center. The tris species proved to be more stable than the mixed ligand systems, since no mixed compound was ever obtained. Clearly the pi-acid approach was not working.

Each system darkened considerably whenever there was an air leak. When the reaction solution was placed onto an inert ion-exchange column, there was usually some uncharged purple compound separated. During the work-up of one of the picolinic acid trials, it was noticed that some of the purple compound had crystallized from methanol in the collection flask. The purple compound was found to contain the thiolate ligand and was air-stable. Therefore, efforts were turned toward producing larger amounts of this purple species. The pi-acids were eliminated from the synthesis, and the purple complex became the new target, a potential model system to represent the thiolate dioxygenase enzymes. The synthesis and characterization of this air-stable iron(III)-thiolate is the subject of the first section of this thesis.[1]

[1] Note added in proof: Suades, et al., mention the synthesis of the title complex in a paper describing a tri-cobalt cluster complex of 3-aminopropanethiol.[76]

Experimental

Materials and Methods. Reagent-grade chemicals were acquired from various sources and were used without further purification. Aldrich: 2-Aminoethanethiol hydrochloride, D-(-)-Penicillamine, 2,2′-Bipyridine, 2-Vinylpyridine, α-Chloropicoline, Picolinic acid. Sigma: Iron(III)chloride (anh.), L-Cysteinesulfinic acid, Hypotaurine, m-Chloroperoxybenzoic acid. Alfa Products: Iron(II)chloride (anh.) Mallinckrodt: 1,10-Phenanthroline monohydrate, Pyridine. MCB: L-Cysteine hydrochloride. Baker: 30% Hydrogen Peroxide. Reagent grade Methanol was distilled over a Grignard reagent and then stored over 4Å Molecular Sieves prior to use. Prepure Nitrogen was used for all purges.

Chloride Analysis. Chloride concentration was determined by the Volhard back-titration method.[42] A 15.0 mg sample was treated with 5 mL 6 M nitric acid in a 125 mL Erlenmeyer flask for 15 minutes to decompose the sample. After the purple color had dissipated, 20 mL H_2O was added to dilute the solution. Roughly 1.0 mL 0.1000 M $AgNO_3$ was added from a 10 mL buret; a white AgCl precipitate formed. Nitrobenzene (3.0 mL) and Fe^{2+} solution (1.0 mL) were added as coagulator and indicator, respectively, and the solution titrated with 0.0100 M KSCN until a faint orange color remained.

Total Iron Analysis.[43] A 15.0 mg sample was dissolved in 0.1 M HCl in a 25 mL beaker and then quantitatively transferred to a 50 mL volumetric flask. Distilled water was used to dilute to the mark. A 5.0 mL aliquot of this solution was pipetted into another 50 mL

volumetric flask to which 1.0 mL 10% sodium citrate, 2.0 mL 10% hydroxylamine hydrochloride and 5.0 mL 0.025% 1,10-phenanthroline were added via pipets. The orange solution was diluted to the mark with water, shaken and allowed to sit for 15 minutes. The absorbance of the 510 nm $[Fe(phen)_3]^{2+}$ peak was measured on a Cary 16 spectrophotometer, referenced to a blank prepared without sample. The average of four successive scans was compared to a line determined from the analysis of $FeSO_4 \cdot (NH_4)_2SO_4 \cdot 6H_2O$ (MW 392.15, %Fe 14.24%)

Fourier Transform Infrared Spectroscopy. FTIR measurements were made from KBr pellets of the solid samples on a Mattson Sirius 100 FTIR spectrometer equipped with a Starlab Computer. Spectral manipulations were carried out with the instrumental software without further modification. Resolution was set at 8 cm^{-1} and 20 scans of the sample and background were averaged in a typical spectrum.

Fourier Transform Proton Nuclear Magnetic Resonance. A 5 mg sample of $Fe[Fe(SCH_2CH_2NH_2)_3]_2Cl_3$ was dissolved in 1 mL d_4-methanol (MSD Isotopes) from a sealed ampule. The solution was filtered through glass wool to remove residual solids and then transfered to an NMR tube. The sample data were collected on a Bruker AM400 400 MHz NMR with TMS as an internal reference. The method was expected to provide results similar to those of Werth[44], who measured the proton NMR of several rubredoxins and rubredoxin analogues containing high spin Fe(III). Chemical shifts for these compounds were found in the region between 0-300 ppm.

Cyclic Voltammetry- CV measurements were made on an IBM EC/225

Voltametric Analyzer and recorded on an IBM 7424 MT Recorder. The Analyzer was operated in 3-electrode mode using a home-made Pt working microelectrode, a Pt wire auxilliary electrode and an Orion 900100 Single Junction Reference Electrode (SCE). All measurements were made at room temperature in a closed Teflon cell. The solutions were purged with prepurified nitrogen for five minutes before the measurement were taken. The first sweep was always a reduction.

Mössbauer Spectroscopy- The MB spectrometer was of the conventional constant-accelerator type. The source was ^{57}Co diffused in rhodium. All isomer shifts are given relative to natural iron foil at 300 K. The iron foil was also used as a standard for velocity calibration. The source was mounted on a LVsyn-loudspeaker system driven by a digitally controlled function generator with a standard feedback loop. The radiation was detected by a proportional counter and a Norland 5300 multichannel analyzer. The sample holder was a two-piece, 2.2-cm diameter Lucite disk with sample area 2 cm^2 and thickness 1.0 mm. It was sealed with silicone grease. Most samples were ground with equal weights of boron nitride, although the x-ray quality crystals were run neat. The data were folded, plotted, and Lorentzian curve fit by a computer procedure on a DEC PDP11 computer.

Magnetic Susceptibility Measurement. The measurement was made on a pure crystalline sample using the Gouy method. An Alpha Model AL7500 water-cooled magnet controlled by an Alpha Model 7500 power supply was used; the field strength was about 5 kilogauss. A Mettler Model H-16 semimicro balance was used to measure the weight change.

$Hg[Co(NCS)_4]$ was used as a susceptibility standard. Effective magnetic moment was calculated from $\mu_{eff} = 2.828(\chi_M T)^{1/2}$, where χ_M is the corrected molar susceptibility. The diamagnetic correction was calculated from Pascal's constants (471.4×10^{-6} $cm^3\ mol^{-1}$)[45].

UV-Visible Spectroscopy- Absorbance measurements of dilute solutions were made on a Hewlett-Packard HP 8451A Diode Array Spectrophotometer, referenced to methanol. The decomposition reactions were followed using the OVERLAY and PEAK FIND functions to plot and collect data. All concentrations were adjusted such that the visible peak at 482 nm would be between values of 0 and 1.5 absorbance units.

Elemental Analyses- Microanalytical results were obtained from Galbraith Laboratories, Knoxville, TN.

X-ray Structure Determination of $Fe[Fe(SCH_2CH_2NH_2)_3]_2Cl_2$. Crystal structure data were collected by Molecular Structure Corporation, College Station, TX. Purple crystals of $Fe[Fe(SCH_2CH_2NH_2)_3]_2Cl_2$ were obtained by a method which will be described later. The determination of the cell dimensions and the collection of intensity data were carried out using Cu Kα radiation (λ = 1.54184Å) on a Rigaku AFC6 diffractometer equipped with a graphite crystal, incident beam monochromator and 12 KW rotating anode generator. As reported by Molecular Structure Corporation, the cell constants were determined from a least-squares refinement using the setting angles of 25 carefully centered reflections in the range $103° < 2\theta < 117°$. Three crystals were surveyed before a crystal that

was suitable for diffraction was found. In general, the crystals diffracted very poorly, if they diffracted at all.

The crystal was mounted on the end of a glass fiber.The data were collected at a temperature of 23 ± 1° using the ω-2θ technique. The scan rate was 16°/min (in omega). The average width at half height was 0.36° with a take-off angle of 6.0°. The system is triclinic with the space group being either P1 or P1-bar. A total of 2383 reflections were collected. The intensities of three standard reflections were measured after every 150 reflections; the average decay for the entire data set was -2.4% on intensity. Corrections were made for the separation of the Kα doublet.

The structure was solved by direct methods and refined by full-matrix least squares techniques. All computations were carried out on a VAX 750 computer by D.A. Keszler and S. Hein using the Texsan program. Table 1 summarizes the crystal and refinement data.

Syntheses. The general synthesis of the cluster is described, through the complete purification of x-ray quality crystals, and then the deviations from that method are detailed. Some of the attempts at producing a mixed ligand pi-acid complex are also reported.

Preparation of The Brown Precursor Complex of $Fe(Fe(SCH_2CH_2NH_2)_3)_2Cl_3 \cdot 3H_2O$. Standard Schlenk techniques were used to prepare the brown iron(II)-cysteamine precursor complex. The central frit was clamped onto the rotating grid. The rest of the apparatus was assembled around the fritte, using plastic clamps to hold the ground glass joints together. (Figure 4)

Table 1. Summary of the Crystal and Refinement Data for $Fe[Fe(SCH_2CH_2NH_2)_3]_2Cl_2$

formula	$Fe_3C_{12}H_{36}N_6S_6Cl_2$
mol wt	694.85
color,shape	purple (black), prismatic
space group	P1 or P1-bar , triclinic
a,Å	8.474(1)
b,Å	11.770(1)
c,Å	8.300(1)
α,deg	106.30(1)
β,deg	92.58(1)
γ,deg	77.46(1)
V,Å^3	775.5(2)
temp, °C	23(1)
Z	1
radiation	Cu Kα (λ=1.54184Å)
cryst dimens, mm	0.25 x 0.20 x 0.15
cryst-detector dist, cm	40
scan speed, deg/min	16
scan type	ω-2θ
scan width	1.26 + 0.300 tan θ
peak bkgd counting time	2:1
maximum 2θ, deg	118
no. of reflecns measd	2383
crystal faces, mm sepn	{1 0 0} 0.25
	{0 1 0} 0.22
	{0 0 1} 0.17
empirical formula	$Fe_3C_{12}H_{40}N_6S_6Cl_2O_2$
mol wt	731.31
space group	P-1 (#2)
D_{calc}, g/cm^3	1.55
D_{exp}, g/cm^3	1.6 - 2.0
mu (Cu K-alpha), cm^{-1}	166.87
no. observations(I>3.50(sig(I)))	1364
no. variables	142
residuals: R;	0.098
R_w	0.134
goodness of fit indicator	2.75
maximum shift in final cycle	0.07
largest peak in final diff. map, e/Å^3	2.22

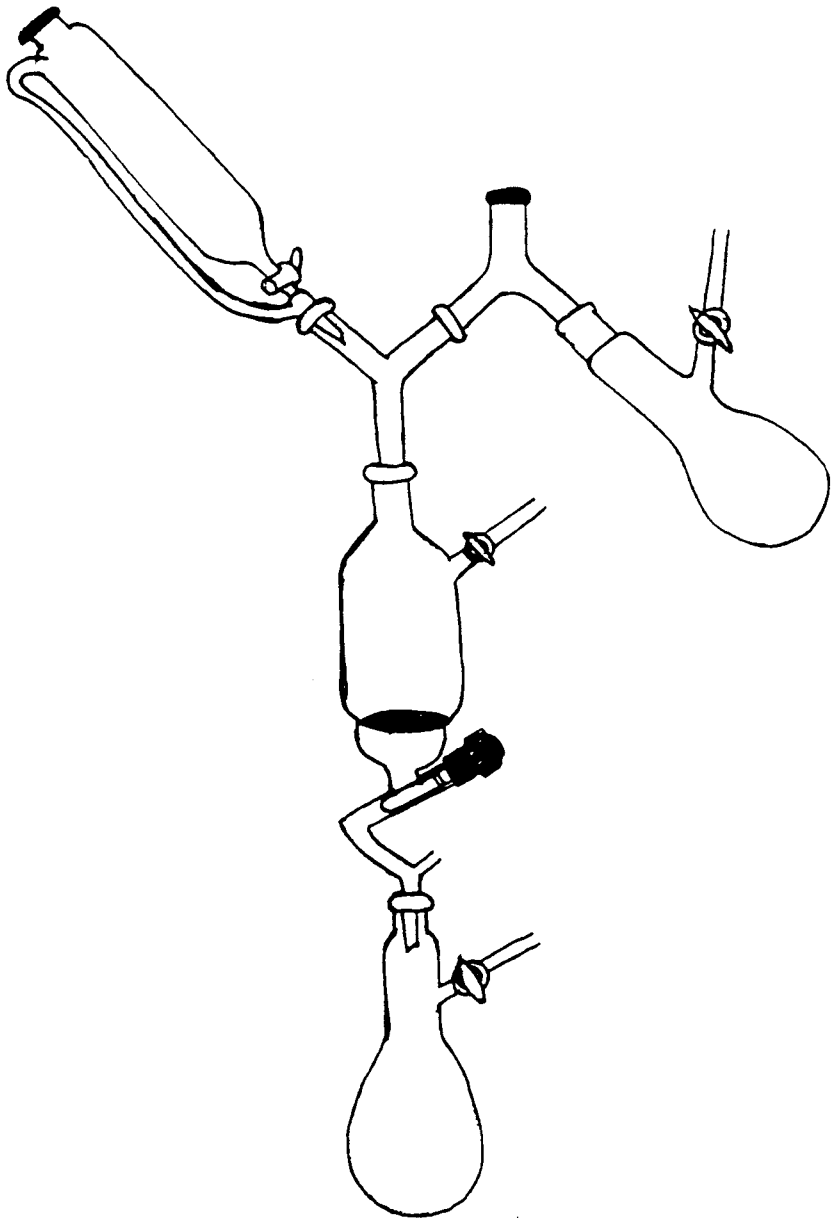

Figure 4. Schematic Diagram of the Schlenk Apparatus Used in the Synthesis of Air-Sensitive Compounds.

Iron(II) chloride (0.634 g, 5.00 mmol) was placed into the reaction flask along with a stir bar. A nitrogen inlet was connected to the side arm of the reaction vessel, an outlet for the N_2 connected from the side arm of the fritte to a mineral oil bubbler and a vacuum line attached to the side arm of the receiving flask, located below the fritte. After the system was swept with nitrogen for 5 min, the stopcock of the dropping funnel was closed and the system rotated to position the funnel vertically.

Cysteamine·HCl (1.14 g, 10.0 mmol) was dissolved in 15 mL MeOH in a 30 mL beaker and the solution added to the funnel. The system was then evacuated to 1 torr with the vacuum pump, then refilled with N_2 in three alternating cycles. A continuous stream of N_2 was allowed to sweep through the system following the purge cycle. When a solution was transferred into the system, the N_2 flow was temporarily halted by closing the inlet stopcock.

Methanol (25 mL) was purged with N_2 and then transferred via a cannula into the reaction flask while stirring. The iron(II) chloride desolved partially in methanol to form an orange slurry. The grid was rotated to allow the cysteamine solution to drip into the reaction flask. The addition was made over a 3 minute period. During this addition the color of the mixture changed from orange to Kelly green.

A solution of base was prepared by transferring 10 mL of the deaerated MeOH into a purged, septum capped Erlenmeyer flask. Triethylamine, NEt_3, (2.8 mL, 20 mmol) was injected into the flask via syringe. This base solution was added via cannula into the dropping funnel and then added dropwise to the reaction flask. The

color of the slurry changed from green to brown, and a light brown precipitate developed after half of the base had been added. Continuing the addition caused total precipitation after three quarters of the base was added; no physical change occured with the addition of the last quarter of the base solution. The solution was light yellow.

At this point the syntheses varied, dependent upon the target of the experiment. Each variation will be discussed separately.

$$12\ FeCl_2 + 24\ HSCH_2CH_2NH_3Cl + 36\ N(CH_2CH_3)_3 + 3\ O_2 \longrightarrow$$
$$4\ [Fe[Fe(SCH_2CH_2NH_2)_3]_2]Cl_3 + 6\ H_2O + 36\ HN(CH_2CH_3)_3Cl$$

Preparations of bis(fac-S)((tris)2-aminoethanethiolatoiron(III)) iron(III) chloride trihydrate.

$$Fe(Fe(SCH_2CH_2NH_2)_3)_2Cl_3 \cdot 3H_2O \cdot CH_3OH$$

Exposure to Air. The reaction flask was removed from the Schlenk system, stirred for ten minutes and the contents poured into a 30 mL M fritted filter. The brown slurry turned purple immediately upon air contact. A large amount of purple solid was collected on the filter. The solid was then washed with two 10 mL portions of MeOH to remove triethylammonium chloride and the excess base. Crude yield, 1.1 g (80%).

In the first few syntheses, KOH was used as the base. The purple solid was found to contain KCl as a coprecipitate. By changing the base to NEt_3, the isolation of a purple material which was free of chloride salt could be accomplished. The procedure for this was to simply wash the precipitate with several extra volumes of MeOH.

Recrystallization. About 1.0 g of crude product was extracted with several 50 mL portions of methanol until the purple color of the solution was no longer very intense. In practice, this corresponds to a volume of 200-300 mL. When a volume larger than 50 mL was used, the decomposition of the complex to disulfide and iron oxide resulted. Each portion was filtered and combined into a 250 mL round bottom flask. A rotory evaporator was used to reduce the volume to 10-15 mL, which resulted in extensive formation of solid. At this point the mixture was filtered. The material collected by filtration was a purple microcrystalline solid, mostly in the form of thin needles and flat plates. A complete discussion of the crystal habits found for the compound appears in the results section. Total yield, 300 mg (27%): large crystals; yield, 35 mg (2.9%).

Anal. Calcd for $Fe_3C_{13}H_{46}N_6S_6O_4Cl_3$: Fe, 20.51; C 19.11; H, 5.68; N, 10.29; S, 23.55; Cl, 13.02. MW = 816.83 Found: Fe, 20.01; C, 19.30; H, 5.50; N, 10.46; S, 24.57; Cl, 13.43.

Molar absorptivity values in methanol are ε_{234}=28,000; ε_{278}=18,000; ε_{336}=11,800; ε_{490}=4,300; ε_{582}=2,700; and ε_{725}=1,150(sh) $\underline{M}^{-1}cm^{-1}$. The complex undergoes slow decomposition in methanol; these values represent a lower limit, with the actual values up to 3% greater.

The filtrate from the recrystallization was placed into a 25mL Erlenmeyer flask which was capped with a septum and stored in a freezer at -15°C. Block crystals formed within 2 days and increased in size when left for longer periods of time. Unfortunately an orange ferrihydrite powder precipitated on top of these crystals when they

were allowed to stand for longer periods of time. The optimum length of growing time for the crystals was 3-4 days. Shorter time periods produced smaller crystals, while much longer standing produced orange coated crystals.

The largest x-ray quality crystals were separated from the ferrihydrite impurity by means of a density gradient. The purple crystals were found to have a density between 1.6 and 2.0 by trial and error methods. Several iron oxide species have reported densities of about 5.5.[46] The mixed crystalline compound was placed into a small amount of CCl_4 (d=1.6) in a 20 mL beaker. CCl_3Br (d=2.0) was added dropwise until the crystals floated. The liquid layer containing the floating crystals was removed into another beaker and the solvent removed by evaporation in the hood.

A vapor diffusion method was attempted as a means of growing x-ray quality crystals. The flask containing the filtrate was set into a 200 mL beaker which contained 25 mL of a solvent in which the purple cluster is insoluble. Both Et_2O and EtOH were used as diffusing solvents. The large beaker was capped with Parafilm and set into the freezer. As the second solvent diffused into the methanolic solution, it caused the precipitation of the solute as needle crystals. The single crystals recovered from concentrated methanol diffracted better than the single crystals obtained from the vapor diffusion method.

Exposure to Oxygen. An attempt was made to quantify the amount of oxygen required to cause the brown iron(II) precursor complex to be fully oxidized to the purple cluster. The stoichiometry of oxygen

uptake should provide an indication of the oxidation state for each component of the system, prior to the complete analysis of the product. The intent was to determine if there were enough equivalents of oxidant used to oxidize both the Fe(II) to Fe(III) and the thiolate to disulfide.

An oxygen tank was connected to a water filled buret by means of a three-way glass stopcock and 1 cm Tygon tubing. The water level in the buret was manipulated by connecting the bottom of the buret to a large funnel, which could be raised and lowered as necessary. This allowed the pressure to be maintained at nearly atmospheric pressure and the volume of gas measured. Initially, the tubing and buret were swept with oxygen five or six times. The reaction flask was removed from the Schlenk apparatus and quickly capped with a rubber septum under a constant flow of N_2. The open end of the oxygen transfer apparatus was connected to the side arm of the reaction flask and the flask set up over a magnetic stirrer.

After another O_2 sweep, the 3-way stopcock was used to fill the buret. Excess pressure in the flask was vented through the septum with a needle. The release of O_2 into the system was accomplished by opening the sidearm stopcock and the volume measured directly from the buret, after equilibrating to atmospheric pressure by adjusting the funnel water level to be equal to the buret water level. The level of oxygen was be adjusted periodically to approximately 20 torr over atmospheric pressure in the reaction flask, by raising the funnel water level above the water level in the buret.

As O_2 was admitted into the closed system under these

controlled conditions, the brown color of the slurry gradually darkened to purple. The change occured over the course of several hours. After 3 hours, the volume of O_2 measured changed at a rate of less than 1 mL/30 min. At this point, the slurry produced was filtered and collected. The average volume of gas taken up by a reaction run on a 5 mmol scale was 30 mL O_2, which corresponds to the oxidation of the iron without oxidation of the thiolate. Crude yield: 1.04 g (75%).

Preparation from Iron(III) Chloride. A completely analogous synthesis was carried out with iron(III) under Schlenk conditions, to see if the compound can be produced without the air oxidation. Anhydrous $FeCl_3$ (0.81 g, 5.0 mmol) was weighed in a glove box under nitrogen atmosphere and placed into the reaction flask, which was then capped with a septum and removed from the glove box. Cysteamine (1.14 g, 10.0 mmol) was dissolved in 10 mL MeOH and the solution poured into the dropping funnel. The system was closed by attaching the reaction flask into place under a positive N_2 atmosphere and purging with three N_2/vacuum cycles.

Methanol (10 mL) was transferred into the reaction flask and the slurry stirred. There was a color change from black to orange when the MeOH was added to the ferric chloride. The thiolate was added dropwise to give a clear, pale green solution. After the mixture was stirred for 10 min, NEt_3 (2.8 mL, 20 mmol) was added to the dropping funnel by cannulus and added dropwise to the reaction flask. Immediately upon addition, the solution darkened and a white cloud formed above the solution. As the addition continued, a khaki green

precipitate formed. At full addition of base, the solution was very dark, almost black. After 10 min of stirring, the solution was filtered to separate a green-black filtrate from a dark green solid.

The air-stable solid was dried in a hood. Once dry, the solid was extracted with 50 mL MeOH, then filtered. A green residue was removed from the deep purple filtrate. The filtrate was taken to dryness using a rotory evaporator and the residue was taken up in 5 mL MeOH and filtered. Purple microcrystals were recovered. The filtrate was placed into a 25 mL Erlenmeyer flask and stored overnight in the freezer. A small crop of large "soccer ball" crystals was recovered after 3 days. Yield: microcrystals, 215 mg (17.6%); large crystals, 15 mg (1.2%).

Attempted Preparation from Disulfide. An attempt to produce the purple compound by the redox reaction of ferrous chloride with cystamine failed. Cystamine (1.14 g, 10.0 mmol) was dissolved in 10 mL MeOH by adding a half equivalent of NEt_3 (0.7 mL, 5 mmol) to the mixture. This solution was placed into the dropping funnel and the standard Schlenk technique used. The ligand solution was added dropwise into $FeCl_2$ (0.634 g, 5 mmol) in methanol. The usual orange to green color change was not observed upon addition of the disulfide. The remaining 2.1 mL (15 mmol) NEt_3 in 10 mL MeOH was transferred into the dropping funnel and then added dropwise. The solution became cloudy and turned pale tan in color. The color gradually changed to light green within 5 min, then deepened in shade until the white component of the cloudiness was completely dissipated. After 20 min, the color was dark brown. The solution was

filtered to produce a dark brown solid and a dark brown filtrate solution. The solid was washed twice with 15 mL portions of methanol.

The solid was collected in the air, causing the surface to lighten in color to a rust orange. A large weight loss accompanied this color change, corresponding to the evaporation of the methanol from the compound. At no point during the synthesis was purple color observed, but when the spent glassware was washed with dilute HCl, the purple color was noticed.

Preparation without Schlenk Technique. The materials were weighed in the same proportions into separate 125 mL Erlenmeyer flasks which were each capped with a septum and purged with a nitrogen stream for 30 min. The $FeCl_2$ flask contained a stir bar. The synthesis was achieved by transferring 15 mL N_2 purged MeOH into each flask, stirring to dissolve and then adding both the ligand and base solutions separately into the flask containing the iron chloride. The slurry was produced with only a slight deepening of the brown color of the system as compared to the standard Schlenk method.

After 5 minutes of stirring, the septum was removed and the brown slurry filtered. The color changed to purple before the solution contacted the filter. A large amount of crude solid was obtained and recrystallization was carried out in a manner similar to the other preparations.

Solid State Reaction with Air. When the initial brown slurry was filtered in the Schlenk system under inert conditions, the brown precipitate was collected on the central fritte. Even under closed conditions, the surface of the solid begans to darken once the

solvent was removed. When the system was opened to air, the color immediately changed to purple at all exposed surfaces. In an experiment where the brown solid was washed with N_2 purged diethyl ether prior to the air exposure and then collected in an open beaker, a spontaneous combustion of the sample occurred. The solid material physically charred, and a burnt organic smell permeated the room. When the ether wash was not used, the solid simply turned purple.

All attempts to collect the brown precursor solid with the rigorous exclusion of O_2 failed. The frit was removed from the Schlenk system after the filtration step, capped with a septum under positive N_2 pressure and taken into a freshly regenerated N_2 glove box. The surface of the solid darkened as soon as the cap was removed. Some O_2 may have been present in the protected N_2 environment, but it could be only a small percentage of the total atmosphere. This indicates that the compound will scavenge oxygen rapidly. The majority of the sample oxidized rapidly in the glove box at every exposed surface. Cutting into the surface with a microspatula exposed a fresh brown surface. An IR pellet was pressed in the glove box using KBr and an attempt was made to follow the oxidation of this brown precursor to the purple compound.

Attempts at Preparation of Mixed-Ligand Pi-Acid Complexes. The complexes were prepared such that a single molar equivalent of pi-acid was used unless otherwise specified. The brown iron(II)-cysteamine precursor was prepared by the same method described for the preparation of the tri-iron cluster.

A) Bipyridine- Bipyridine (643 mg, 4.12 mmol) was weighed into a

50 mL Erlenmeyer flask, which was then septum capped and purged with N_2. Purged MeOH (10 mL) was added and the solution stirred until the solid was completely dissolved. The solution was transferred into the dropping funnel and added dropwise into the brown slurry. The slurry immediately turned red-violet, the color of grape juice.

The solution was stirred for half an hour. The grid was rotated to pour the contents of the reaction flask onto the fritte. The N_2 stopcock was closed and the vacuum used to pull the filtrate solution into the collection flask, leaving any solid formed in the reaction on the frit. A one atmosphere pressure of nitrogen was restored to the system. The flask was then quickly removed from the apparatus and capped with a septum. In different experiments, the red solution was either transferred via cannula onto an cation exchange column, evaporated to near dryness, or cooled to induce crystallization.

The red material isolated was recrystallized from hot CH_3CN by slow cooling of the saturated solution. The intended stoichiometry for the reaction was not observed. The red compound produced was found to be $Fe(bpy)_3Cl_2$. A small amount of the purple iron-cysteamine cluster was separated from the red compound by the cation exchange chromatography. Elemental analysis of the red compound demonstrated that no sulfur was present. The UV-Vis spectrum of the red compound had peaks at 248, 292, 352, and 524 nm.

B) 1,10-Phenanthroline- The reaction was the same as the bipyridine reaction except that the o-phen product was a bit more orange than red. 1,10-phenanthroline (817 mg, 4.2 mmol) was dissolved in 15 mL purged MeOH, transferred into the Schlenk system and added

dropwise to the brown slurry. An orange solution was formed, which was stirred for 30 min, then filtered to produce an orange solution and a brown-orange solid. The solid was recrystallized from hot CH_3CN. UV peaks were found at 226, 268 and 508 nm for tris(o-phenanthroline)iron(II) chloride.

C) Pyridine- Pyridine (0.20 mL, 1.2 mmol) was injected via syringe through the septum into the dropping funnel along with 5 mL MeOH. There was no significant color change upon the dropwise addition of the pyridine to the brown slurry. The slurry darkened slightly and turned considerably darker upon air exposure. The mixture was filtered to separate a dark brown solid from a slightly yellow solution. A white solid was forced out of the filtrate by diethyl ether, which was shown to be cystamine by FTIR.

D) Pyrazine- A pyrazine bridge between two $Fe(CySte)_2$ units was envisioned. Pyrazine (93.3g, 2.3 mmol) was dissolved in MeOH and then transferred into the system. The brown solution which resulted turned violet when exposed to air. UV-Vis evidence showed that no pi-acid was incorporated in the product.

E) Picolinic acid- 2-Picolinic acid (287 mg, 2.33 mmol) was dissolved in MeOH and added dropwise from the funnel. The solution turned bright red as the addition was continued. After stirring, the solution was filtered to give a light orange solid and a red solution. A portion of this methanolic solution was placed onto an air-protected anion exchange column, from which a neutral purple band eluted while a red band remained bound to the column. This latter compound was removed with NEt_4Cl. The compound was worked up to

remove the iron and the resulting free ligands were dissolved in D_2O in order obtain the ^1H NMR spectrum. The result suggested that both ligands were present, but this was later found to be incorrect, due to incomplete separation of the red tris(picolinato)iron(III) and disulfide on the column. The UV of this red complex has peaks at 284, 330, and 462 nm.

1,6-Bis(2'-pyridyl)-2,5-dithiahexane.

α-Chloropicoline (23.1 g, 14.1 mmol) was dissolved in 50 mL 100% EtOH with stirring in a three-neck 500 mL R.B. flask. The flask was equipped with a 125 mL dropping funnel, a reflux condenser, and a standard powder funnel. NaOEt (21.1 g, 28.2 mmol) was added through the funnel while stirring. 1,2-ethanedithiol (6.6 g, 7.1 mmol) was added to 25 mL 100% EtOH in the dropping funnel and this solution was added dropwise to the stirring slurry. The funnel was replaced with a ground glass cap. The solution was refluxed in a hood for 3 hours.

The solution was allowed to cool and then filtered through a 150 mL M frit to remove the co-product, NaCl. The salt was rinsed with two 15 mL portions of absolute EtOH, which were added to the filtrate, and the salt discarded. A 10% w/w HCl solution in EtOH was used to acidify the ligand solution until water-moistened pH paper turned orange (pH≈4). The solution was filtered again and then placed into a 250 mL R.B. flask. The solvent was removed by rotary evaporation to yield a red oil and more NaCl (est. 1.5 g).

The metal salts of the (1,6) ligand were prepared by a modification of the method of Livingstone and Nolan[47]. 50 mL 100% EtOH was added to the oil/salt mixture. A slurry of anhydrous $FeCl_2$

(6.9 g, 5.4 mmol) in 100 mL EtOH was added with stirring. A condenser was placed onto the flask and the solution heated to reflux for 10 min. The hot solution was filtered through a 150 mL M fritte. A light green product was collected and the brown filtrate discarded.

The crude solid was dissolved in 200 mL warm MeOH, and filtered to remove a small amount of insoluble brown $FeCl_2$ from the lemon yellow solution. 300 mL anhydrous Et_2O was added all at once to induce the precipitation of bright yellow needle crystals. After 3 hours these crystals were collected by suction filtration, washed twice with 25 mL Et_2O, and stored in a vial. Yield: 3.0 g (39%) ε_{262}=9000, mp 186°d, μ_{eff}= 4.91 B.M. (high spin Fe^{2+}).

The green copper(II) salt and purple cobalt(II) salt of the (1,6) ligand were prepared on a much smaller scale by adding the corresponding metal chloride in place of the iron(II) chloride. (1,6)$CuCl_2$ (38%); (1,6)$CoCl_2$ (45%)

(1,6)Fe(SR). In the typical (1,6)Fe(SR) synthesis, (1,6)$FeCl_2$ (0.61 g, 2.0 mmol) was placed into the reaction flask of the Schlenk system along with a stir bar. 2.0 mmol of thiolate was dissolved in 15 mL solvent and placed into the dropping funnel. The system was purged with 3 alternating cycles of vacuum/N_2 and then 10 mL solvent was transferred into the reaction flask. The color remained yellow as the thiolate was added dropwise to the stirring iron solution, but turned purple when O_2 was present in the system. 10 mL solvent was added to dissolve the base in a septum capped 25 mL Erlenmeyer flask and this solution was added to the dropping funnel via cannula. The grid was rotated to allow the stepwise addition of

this solution to the reaction mixture, causing a gradual darkening of the solution to root beer brown.

After 45 min, 50 mL anhydrous Et_2O was added, giving a cream colored precipitate. The system was filtered in a glove bag under an N_2 atmosphere, separating the yellow filtrate from an orange-brown solid. Air exposure at any point caused the system to turn purple-grey. The solid held the grey color, but the solutions faded from purple to orange gradually over 5-10 minutes. Evaporation of the filtrate solution produced crystals of the (1,6) ligand, indicating that the thiolate ligand had displaced the tetradentate ligand from its coordination sites.

Several variations of this procedure were used in attempting to prepare a thiolate-macrochelate complex. Four solvents (EtOH, MeOH, CH_3CN, $CHCl_3$); four thiolates (cysteine, cysteamine, penicillamine, thiosalicylic acid) and three bases ($NaOCH_3$, NEt_3, NaOH) were tried. These reactants were mixed in different combinations with similar negative results.

The synthesis of alanine and cysteine sulfinic acid complexes of the (1,6)Fe salt were also attempted, but no unique materials were isolated. Bromine was added to see if the yellow salt could be oxidized to a ferric form, but the product of this reaction was not cleanly separated. The disulfide cystine was added to the purple $(1,6)CoCl_2$ to see if (1,6)CoCys, a cobalt(III) complex could be formed via an oxidation-reduction pathway. No discrete compounds were isolated from this attempt.

1,8-Bis(2'-pyridyl)-3,6-dithiaoctaneiron(II)chloride. (1,8). The ligand was prepared by the condensation of 2-vinylpyridine with 1,2-ethanedithiol. 11.7 mL of 2-vinylpyridine (11.4 g, 108 mmol) was placed into a 100 mL R.B. flask. 5.9 mL (5.2 g, 55 mmol) of 1,2-ethanedithiol was added via graduated pipet and the solution heated to 60° in the hood with stirring. The yellow solution was cooled to room temperature and the color changed to orange. The solution was reheated to 85°C and cooled in an ice bath, which caused the formation of white needle crystals and a tan, amorphous solid. The solution was filtered, the solid washed twice with 25 mL cold petroleum ether and air dried in a hood. The solid was recrystallized from warm petroleum ether at a slower rate of cooling. Yield: 14.4g 86.0% mp 48-49°C.

The iron complex was formed by dissolving 0.6 g (2.0 mmol) of the (1,8) ligand in 10 mL absolute EtOH in a 100 mL R.B. flask. 0.25 g (2.0 mmol) anhydrous $FeCl_2$ was added to the stirring solution causing the color to become mustard yellow.[48] The solution was heated to 65°C, then filtered to yield a mustard brown solid, which was recrystallized from hot MeOH. Yield 0.658 g (76.3%). ^1H NMR: D_2O δ 7.76, 7.09, 2.54, 2.25, 1.19.

The (1,8) iron-thiolate syntheses were carried out in the Schlenk system under anaerobic conditions. (1,8)$FeCl_2$ (0.87 g, 2.0 mmol) was dissolved in purged MeOH (10 mL) and L-cysteine·HCl·H_2O (0.35 g, 2.0 mmol) was added. NEt_3 (0.56 mL, 4.0 mmol) was syringed into the mixture, resulting in the formation of a brown air-sensitive solid. The solid turned grey upon air exposure. After the solution

was filtered and exposed to air, the filtrate turned purple and then rapidly faded to orange. Neither the brown, nor the grey solids were soluble in any solvents, but both decomposed to rust in water.

If the base was added to the mustard yellow slurry first, the color turned dark green. As cysteine was added, the color turned grey. The solution was filtered and the grey solid collected in a glove bag. The grey and brown complexes were compared to the mustard colored complex using IR spectroscopy, and were found not to contain the (1,8) ligand.

The synthesis was also attempted on a 2 mmol scale by mixing together the (1,8) and cysteine ligands in an evacuated 125 mL Erlenmeyer flask in 20 mL 100% EtOH. Purged ethanol (20 mL) was added to $FeCl_2$ within the Schlenk system and the ligand solution then transferred into the metal solution while stirring. Addition of NEt_3 caused a yellow/orange to brown color change, and an air leak caused the solid to turn black. The black solid did not show characteristic (1,8) infrared absorbances.

Results and Discussion

Synthesis of $Fe[Fe(SCH_2CH_2NH_2)_3]_2Cl_3 \cdot 3H_2O \cdot CH_3OH$

Thiols are oxidized to disulfides by O_2 in the presence of ferric ions. By mixing one mole of ferrous chloride with two moles of cysteamine under rigorously oxygen free conditions, the thiolate was coordinated to the iron without being oxidized. Cysteamine serves as a bidentate ligand, bonding through both the thiolate and amine ends.

The initial green color of the system is associated with an iron(II)-thiol chromophore. As base is added, deprotonation of the thiol occurs, which causes the color to change from green to brown. A light brown precipitate deposits with further base addition, likely due to deprotonation of the $-NH_3^+$ function on the ligand, followed by $-NH_2$ coordination to the metal.

Under these conditions thiolate sulfur has a great tendency toward bridging between two metal atoms. This type of bonding to iron reduces the propensity for internal oxidation to a disulfide. The brown precursor compound is highly reactive and could not be isolated without undergoing further oxidation. One possible composition would be a three dimensional polymer lattice consisting of FeS_6 units in which each thiolate atom is bridging between two iron atoms. The amine ends of the cysteamine ligands would be protonated, with a chloride ion providing the charge balance. As a third mole of base is added, the pendant $-NH_3^+$ groups are deprotonated, which causes a free $-NH_2$ end to displace a thiolate from the coordination sphere of iron.

Oxidation of this brown solid produces the purple iron(III)-thiolate complex. The iron is oxidized from +2 to +3, but the bridging thiolate ligands remain unoxidized. The change in iron chromophore, a replacement of a bridging thiolate with a non-bridging amine, destroys all possibility for an extended polymer network. The reorganization takes place concurrently with oxidation of iron. The chloride remains present to counterbalance the positive charge on the entire cation. The product of the oxidation remains the same despite several variations of oxidative conditions.

The elemental analysis of the purple crystals demonstrates that there are two thiolate ligands and one chloride per iron. There are two reasonable structures that correlate well with this composition. Besides the trinuclear iron-thiolate structure having six bridging thiolate ligands and three chloride ions, a binuclear compound with two bridging and two non-bridged thiolates fits the analysis. In

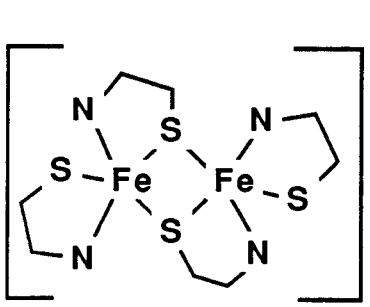

$[Fe_2CySte_4]^{2+}$

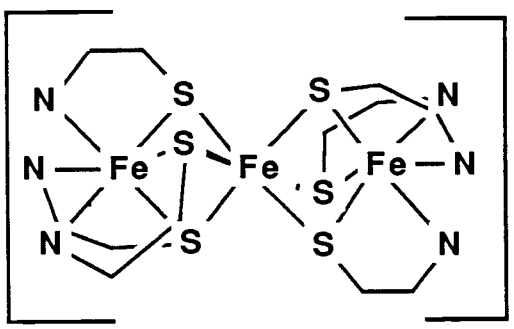

$Fe(Fe(CySte)_3)_2^{3+}$

the solid state, this purple compound is stable with respect to internal oxidation-reduction and can be handled in the air without

precaution. The compound has a melting point of 126°C.

Solubility tests on the purple solid demonstrate that it is soluble in water and methanol, both highly polar, hydrogen-bonded solvents. The compound has a solubility of about 640 mg/100 mL in methanol at room temperature. It is insoluble in other common organic solvents: DMF, THF, ether, ethanol and higher alcohols, acetonitrile, and toluene. The compound is slightly soluble in DMSO, but spectral changes suggest that DMSO will coordinate to the metal by displacing the thiolate ligands.

A fairly large yield of crude material can be obtained, but much of it is lost during attempts to recrystallize it. A substantial portion of the material decomposes to ferrihydrite, an iron oxide species. The ferrihydrite is insoluble and appears as either an orange or brown precipitate. (This material is discussed further in the Mossbauer section.) The recrystallization of the crude product from MeOH will produce quite a bit of this brown precipitate, which can be filtered off. The filtrate solution will then hold its purple color indefinitely when cold (-15°). Under such cold conditions, the ferrihydrite will gradually precipitate over several weeks. If the methanol is removed by concentrating the solution by rotary evaporation at reduced pressure, the purple material will precipitate as needle or block crystals, which are too small for x-ray analysis. Evaporation to complete dryness will induce the decomposition of the compound. This is likely due to water being present in substantial excess over methanol.

The absorption spectrum of the purple compound in MeOH has six

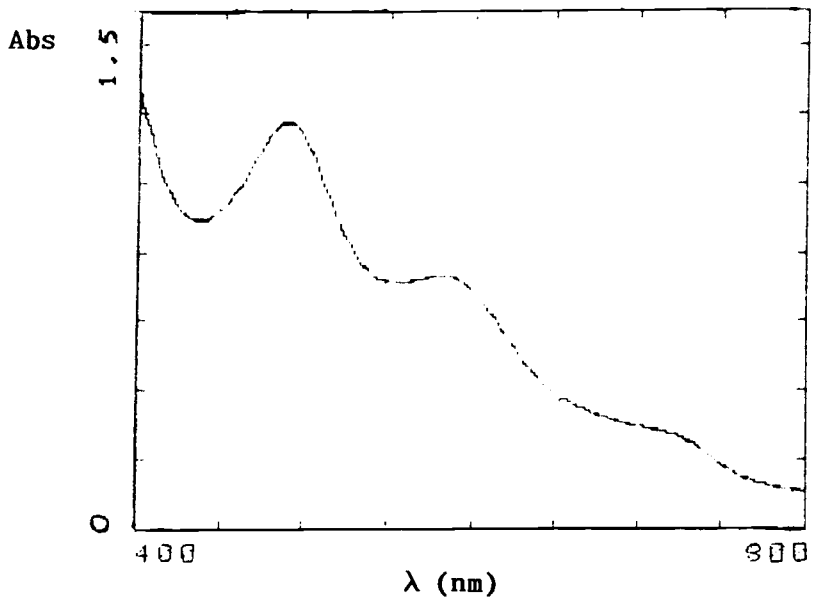

Figure 5. Visible Spectrum of $Fe[Fe(SCH_2CH_2NH_2)_3]_2Cl_3$ in MeOH.

peaks, three in the UV and three in the visible region (Figure 5). The height of the 490 nm charge transfer band is used to establish the concentration of the species in solution. The peak at 725 nm is a shoulder off the peak at 580 nm. Since the complex undergoes slow decomposition in methanol, the molar absorbtivity values reported earlier represent a lower limit, with the actual values up to 3% greater.

A concentrated methanol solution fades over a three-week period, and gives a yellow solution containing a small amount of orange precipitate. There are no peaks in the visible spectrum for this yellow solution. The rate of the decomposition depends upon whether or not the solution has been protected from air. There is no change in the intensity ratio of the peaks.

Addition of water to a methanol solution of the complex accelerates the decay of the chromophore. Since water itself cannot be the oxidant, it must be enabling the air oxidation to proceed at an enhanced rate. The purple solid dissolves readily in water, but is air-oxidized completely to the ferrihydrite. The orange precipitate is suspended throughout the solution in the cell, which no longer has a purple color. The precipitate contains no thiolate and the solution has a UV peak at 244, demonstrating that oxidation of thiolate to disulfide has taken place. The rate of this reaction is dependent upon the initial concentration; decomposition occurs more rapidly at lower initial concentration. The process begins immediately upon dissolution and is completed within an hour.

The compound reacts with dissolved oxygen much more rapidly in water than in methanol. The aqueous solution might hold its color for up to 1.5 h, but the visible spectrum showed a steady decrease in the intensity of the 490 nm band (Figure 6). Complete loss of spectral features occurs all at once, after the species has gradually decomposed a portion of the way. Addition of dilute acid will stabilize the color for longer periods of time. In methanol, monitoring a solution at the same concentration showed only a 3% loss of intensity of the 490 nm peak over 24 hours.

Addition of a small amount of water to a concentrated methanol solution tends to help the formation of good crystals, even though the presence of the water will also promote the decomposition reaction. The criteria for 'good' crystals are color, crystal habit and reproducible spectral data (UV-Vis and FTIR). In mixed $MeOH/H_2O$

and reproducible spectral data (UV-Vis and FTIR). In mixed MeOH/H_2O solutions, the rate of decomposition is only marginally affected by the amount of water present, even up to 50% water by volume. In very dilute methanol solutions, the decomposition is as rapid as in water.

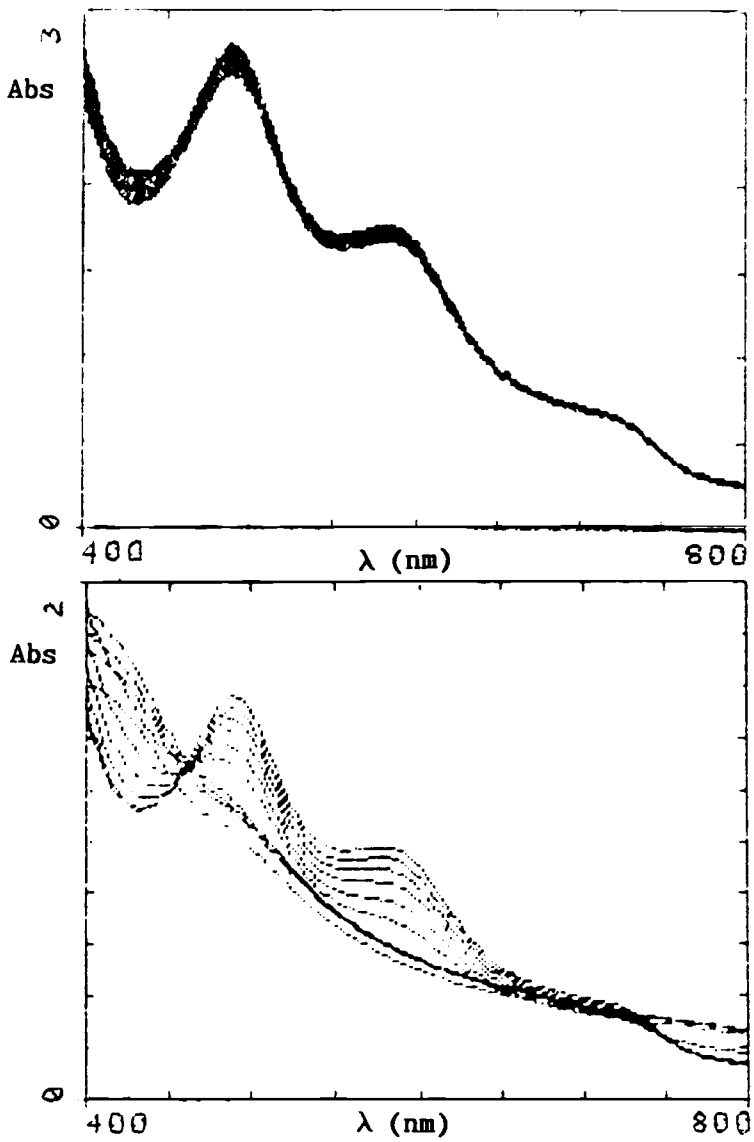

Figure 6. Changes in the Visible Spectrum of $Fe[Fe(SCH_2CH_2NH_2)_3]_2Cl_3$ Upon Air Oxidation: (a) spectra in methanol, rerun every half hour for 20 hours, (b) spectra in water rerun every 15 minutes for 2.5 hours.

Crystal Habits. There are several different distinct crystal habits for $Fe[Fe(SCH_2CH_2NH_2)_3]_2Cl_3$. Each crystal habit is defined by a regular geometry, with specific angles that recur throughout the individual crystals.

The most stunning crystal shape takes the form of a soccer ball. Each of the individual crystals is a regular pentagonal bipyramid, with five faces sharing edges, which are capped at a single point. The angles are distinctive, at about 72° between faces. The three dimensional character stands out, and the faces sparkle as they reflect light. These crystal are produced in small yield, by slow cooling of a saturated methanolic solution of the complex at -15°C for 48 hours. There are minor amounts of ferrihydrite dust associated with this type of crystal in some of the batches. The soccer balls are much larger than any of the other types of crystals, although some small balls are found.

The most prevalent crystal type is the rod shaped crystal, which can give the appearance of a hexagon. Each rod is extended in length and the edges meet in a triangular array. The crystals have the appearance of bars of gold, only purple in color. The surface is generally of a mosaic consistency, but is rarely dusted with the rust powder. This shape is most often found in the microcrystals.

The third major crystal type is a flat plate. These are two dimensional crystals that have a hexagonal shape, but are wafer thin. They tend to stick to rod or soccer ball crystals and are produced in much smaller yield in mixed crystal systems. On two occasions these flat plates were the majority species of crystal produced in the

batch. There are also some plate type crystals that are square, with angles very close to 90°.

In most of the crystal sets, needle crystals are produced. When crystals were grown by vapor diffusion of ether into the methanol solution, the needles were predominant. In several cases, the needles were clustered into the shape of microscopic Christmas trees with branches extended in every direction. The needle crystals would often have a shiny surface and appear pitch black rather than purple.

The crystals of each type have been produced in isolation and in mixed sets. The first crop is collected by reducing the volume of methanol (rotoevaporation at 0°C) and then filtering. This tends to produce shiny crystals that congregate with each other. Distinctive angles can be seen, but the crystals are far too small for x-ray study. The saturated filtrate is placed into a freezer and better defined crystals are collected in 24-72 hours. As the time is extended, larger crystals are produced, but there also tends to be more ferrihydrite. In some cases fissuring occurs at the edges of the crystals. The fissures are small cracks that extend into the crystal faces a short way. This may be due to loss of solvent, but further fissuring was not observed upon allowing crystals to stand out in the air. One of the soccer ball crystals, which had developed a fissure, was observed to explode spontaneously. The majority of the samples do not develop fissures.

The recrystallization process will always reduce the yield of the material. A good portion of the solid will not come out of the saturated methanol solution unless forced out by the addition of a

second solvent. In these cases the material collected is not crystalline. There does not appear to be a method of predicting which type of crystal (soccerballs, blocks, rods, plates or needles) will be produced. Rods and needles tend to dominate first crop crystals, whereas blocks, plates and soccerballs require more time to develop and form after the first crop has been removed. There are only minor differences between materials produced in Fe(II) vs. Fe(III) preparations, or between air vs. pure oxygen preparations.

Crystal Structure. The crystal structure of the +3/+2/+3 trinuclear iron cluster is shown in the ORTEP diagram (Fig. 7). The complex can be viewed as two identical fac-S tris(2-aminoethane-thiolato)iron(III) ligands, connected to a central iron(II) ion by triple bridges through the coordinated thiolate sulfur atoms. The cation has an inversion center that relates its two hemispheres, such that all the bond lengths and angles are duplicated in each half molecule. The three thiolate bridges on each subunit are similar, but not identical in this respect.

The net +2 charge on the complex is determined by the presence of two chloride anions in the unit cell. There is not enough residual negative charge density for presence of a third chloride ion at any other location, even with the consideration of partial site occupancy.

The central iron ion is coordinated between the two fac-S_3 ligands in a slightly distorted octahedral geometry. The bond angles for S-Fe_c-S are within 3° of 90° (87.2°, 88.5°, 91.5°, 92.8°), while each opposite sulfur pair is fixed at 180° by symmetry.

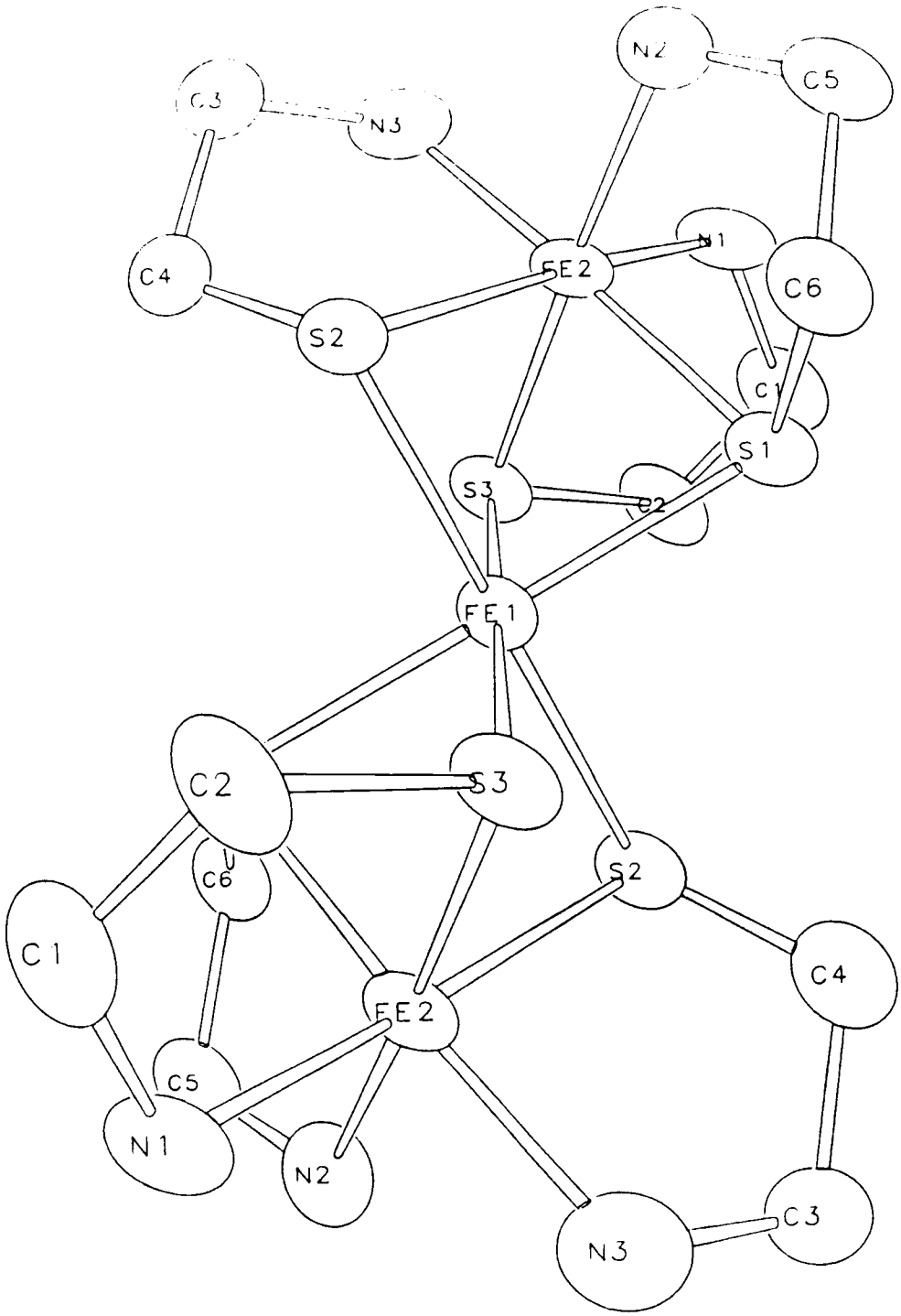

Figure 7. ORTEP Diagram of $Fe[Fe(SCH_2CH_2NH_2)_3]_2Cl_2$ with 50 % Probability Thermal Ellipsoids. Structure is refined to R= 0.098

For the terminal iron atoms, the N-Fe-N angles are all obtuse, while the S-Fe_t-S angles are acute. As expected with a bidentate chelate, the octahedron of the terminal iron is more distorted than that of the central iron. The geometry of the Fe-S-Fe angles is a function of the iron-iron separation. The Fe···Fe distance of 2.686 Å is 0.171 Å shorter than that of the similar trinuclear three cobalt(III) cluster.[40] A comparison of selected bond lengths and angles is given in Tables 2 and 3, respectively. There may be a stabilizing interaction between iron atoms as in $[FeS(SCH_2)_2(C_6H_4)]_2^{2-}$, a tetrahedral iron-sulfur cluster studied by Holm, et al.[49]

The plane formed by the three bridging thiolate atoms is 2.251 Å from the terminal iron and 2.284 Å from the central iron. The location of the fac-S_3 plane 0.033 Å closer to the terminal iron compares very closely with the 0.037 Å difference in the Co system. This suggests that perhaps the complex contains three, low-spin ferric irons and that a smaller counterion such as OH^- is present. The repulsion of the three extra electrons in the cobalt system cause a longer cobalt-cobalt bond, causing the M-S-M bond angles in the complex to be less acute than those of the analogous iron complex.

The intraligand bond lengths are comparable between the two complexes. The R factor (0.098) is larger than that of well-resolved crystallographic structures. This large R is a consequence of some disorder within the crystal. Nevertheless, most of the distances and

Table 2 : Selected Bond Lengths for $[Fe(Fe(CySte)_3)_2]Cl_2$ and $[Co(Co(CySte)_3)_2]_2SO_4Cl_4$.[40] Units in Å

$[Fe(Fe(CySte)_3)_2]Cl_2$		$[Co(Co(CySte)_3)_2]_2SO_4Cl_4$	
Fe_t-S	2.241(5)	Co_t-S	2.238(7)
	2.250(6)		
	2.261(5)		
Fe_c-S	2.282(4)	Co_c-S	2.262(11)
	2.285(4)		
	2.285(5)		
Fe...Fe	2.686(3)	Co...Co	2.857(1)
Fe-N	1.99(1)	Co-N	1.996(8)
	2.02(2)		
	2.04(2)		
S-C	1.81(2)	S-C	1.821(7)
	1.79(3)		
	1.84(2)		
N-C	1.47(2)	N-C	1.489(14)
	1.46(3)		
	1.50(3)		
C-C	1.46(3)	C-C	1.526(12)
	1.53(3)		
	1.49(3)		

Table 3: Selected Bond Angles for $[Fe(Fe(CySte)_3)_2]Cl_2$ and $[Co(Co(CySte)_3)_2]_2SO_4Cl_4$.[40]

$[Fe(Fe(CySte)_3)_2]Cl_2$		$[Co(Co(CySte)_3)_2]_2SO_4Cl_4$	
Fe_t-S-Fe_c	72.6°(2)	Co_t-S-Co_c	78.8°(4)
	72.5°(1)		
	72.8°(2)		
S-Fe_c-S	87.2°(2)	S-Co_c-S	83.5°(9)
	92.8°(2)		
	88.5°(2)		
	91.5°(2)		
S-Fe_t-S	90.5°(2)	S-Co_t-S	84.5°(8)
	88.9°(2)		
	88.6°(2)		
N-Fe_t-N	95.4°(6)	N-Co_t-N	94.6°(6)
	93.2°(7)		
	92.2°(7)		
N-Fe_t-S	86.3°(5)	N-Co_t-S	88.3°(2)
same ligand	86.4°(5)		
	84.7°(4)		
N-Fe_t-S	90.9°(5)	N-Co_t-S	88.3°(2)
cis	91.1°(4)		
	92.1°(5)		
N-Fe_t-S	173.5°(5)	N-Co_t-S	180.00°
trans	176.9°(5)		
	174.7°(5)		

angles in the tri-iron cluster are chemically reasonable with the exception of the C_3-C_4 bond length, which is a bit too short.

NMR. In d_4-methanol, a very broad single band was spread over the region 40-260 ppm, which was not present in a background scan of the probe without sample. This extreme broadening and large chemical shift is likely to be due to the interaction of the cysteamine protons with the paramagnetic iron centers.

IR. The FTIR spectrum of the complex contains a characteristic pattern which helps to demonstrate the formation of the trinuclear cluster. (Figure 8) The fingerprint region from 1800-600cm^{-1} is consistently reproduced in various sets of crude material and crystals. The peaks appear at the same locations, but have differing degrees of splitting and some variation of intensity. Even though the crude material gives the same IR as the best crystals, this material will not go completely into methanol without the production of some iron rust. The spectral region between 1800 cm^{-1} and 400 cm^{-1} is displayed for both the crude solid and x-ray quality crystals in Figure 9.

The assignments of individual peaks follow those for similar compounds listed by Nakamoto.[50] The 1590 cm^{-1} band is an asymmetric stretch from the coordinated NH_2 ligands. The three sets of major bands between 1200-1500 all arise from ligand modes. Each peak is only slightly shifted from its location in the spectrum of $HSCH_2CH_2NH_3Cl$. The NH_2 rock modes at 919 and 843 cm^{-1} are lowered in intensity by metal coordination. The 1635 cm^{-1} shoulder is likely due to a bending mode of water, which is contained in the

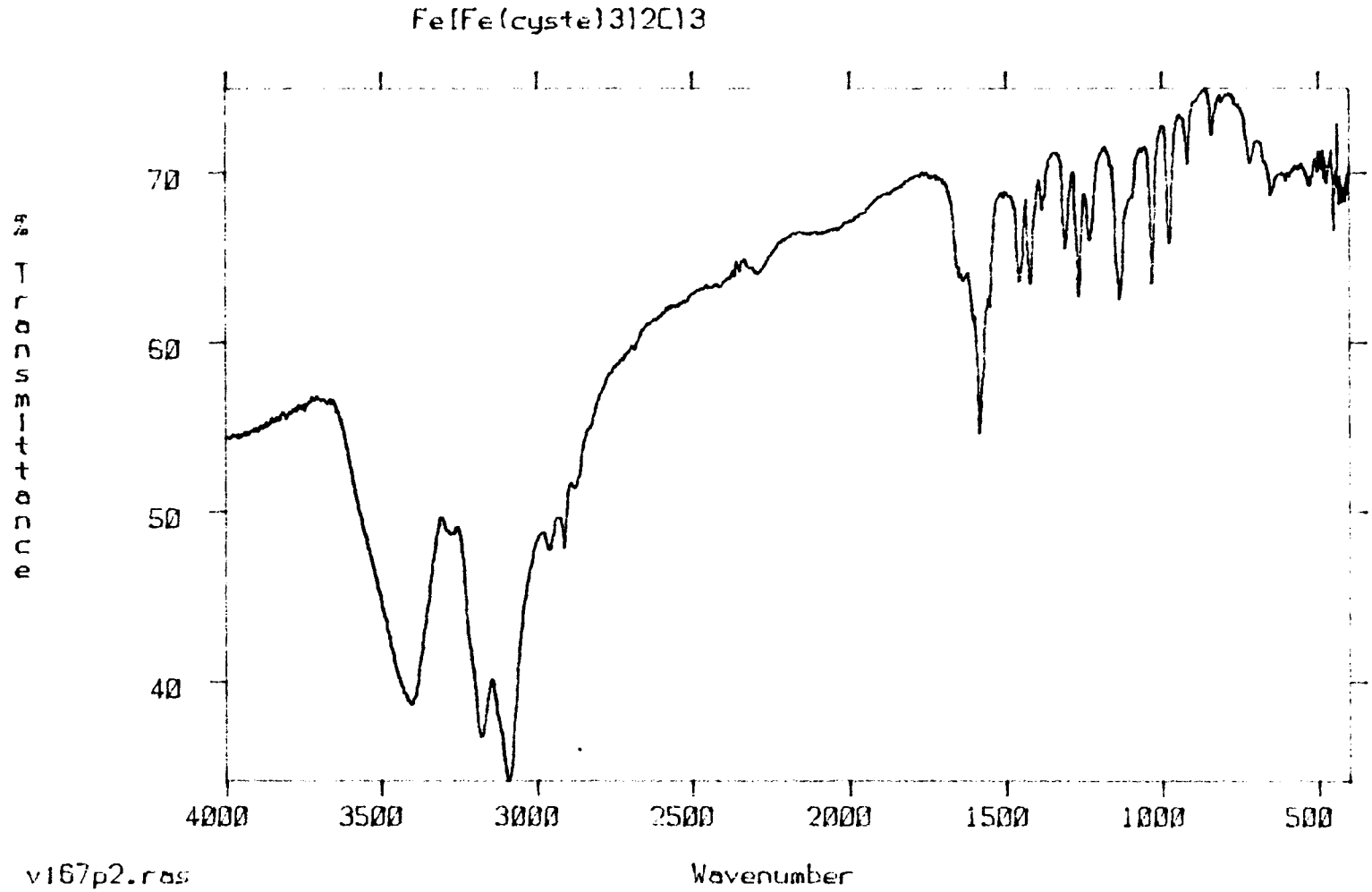

Figure 8. FTIR Spectrum of $Fe[Fe(SCH_2CH_2NH_2)_3]_2Cl_3$ Crystals.

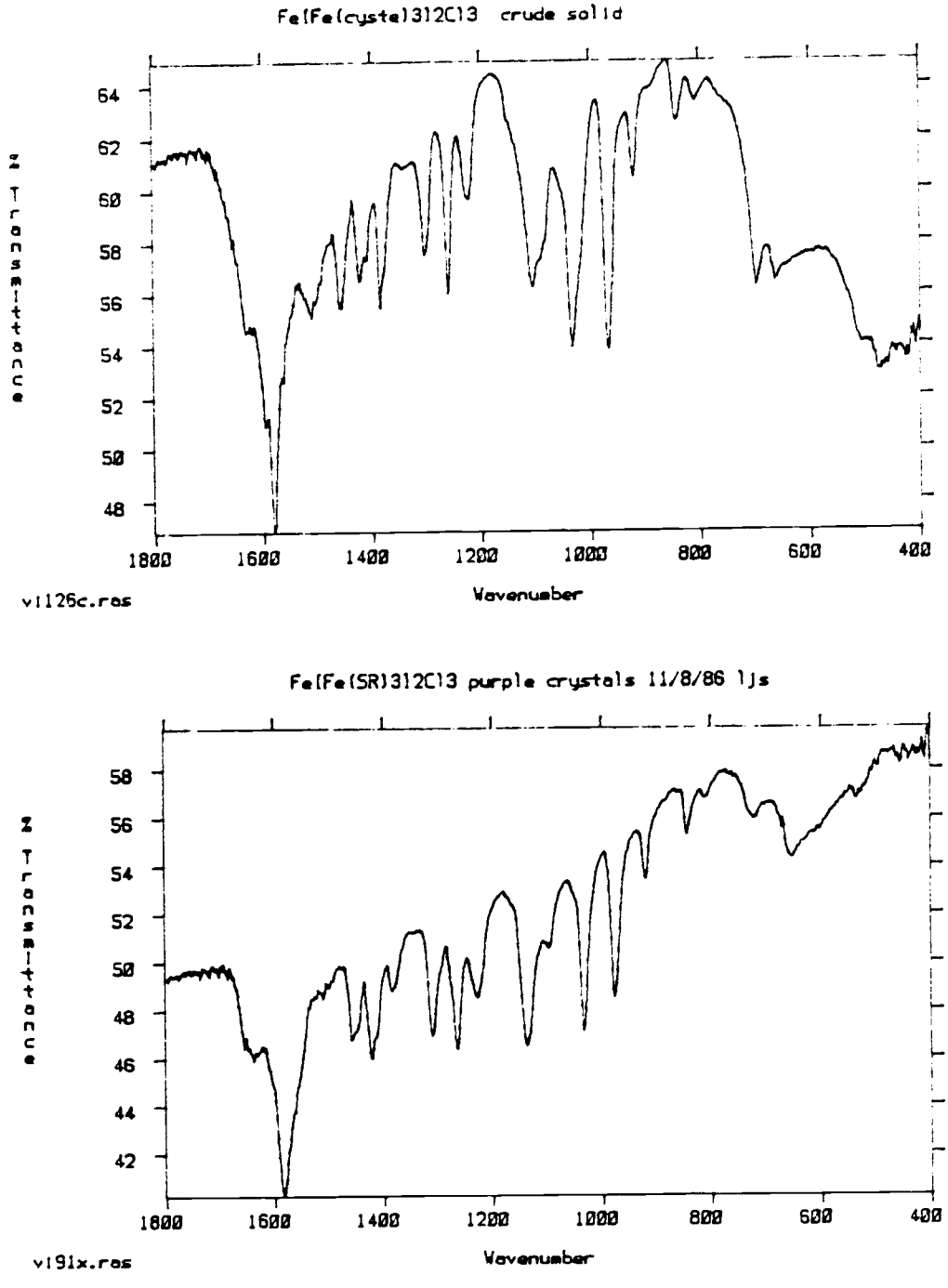

Figure 9. FTIR Spectra of the Fingerprint Region (1800–400 cm^{-1}) for $Fe[Fe(SCH_2CH_2NH_2)_3]_2Cl_3$. Comparison of the Crude Solid vs. Microcrystals.

crystal lattice.

In the far IR region, peaks at 3400 cm^{-1}, 3150-3100 cm^{-1}, and 2950 cm^{-1} correspond to O-H, N-H and C-H stretching modes respectively. The intensity of the O-H band tends to vary between samples, but it is clear from the IR that -OH is present, consistent with the analytical data for the complex.

$Fe[Fe(SCH_2CH_2NH_2)_3]_2Cl_3 \cdot 3H_2O \cdot CH_3OH$ 3400, 3150, 3100, 2950, 1635, 1583, 1457, 1420, 1384, 1310, 1265, 1230, 1134, 1032, 977, 919, 843, 720, 652 cm^{-1}.

The infrared spectrum has been used to verify the presence of the purple complex, and also to detect impurities present to a significant extent in the sample. The two major impurities other than ferrihydrite that might be present are $HNEt_3Cl$ and cystamine. The $HNEt_3Cl$ byproduct is completely removed by the methanol wash. The IR spectrum of this material has several intense spikes at 1476, 1434, 1398, 1171, and 1036 cm^{-1} which would be readily observed in a mixture containing even a small amount of $HNEt_3Cl$. Cystamine, the disulfide formed by oxidation of the product, has a pair of sharp peaks at 1478 and 1462 cm^{-1}, which are readily apparent when overoxidation of the species has taken place.

The IR spectrum of the orange-brown ferrihydrite produced during the recrystallization does not contain the cysteamine features (Figure 10). The three sets of ligand peaks between 1200-1500 cm^{-1} were absent. The C-H and N-H stretching modes around 3000 cm^{-1} were also absent. However, the strong O-H stretch at 3400 cm^{-1} indicates that this iron residue is partially hydrated iron(III)oxide.

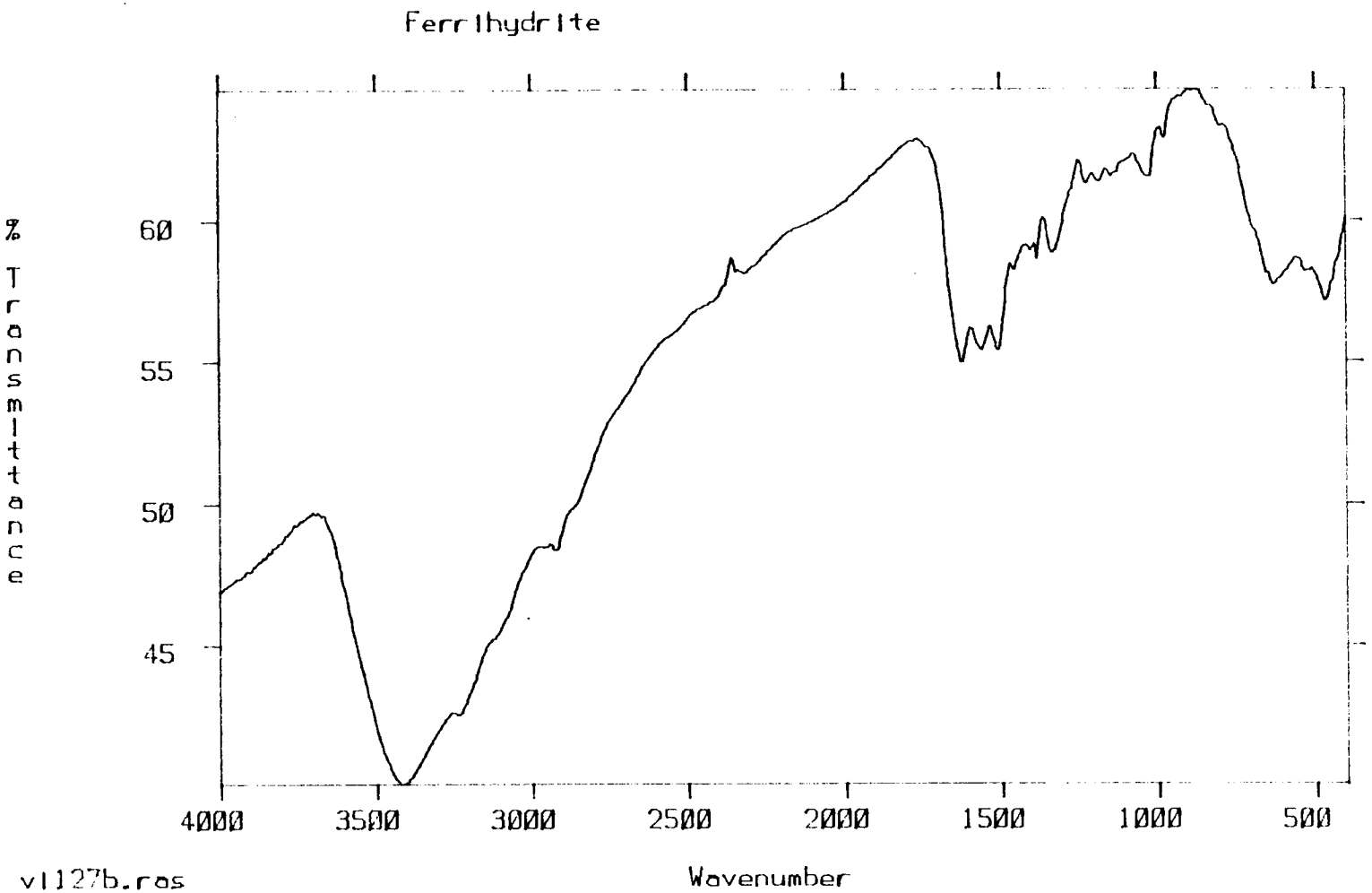

Figure 10. FTIR Spectrum of Brown Ferrihydrite, Produced from Reaction of $Fe[Fe(SCH_2CH_2NH_2)_3]_2Cl_3$ with O_2 in MeOH During Recrystallization.

An effort was made to investigate the brown, ferrous-iron precursor complex and the O_2 oxidation that transforms it into the purple trinuclear compound. The brown solid is so susceptible toward oxidation, that its surface turned purple in a glove box whose N_2 atmosphere had been freshly regenerated. An IR pellet of the brown material was pressed in the glove box from a freshly cut filter cake, and exposed to air in the KBr lattice. The air oxidation to the ferric state was followed in a series of spectral data collections. Distinct increases in spectral intensity at 500 and 620 cm^{-1} were observed. These correspond to ν(M-N) and $\rho_r(NH_2)$ modes. There are also intensity gains at 1020, 1130, and 1600 cm^{-1}. These spectral changes imply that the air oxidation of the brown precursor is accompanied by the formation of a new iron-nitrogen bond. A second pellet was pressed from the same material after the solid was air exposed. The spectrum was similar to that of the crude purple compound.

Mössbauer- Mössbauer spectra were collected on the purple product prepared by both the $FeCl_2$ and $FeCl_3$ methods. The spectrum for each sample consists of three quadrupole doublets (Figures 11,12; Table 4). The outer two doublets originate from the purple complex, while the central doublet arises from the iron oxide impurity. The intensity ratio of the two outer doublets is 1.7:1. The quadrupole splittings and isomer shifts are consistent with a compound having three low spin ferric iron atoms.

The Mössbauer results are consistent with the cation environment determined by x-ray crystallography, where the central iron has six

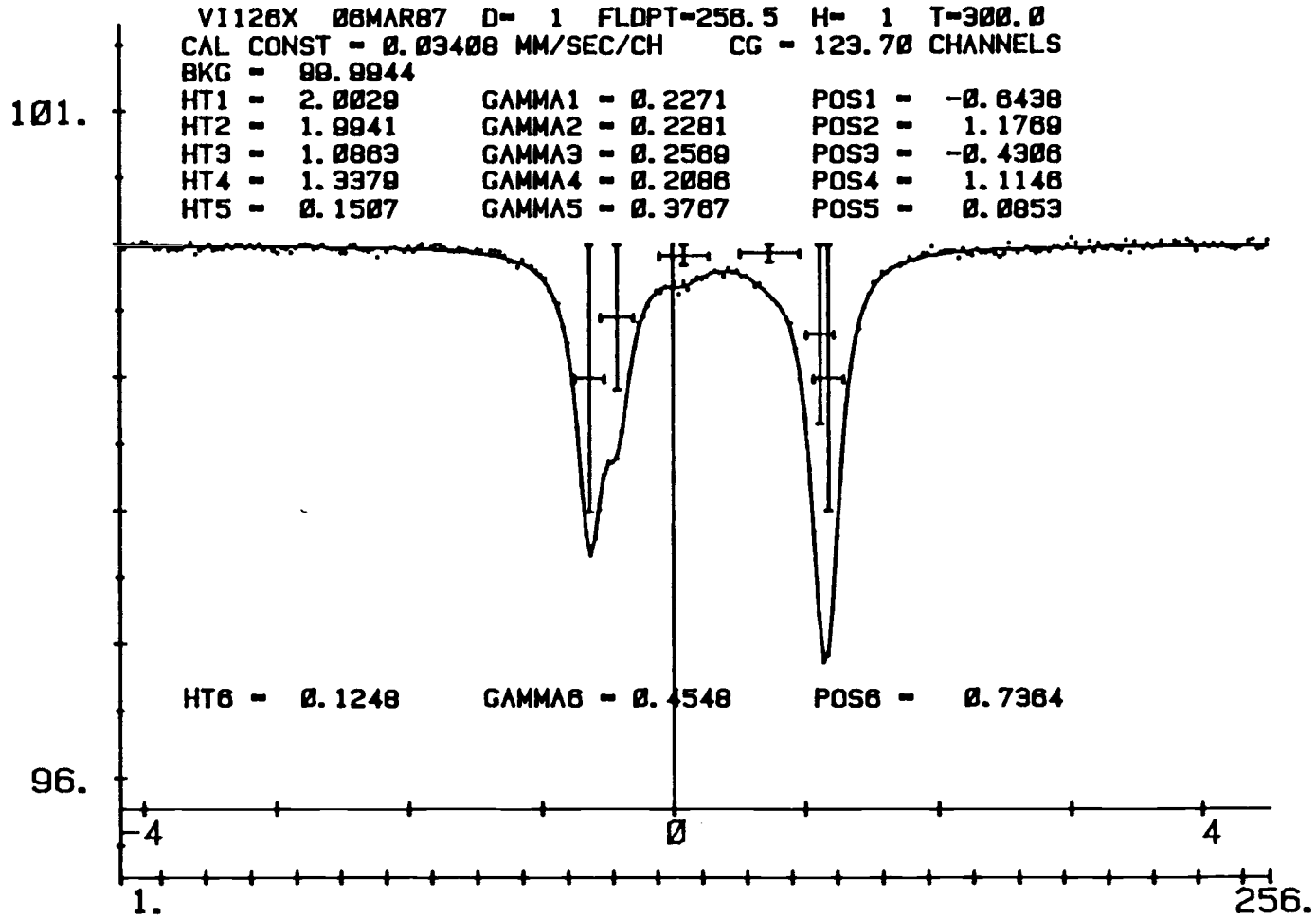

Figure 11. Mössbauer Spectrum of $Fe[Fe(SCH_2CH_2NH_2)_3]_2Cl_3$

Produced from Fe(II) Synthesis.

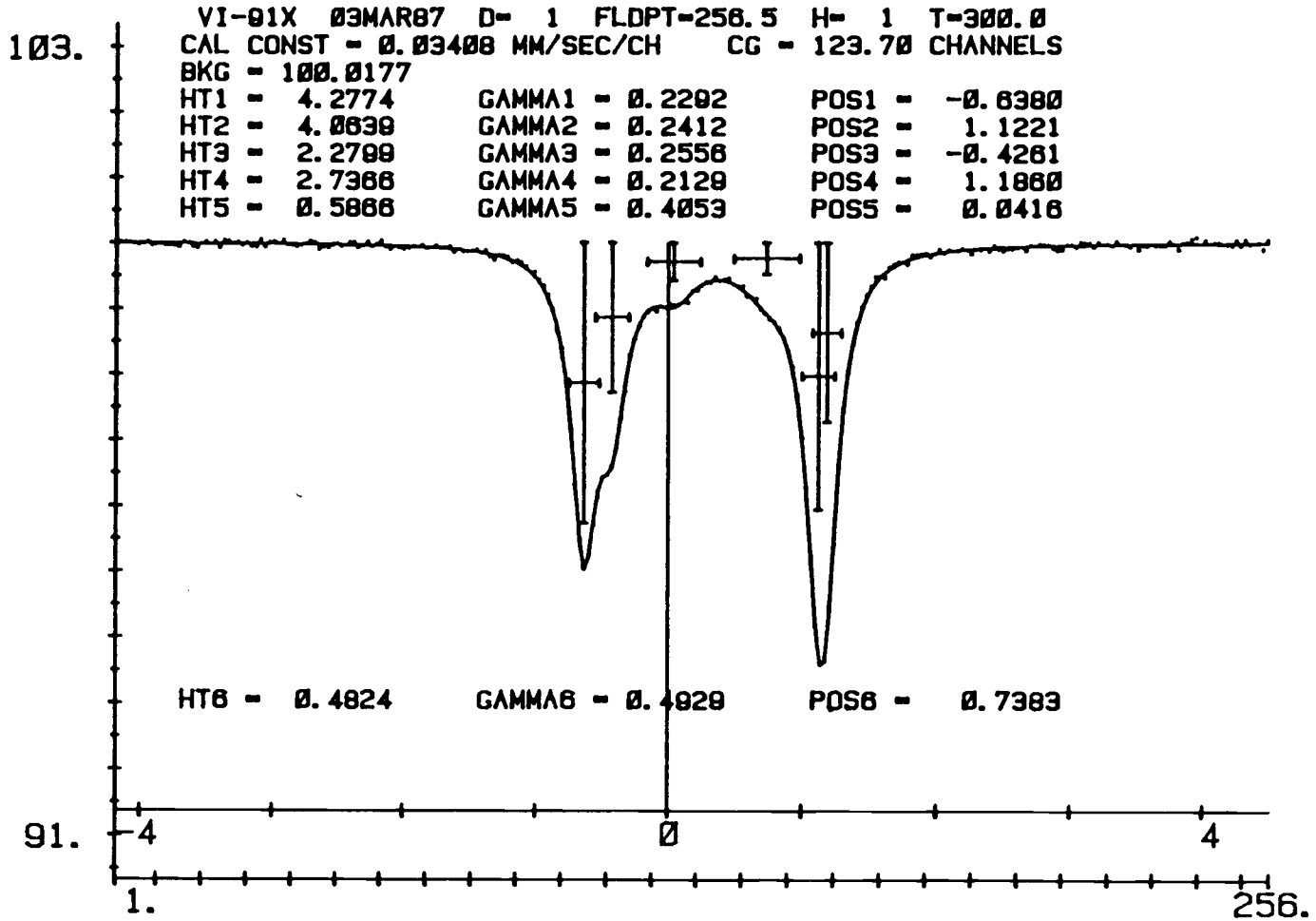

Figure 12. Mössbauer Spectrum of $Fe[Fe(SCH_2CH_2NH_2)_3]_2Cl_3$

Produced from Fe(III) Synthesis.

Table 4: Mössbauer Results for Tri-iron Cluster[a] and for Brown Rust (Ferrihydrite).

	Peak locations mm/sec		ΔE_Q Quad split mm/sec	δ Isomer shift mm/sec	Heights net	Heights rel
Cluster microcrystals[b]						
A	-0.638	+1.122	1.76	+0.24	8.34	1.66
B	-0.426	+1.186	1.61	+0.38	5.02	1.00
C	+0.042	+0.738	0.70	+0.35	1.07	0.21
Cluster microcrystals[c]						
A	-0.655	+1.106	1.76	+0.23	6.11	1.67
B	-0.422	+1.031	1.45	+0.30	3.65	1.00
C	-0.009	+0.739	0.75	+0.37	2.71	0.74
Cluster block crystals[b]						
A	-0.644	+1.177	1.82	+0.27	4.00	1.65
B	-0.431	+1.115	1.55	+0.34	2.42	1.00
C	+0.085	+0.736	0.65	+0.41	0.28	0.11
Brown Rust (Ferrihydrite)[b]						
A	-0.404	+1.084	1.49	+0.34	3.25	0.21
C	+0.023	+0.753	0.73	+0.37	15.53	1.00

[a] A, B, and C refer to the quadrupole doublets; outer, middle and inner respectively. [b] Prep'd from $FeCl_2$. [c] Prep'd from $FeCl_3$.

Table 5: Literature Mössbauer Results

Murad[51]			
Ferrihydrite	0.89	+0.34	H.S. Fe(III)
	0.54	+0.35	H.S. Fe(III)
Lane[26]			
$[Fe(S_2\text{-}o\text{-}xyl)]^-$	0.57	+0.57	H.S. Fe(III)
$[Fe(S_2\text{-}o\text{-}xyl)]^{2-}$	0.61	+3.20	H.S. Fe(II)
$[Fe(SPh)_4]^{2-}$	0.64	+3.24	H.S. Fe(II)
Lippard[22,23]			
$(FeL)_2$	0.71	+3.48	H.S. Fe(II)
$(FeL')_2$	0.76	+3.23	H.S. Fe(II)
$Fe(cys)_2 \cdot 2H_2O$	0.88	+3.02	H.S. Fe(II)
Tao[52]			
$[Fe(Pypep)_2]Cl \cdot 2H_2O$	1.28	+0.10	L.S. Fe(III)
Eley[53]			
$Fe(dtc)_3$ (N,N-Diisopropyl) $\mu_{eff}=2.62$	0.63	+0.46	L.S. Fe(III)

thiolate bridges and each terminal iron, identical by symmetry, has three thiolates and three amine donor atoms. The slightly different quadrupole splittings are indicative of two similar, distinct iron (III) environments. The intensity ratio indicates that two irons are in identical environments.

The Fe(II) and Fe(III) based samples differ slightly in the inner doublet region. For the Fe(III) based sample, there is much more intensity in the inner doublet. The positions of the other peaks, and the relative intensity between the first doublet pairs are similar within the two different samples. Both the isomer shift and quadrupole splitting of these inner doublets match the spectrum of the iron oxide material.

This iron oxide material was isolated from the recrystallization of the purple compound and was examined separately by the Mössbauer technique. (Figure 13) The spectrum appears to be the same as that measured by Murad and Schwertmann for ferrihydrite, a naturally occurring iron oxide with the composition $Fe_2O_3 \cdot 2FeOOH \cdot 2.6H_2O$ with an FeO_6 iron environment.[51] The quadrupole splitting of 0.73 mm/sec is close to the average of the two isomer shifts found for ferrihydrite. It is on this basis that the orange-brown residue has been referred to by this name.

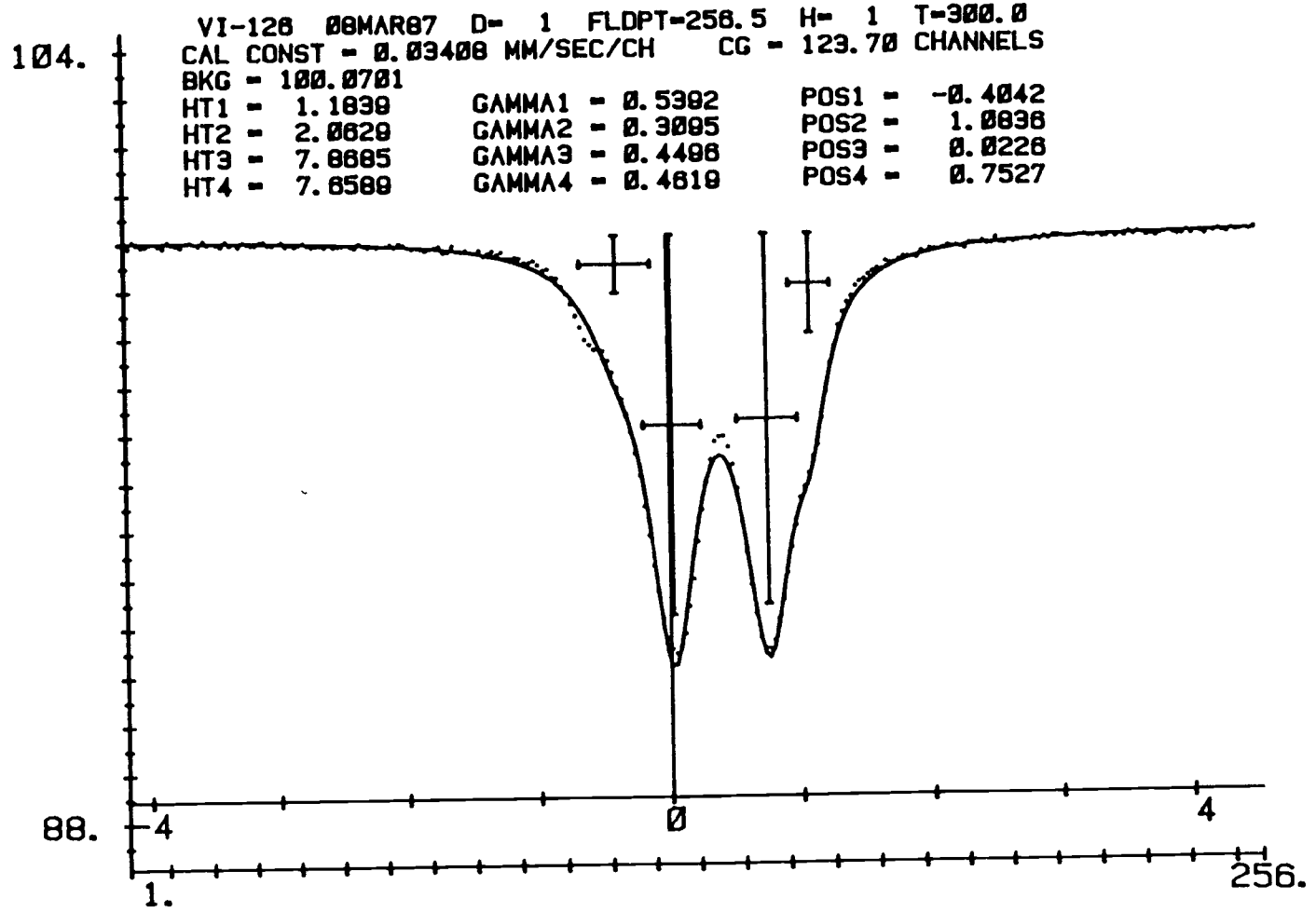

Figure 13. Mössbauer Spectrum for Ferrihydrite, Produced from Reaction of $Fe[Fe(SCH_2CH_2NH_2)_3]_2Cl_3$ with O_2 in MeOH during Recrystallization

Magnetic Measurement. The Gouy method was used to determine the magnetic susceptibility of the complex. The corrected magnetic susceptibility is calculated by measuring the gram susceptibility of the sample, multiplying by the molecular weight and then correcting for diamagnetism by the use of Pascals constants.[45] The μ_{eff} can then be calculated based on the temperature, using the formula $\mu_{eff}=2.828((\chi_{corr})(T))^{1/2}$. For a crystalline sample of the purple complex, the moment is found to be 2.61 Bohr Magnetons.

The spin-only magnetic moment of the tri-iron cluster can be calculated for several combinations of individual spins using the formula $\mu_{eff}=g[S(S+1)]^{1/2}$ B.M. where g=2.0 for an electron with no angular momentum. Values for S, $[S(S+1)]^{1/2}$, and μ_{eff} are given in Table 6 below.

For $Fe[Fe(SCH_2CH_2NH_2)_3]_2Cl_3 \cdot 3H_2O$ (MW=784.79), the Mossbauer spectrum clearly indicates two unique Fe(III) strong field environments. This gives two possibilities for the magnetic interactions between the single unpaired electron of each of the three iron ions. For the tri-iron complex, there can be either three unpaired electrons (spin = 3/2) or one (spin = 1/2). In the former case, the magnetic spins would all be parallel to each other, whereas in the latter case one of the spins, presumably the central-iron spin, would be aligned opposite to the other two irons. This gives

Table 6: Selected Values for S, $[S(S+1)]^{1/2}$, and μ_{eff}

S	$[S(S+1)]^{1/2}$	μ_{eff}
1/2	0.87	1.73
1	1.41	2.82
3/2	1.93	3.87

S=1/2, μ_{eff}=1.73 B.M., while the uncoupled spins give S=3/2, μ_{eff}=3.87 B.M.. However, the spin-only calculation assumes that orbital angular momentum is quenched, which may not be the true. For low-spin Fe(III), typical observed values for μ_{eff} are about 2.4 B.M.[45]. This is sufficiently close to the experimentally measured value of 2.61, to indicate that the spins are up-down-up.

It may be possible to alter the magnetic coupling by changing the temperature.[54] The S=3/2 state might be close enough to the ground state to be populated at accessible temperatures. A magnetic flip of one iron spin could then lead to a restructuring of the total magnetic state of the cluster. The linear array of iron ions is different from that of most other iron cluster compounds and might possess an interesting spin temperature dependence.

Chemical Reactivity of $Fe[Fe(SCH_2CH_2NH_2)_3]_2Cl_3$ (1) Reaction with Penicillamine - 1.0×10^{-4} M stock solutions of the title complex and penicillamine were prepared in MeOH, which allowed the absorption spectra to be followed over the entire course of the reaction. Absorbances of several mixtures of different initial ratios of thiolate:complex were monitored to the point where the spectrum was no longer changing.

There was a significant effect on the visible spectrum induced by the addition of penicillamine (Figure 14). Both the 490 and 580 nm peaks grew in intensity immediately upon the addition of PenSH to the complex solution, the 580 peak increasing by a greater amount as the PenSH concentration was increased. The 490 nm peak shifts to lower energy. A plot of absorbance (490nm) vs. thiol/iron ratio showed

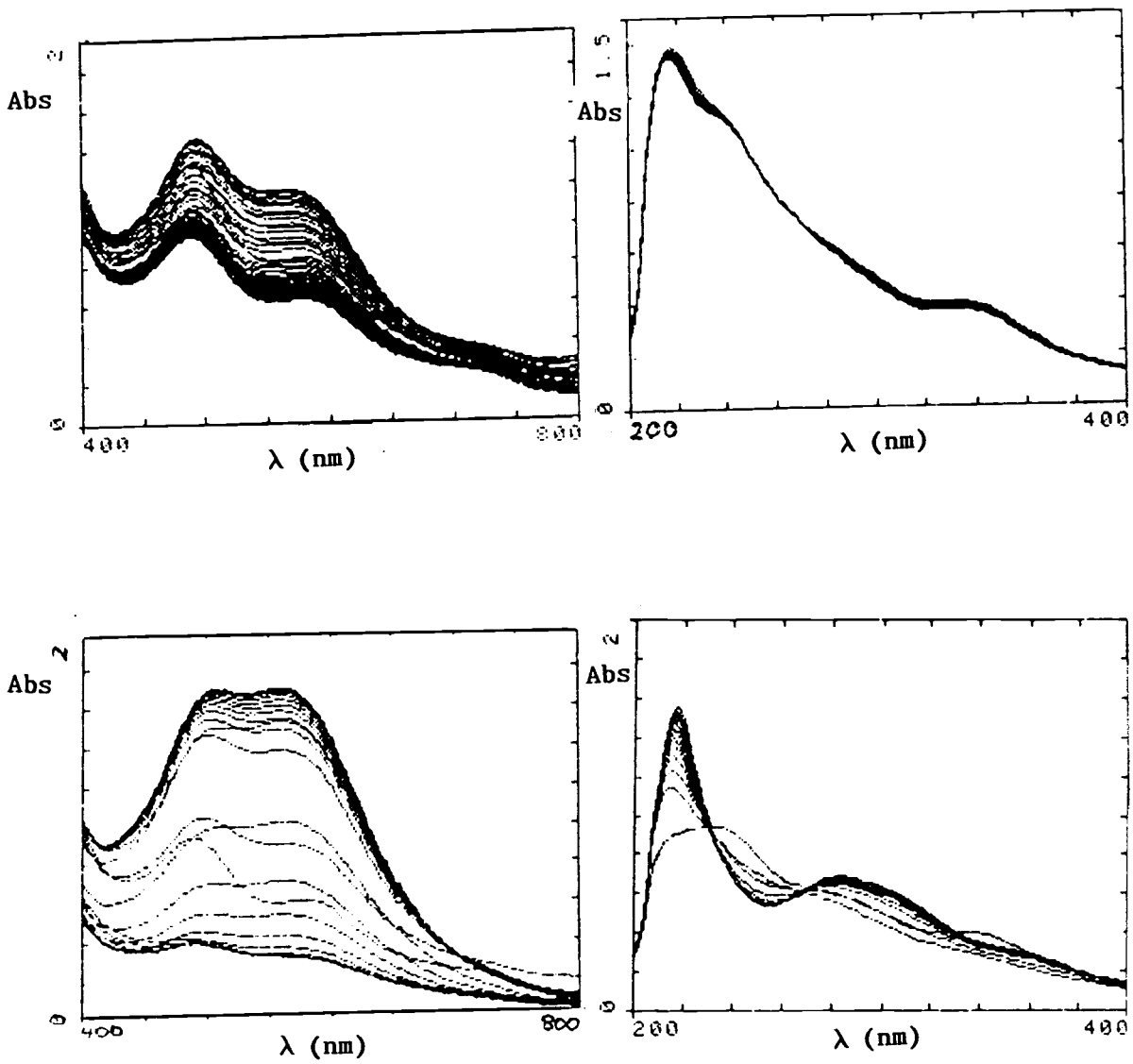

Figure 14. Visible and UV Spectral Changes of Dilute MeOH Solutions of $Fe[Fe(SCH_2CH_2NH_2)_3]_2Cl_3$ upon Addition of Thiols: A) Penicillamine B) Cysteamine.

that the intensity gain was linear up to 2.3 PenSH/Fe, then leveled off with only slight increases in absorbance upon further addition.

Once the intensity reached a maximum (2-3 minutes), the new chromophore began to decompose rapidly. The resulting spectrum corresponded to that of the initial spectrum of the iron complex, but at lower concentration than the original stock solution. When the solution was monitored further, the visible absorbance (400-800 nm) increased again, suggesting a regeneration of the initial compound after oxidation of the additional thiolate had taken place. The final absorbance value remained less than the initial value. The plots of both the final absorbance and the minimum absorbance vs. the PenSH/Fe ratio were linear.

(2) Reaction with Cysteamine - A similar experiment was conducted with cysteamine as the thiol. When cysteamine was added to the iron complex solution in small increments, there was no increase in the visible absorption values. The 490 nm peak gradually decreased, culminating in a final spectrum that matched the initial spectrum but at lower intensity.

There was also an initial increase in intensity of the 218 nm band in the UV, followed by a steady decrease in absorbance of this band and the growth of a new peak at 244 nm. This spectral change can be associated with the oxidation of the thiolate to disulfide. There were also some slight changes in intensity in the 300-400 nm region. The effects of this oxidation on the visible spectra leveled off after a short period of time, as long as there was not a large excess

of cysteamine added. After 20 min, the reaction was complete, the absorption spectrum was consistent with that of the iron complex, but at a lower concentration.

(3) Reaction with MCPBA - The organic oxidizing agent m-chloroperoxybenzoic acid was added to a solution of the purple complex to see if oxidation of the coordinated thiolate would occur. There were no new features in the spectrum. Thus, there is no evidence for oxidation of sulfur to a sulfenate or any other S=O bonded species. Absorbance decreased throughout the course of the reaction, similar to the effect of the addition of water to the methanolic solution of complex. The oxidation was attempted in dilute solution only, with up to six-fold excess of MCPBA over iron complex.

(4) Reaction with H_2O_2 - At low concentration, the results were similar to those of MCPBA, but a hundred-fold excess of peroxide led to rapid bleaching of all purple color. The resulting orange solution had two significant features, a huge UV peak at 244 nm and a broad shoulder in the 350 nm region. An isosbestic point occurs at 360 nm.

The failure to observe oxidation chemistry of the thiolate ligands is not surprising in view of their bridging nature. There is no mechanism available for the oxidation to a S=O bonded species to take place. A four-coordinate sulfur atom would have to exist in a highly hindered environment. If the bridge bonds are broken, then the oxidation to disulfide is expected.

Cyclic Voltammetry. A 4.92×10^{-4} M solution of $Fe[Fe(SCH_2CH_2NH_2)_2]Cl_3$ was prepared in 0.10 M methanolic $(CH_3)_4NCl$. A series of cyclic voltammograms was run on 25 mL of N_2 purged solution using a Pt working electrode vs. SCE at 25°. The solutions were not stirred and the first wave was reductive. The scan range was initially +0.9 to -0.6 V, later scaled down to +0.7 to -0.5 V.

A typical CV curve for the complex is given in Figure 15a. There is a reductive wave at -0.31 V and an oxidative wave at -0.24 V. The reductive wave is slightly larger (0.36 μA vs. 0.31 μA) at 50 mV/s. On successive scans, the reductive wave decreased slightly, whereas the oxidative wave either increased or did not change. (Figure 15b) This implies an essentially reversible reaction, with a small amount of irreversibility. This may be due to diffusion of the species away from the proximity of the electrode. For a fresh solution, current was measured as a function of scan rate. The results confirm that the reaction is diffusion limited (Table 7). After five minutes of this essentially reversible scanning, the spectra began to undergo drastic shape changes.

During the next 5 minutes, the reductive wave was totally lost, indicating decomposition of the tri-iron cluster. (Figure 16c) At the same time, the oxidative wave was shifted to a less negative potential. A brown precipitate was found in the spent solution, and the concentration of the purple species was halved, based on the 490 nm absorption peak. A solution of the initial stock solution was also monitored as a reference and found to undergo only a 0.15% loss of

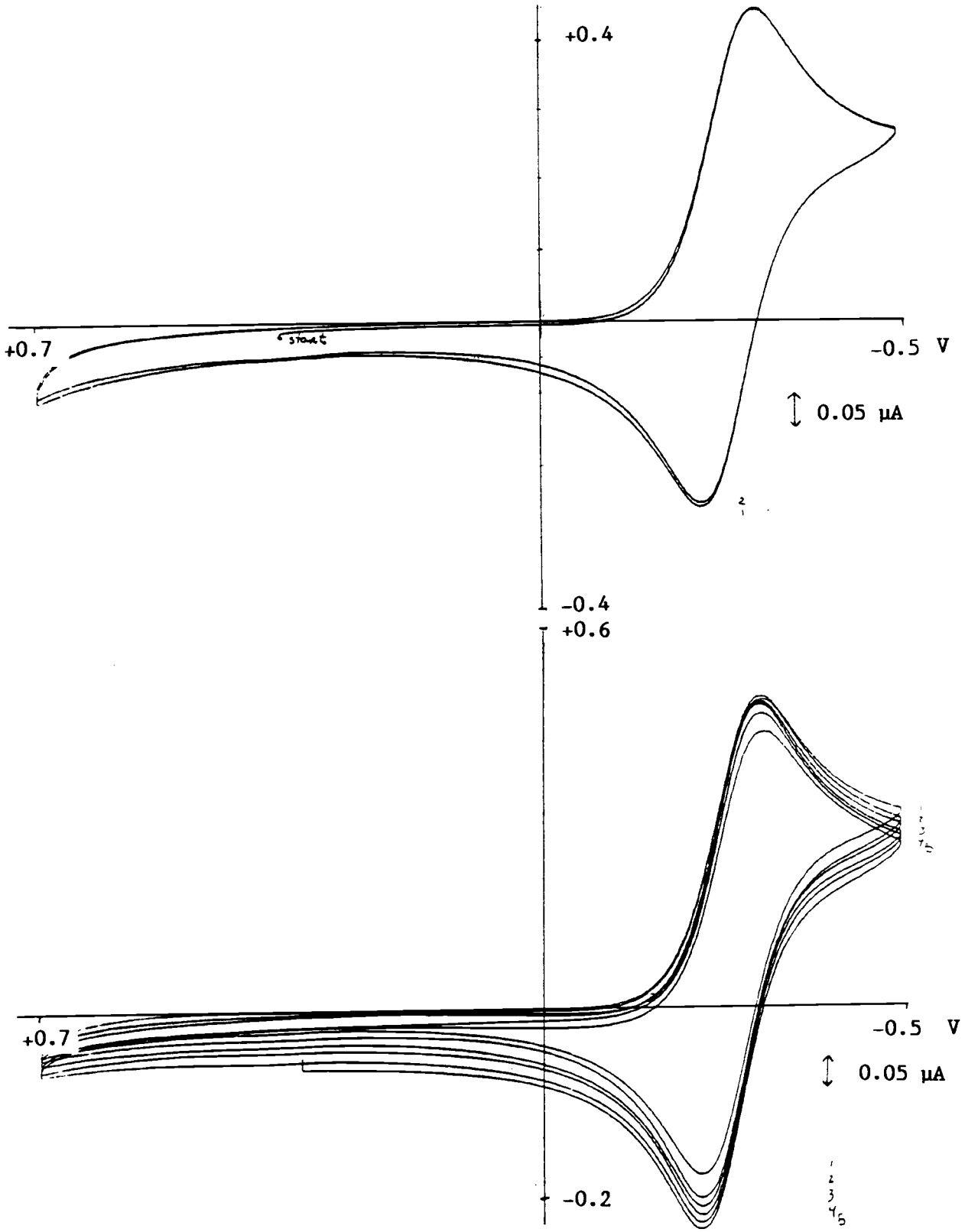

Figure 15. Cyclic Voltammogram for $Fe[Fe(SCH_2CH_2NH_2)_3]_2Cl_3$ with a) a Single Reduction/Oxidation Sweep, b) Five Consecutive Sweeps.

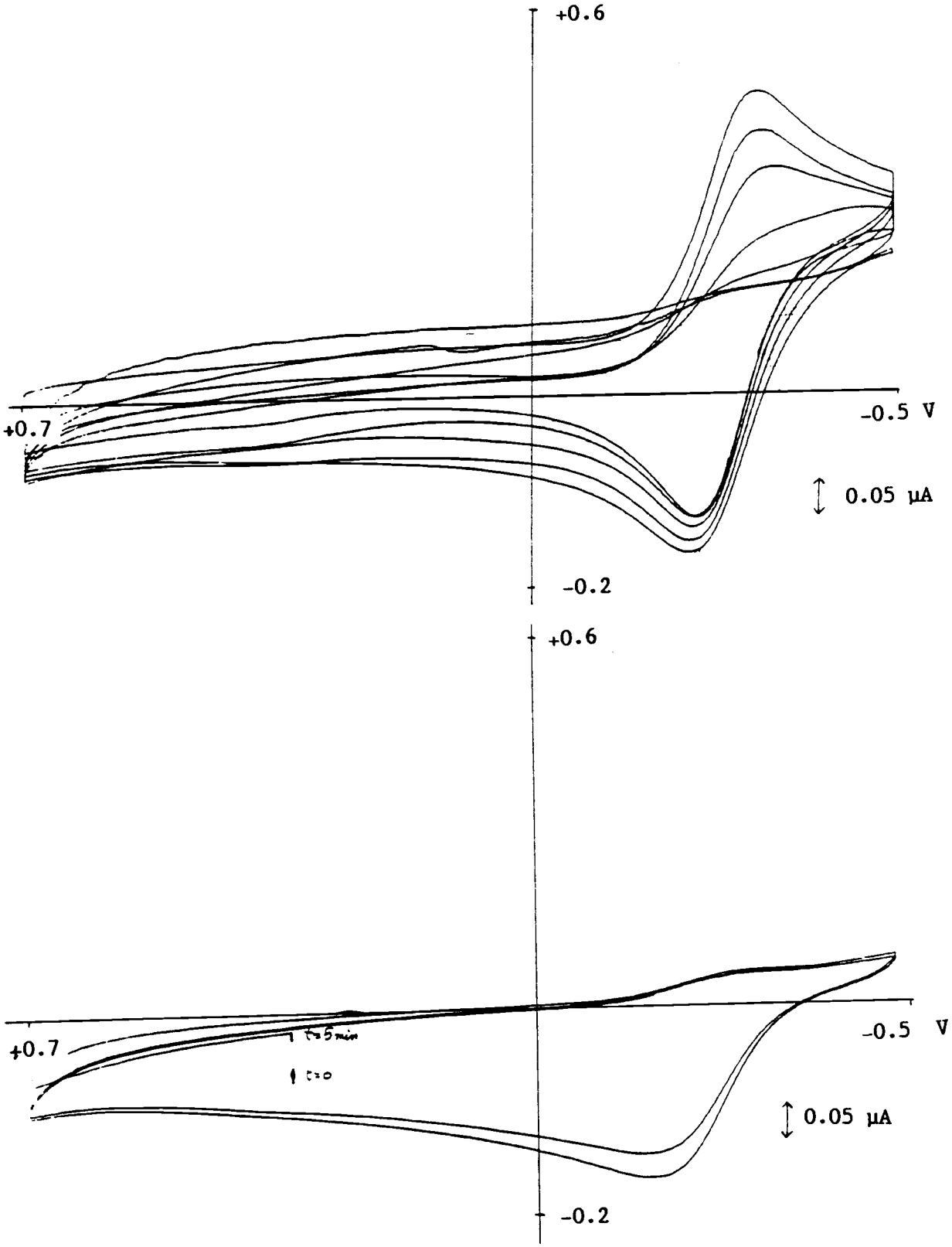

Figure 16. Cyclic Voltammogram for $Fe[Fe(SCH_2CH_2NH_2)_3]_2Cl_3$ with c) Ten Consecutive Sweeps and d) Final Sweep After 15 min.

chromophore in the same time span.

The CV was repeated on a 2nd 25 mL portion of the initial solution. After the N_2 sweep, a series of spectra with different scan rates was recorded. The reduction wave at -0.29 V and the oxidation wave at -0.22 V showed the same relative intensity throughout. After 6 successful scans (estimated time; 10 min), rapid decomposition of the chromophore occurred. The final spectrum recorded 5 minutes later is shown in Figure 16d.

Table 7: Electrochemical Potentials for Cyclic Voltammetry of $Fe[Fe(SCH_2CH_2NH_2)_2]Cl_3$ as a Function of Scan Rate.

	Reduction		Oxidation		
Rate	Potential	Current	Potential	Current	Irrev.loss[a]
mV/s	mV	µA	mV	µA	%
20	-300	0.29	-225	0.27	7.0%
50	-295	0.44	-220	0.34	22.7%
100	-295	0.63	-220	0.51	19.0%
200	-295	0.85	-220	0.72	15.3%
500	-300	1.40	-215	1.10	21.4%

a) irreversible loss is the percent decrease in current between the reduction and oxidation scans.

Table 8: Electrochemical Potentials for Successive Cyclic Voltammetric Scans for $Fe[Fe(SCH_2CH_2NH_2)_2]Cl_3$ at 50 mV/s

	Reduction		Oxidation	
Scan	mV	µA	mV	µA
i	-295	0.440	-225	0.340
1	-295	0.435	-220	0.365
2	-300	0.430	-225	0.380
3	-290	0.425	-225	0.385
4	-290	0.425	-225	0.390
5	-300	0.415	-225	0.390
6	-305	0.390	-225	0.380
.	.	.	.	.
7	-310	0.330	-225	0.280
8	-310	0.330	-225	0.275
9	-315	0.275	-220	0.225
10	-450	0.050	-215	0.240
11	----	0.050	-210	0.230
.	.	.	.	.
f	-255[a]	0.030	-150	0.180

a) the final scan was taken 5 minutes after the completion of the previous scans. The current measured is very small and the potential well is centered at -255mV.

Conclusion

We have isolated and characterized an air-stable trinuclear, iron-thiolate complex in an attempt to produce a model for non-heme, iron-thiolate dioxygenases. The compound contains three low-spin octahedral ferric iron ions in a linear array, bridged by thiolate sulfurs. The ferric ions are magnetically coupled. The central iron is in a six-thiolate environment, while each terminal iron has an identical three-sulfur, three-amine ligand environment.

The unique air stability of the compound probably is due to the spatial arrangement of atoms about the sulfurs. The rigidity of the cluster and the steric crowding around the bridged thiolates prohibit the sulfur atom from bonding with an adjacent thiolate sulfur to form a disulfide.

The compound consists of a tripositive, tri-iron cluster and three chloride counterions. The compound is not retained on either an anion or a cation exchange column when eluted with methanol, indicating strong ion-pairing between the Cl^- ions and the cluster in this solvent.

As in the Holm-type iron-sulfur clusters, $[Fe_2S_2(SR)_4]^{2-}$ and $[Fe_4S_4(SR)_4]^{2-}$,[2] there are two distinct oxidation states available for this linear cluster. $Fe[Fe(SCH_2CH_2NH_2)_3]_2Cl_3$ undergoes reversible one-electron reduction. Cyclic voltammetry was used to measure the potential difference between the two different oxidation states. A one-electron reversible couple was found at -310, -240 mV through the first few

scans. As the scans were repeated, a gradual change in the voltammogram occurred. The decrease in the current generated during the reduction wave relative to that of the oxidation wave is due to diffusion of the reduced species away from the surface of the electrode. As the concentration of the reduced species increases, an autocatalytic decomposition appeared to take place. The 490 nm absorption peak had decreased considerably relative to that of an aliquot of the original solution.

The diffraction study provides useful structural results and information about the general nature of the crystals of the tri-iron species. A few crystals diffracted weakly; most did not show any diffraction spots. The crystal selected by MSC yielded usable data. It is unclear as to whether this crystal was unique, or had the same lattice as the many other crystals which failed to diffract. The crystal structure was shown to have a III-II-III array of irons, from the presence of only two chloride counterions per cluster. The R factor of 9.8% is rather large because of disorder in the crystal. However, the angles and distances are reasonable and the presence of a dipositive, tri-iron cluster is well established.

A reasonable amount of 'pure' compound was collected by filtration after reducing the volume of solvent by rotoevaporation. The elemental analysis of the resulting microcrystals gave ratios of 1:1 for Fe/Cl, 1:1 for N/S, and 1:2 for Fe/N. This leads to the conclusion that only ferric iron is present in the bulk microcrystalline material. Both the magnetic data and the Mossbauer results support this conclusion.

Therefore, the crystal on which the diffraction results are based cannot be representative of the bulk material. Although the III-II-III form seems much less stable in solution, at least one crystal of it has been observed (in the MSC study). A resolution of this situation must await the acquisition of a new departmental diffractometer which will be used to make a survey of the variety of crystal types possible.

A mechanism for the facile interconversion of the two forms of the cluster can be proposed. The initial reversible reaction is likely the one-electron reduction of the central iron of the cluster.

$$Fe[Fe(SCH_2CH_2NH_2)_3]_2^{3+} + e^- \longrightarrow Fe[Fe(SCH_2CH_2NH_2)_3]_2^{2+} \qquad (13)$$

The reduced trinuclear cluster is not nearly as stable in solution as the oxidized form. Under conditions of limited O_2 access and cold temperatures, at least one single crystal of the reduced form has been isolated. However, in air it will either be oxidized back to the triferric form, or be dissociated into a ferrous ion and two tris(2-aminoethanethiolato)iron(III) molecules. As these species build up in the solution, more oxidation-reduction chemistry can occur. The thiolate of the tris ligand is no longer protected from oxidation by bridging; reaction with O_2 can take place, as can internal oxidation-reduction. Both routes lead to disulfide and Fe(II). The ferrous ion may also promote further redox decomposition of the cation cluster.

$$Fe[Fe(SCH_2CH_2NH_2)_3]_2^{2+} \longrightarrow 2\ Fe(SCH_2CH_2NH_2)_3 + Fe^{2+} \qquad (14)$$

$$Fe^{2+} + Fe[Fe(SCH_2CH_2NH_2)_3]_2^{3+} \longrightarrow Fe^{3+} + 2\ Fe(SCH_2CH_2NH_2)_3 + Fe^{2+} \qquad (15)$$

This mechanism is supported by the cyclic voltammetry data. As the reduction occurs, a gradual irreversible oxidation is observed. This would correspond to loss of the reduced form of the cluster. When the dissociated species build up to significant concentrations, the decomposition proceeds at an accelerated pace. The reduction wave disappears, and the oxidation wave shifts to a higher positive potential. This latter observation provides evidence for the oxidation of the non-bridging thiolates to disulfide.

$$2\ Fe(SCH_2CH_2NH_2)_3 \longrightarrow NH_2CH_2CH_2S\text{-}SCH_2CH_2NH_2 + 2\ Fe^{2+} + 4\ NH_2CH_2CH_2S^- \qquad (16)$$

This oxidation does not takes place to an appreciable extent in the solid state, because there is no medium for diffusion of the tris ligand away from the ferrous ion. The lattice is fixed and the only oxidation that can take place returns the molecule to the original trivalent cluster.

The compound appears to be the first air-stable aliphatic iron-thiolate reported in the literature. The major difference between this tri-iron cluster and the iron-sulfur species previously reported in the literature is that irons are in octahedral sites, rather than tetrahedral or trigonal-bipyramidal configurations. Its closest non-iron analogue in the literature is $Co(Co(SCH_2CH_2NH_2)_3)_2^{3+}$ [40] The closest tri-iron analogue reported appears to be Walters' hexakis(μ-benzenethiolato)triiron(II) hexacarbonyl cluster.[34]

The solubility behavior of the compound is unusual. The cluster is insoluble in most of the common organic solvents. Only the highly

polar solvents water and methanol will dissolve the compound, but they also mediate the redox decomposition to disulfide and iron oxide. It is fortunate that the species remains intact in methanol long enough to be recovered in a pure crystalline form.

The behavior upon the addition of penicillamine is fascinating. The initial increase in the intensity of the 490 nm peak indicates coordination of some of the added thiol. After a gradual building of a new species, the autoxidation to disulfide occurs rapidly. After this reaction is spent, the original chromophore begins to reestablish itself. This suggests that there is a strong thermodynamic stability associated with the formation of the cluster.

The model suggests a possible mechanism for the chemistry occurring at the active site of the thiolate dioxygenase enzymes. The thiolate bridge between two metal centers demonstrates how an enzyme might protect the cysteinyl thiolates of its protein shell while binding and catalyzing the oxidation of the thiolate substrate. Both of the thiolate dioxygenases require a ferrous iron cofactor for enzymatic activity. It seems possible that this ion coordinates to two or three cysteinyl sulfurs to form a bridge with the iron intrinsic to the enzyme. The substrate interacts with the extrinsic iron in a non-bridged manner, making it available for oxidation to the sulfinate. The entire iron thiolate network mediates the charge distribution during the oxidation, preventing the reaction from producing the disulfide.

The tri-iron cluster does not display the ability to mimic the oxidation to give sulfur-oxygen bonds. However, the demonstration of

the existence of an air-stable iron-thiolate compound should lead to the development of other air-stable systems which more closely mimic the thiolate dioxygenase active site functions. The burden of conducting complete characterizations under inert conditions is lifted, so that both chemical and physical properties of such models can be readily explored.

Part II: Characterization of the Products of the H_2O_2 Oxidation of Potassium Bis(N,S,O-penicillaminato)cobaltate(III).

Historical (3) Oxidations of Cobalt-Thiolate Complexes. Bonding to a metal center modifies the chemical reactivity of thiolate sulfur. In order to study the oxidation reactions of thiolate sulfur bound to metal centers, a series of complexes with the CoN_5S chromophore have been characterized in several laboratories.[55-67] Several of these complexes are pictured in Figure 17. Each complex has two ethylenediamine ligands bound to a central cobalt(III). A bidentate N,S ligand (which contains a thiolate functional group) occupies the remaining two sites of the cobalt octahedron. This ligand is the site of further oxidation; the final products are dependent upon the nature of the oxidant. The ethylenediamine ligands are inert, so that spectroscopic changes are due to the chemical nature of the oxidized sulfur atom.

Coordination of thiolate to cobalt(III), or any metal center, causes an decrease in nucleophilicity of the sulfur atom.[55] However, the thiolate retains significant reactivity and oxidation can take place to produce several different coordinated sulfur-bonded species: sulfenates[55-59], sulfinates[60], thioethers[61-64], disulfides[65], and sulfenamides[66,67], dependent upon the oxidant. Table 9 lists the spectral properties of several compounds of this type. The rate of nucleophilic addition is sensitive to the nature of the sulfur atom; a 2-coordinate sulfur reacts much faster than a 3-coordinate atom.[68] A portion of this rate enhancement can be

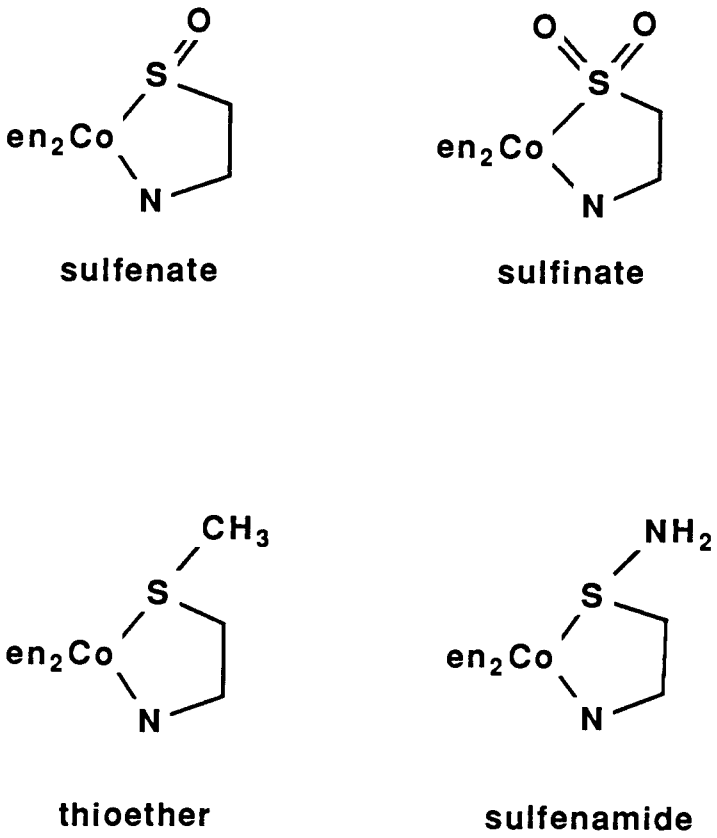

Figure 17. Several Different Complexes Available by Electrophilic Addition to the $(en)_2Co(SCH_2CH_2NH_2)^{2+}$ Ion. Analogous Compounds Exist for the Cysteinato Complex.

Table 9: Visible-UV Spectrophotometric Parameters of some Relevant Cobalt Complexes

Complex	$\lambda_{max}(\varepsilon)$ nm($M^{-1}cm^{-1}$)		
$[(en)_2Co(SCH_2CH_2NH_2)]^{2+}$ [a]	482(142)	370sh(315)	283(13,800)
$[(en)_2Co(S(O)CH_2CH_2NH_2)]^{2+}$ [a]	470(500)	365 (6700)	285 (3,100)
$[(en)_2Co(S(O)_2CH_2CH_2NH_2)]^{2+}$ [a]	432(220)		288(14,200)
$[(en)_2Co(S(SCH_3)CH_2CH_2NH_2)]^{3+}$ [b]	489(149)	343 (1840)	278 (7,550)
$[(en)_2Co(S(NH_2)CH_2CH_2NH_2)]^{2+}$ [c]	474(212)		296 (6,400)
$[(en)_2Co(SCH_2CH(COOH)NH_2)]^{2+}$ [d]	483(126)		283(11,700)
$[(en)_2Co(S(O)CH_2CH(COOH)NH_2)]^{2+}$ [d]	480(600)	371 (5800)	287 (3,750)
$[(en)_2Co(S(O)_2CH_2CH(COOH)NH_2)]^{2+}$ [d]	430(190)		287(11,900)
$[(en)_2Co(SCH_2COO)]^{+}$ [a]	518(152)	360sh(340)	282(11,700)
$[(en)_2Co(SC(CH_3)_2COO]^{+}$ [a]	514(153)	360sh(340)	282(10,900)
cis,cis,cis-N,S,O-$[Co(SC(CH_3)_2CH(COOH)NH_2)(SC(CH_3)_2CH(COOH)NH_2)]^{-}$ [e,h]	474(162)	410 (708)	296(17,800)
trans-N-$[Co(SC(CH_3)_2CH(COOH)NH_2)_2]^{-}$ [f]	489(336)		292(16,600)
trans-O-$[Co(SC(CH_3)_2CH(COOH)NH_2)_2]^{-}$ [g]	454(240)	353 (1900)	286(12,900)
trans-N-$[Co(S(O)C(CH_3)_2CH(COOH)NH_2)_2(SC(CH_3)_2CH(COOH)NH_2)_2]^{-}$ [f]		365 (6100)	280(9,000)
trans-N-$[Co(S(O)C(CH_3)_2CH(COOH)NH_2)_2]^{-}$ [f]		383 (9500)	295(5,400)

[a]Ref 57. [b]Ref 65. [c]Ref 66. [d]Ref 55. [e]Ref 77. [f]Ref 58. [g]Ref 78. [h]All penicillamine complexes have the S configuration at carbon with the exception of this molecule which has one R and one S ligand.

attributed to steric effects, which hinder the approach of the electrophilic oxidant to a 3-coordinate sulfur atom. Both the net charge on the ligand and extent of back pi-bonding between metal and ligand orbitals may also play significant roles in the reaction rate.

A key distinguishing feature of this type of system is the UV-Vis spectrum. The strong absorption band at ≈280 nm is caused by a S-->Co ligand-to-metal charge transfer (LMCT). The location and intensity of this LMCT band are related to the oxidation state of sulfur. The presence of this band can be used as confirmation of the sulfur-cobalt bond. Upon oxidation, if the atom added to the sulfur has a lone pair of electrons, a second LMCT band will be observed.[64] The second charge transfer will 'borrow' intensity from the first, a phenomenon known as the lone pair perturbation effect. There are two other lower energy d-d transitions that arise in these types of complex, which vary in energy dependent upon the structure of the thiolate ligand.

Sloan and Krueger used the bis(ethylenediamine)cysteinato-cobalt(III) ion to demonstrate that the H_2O_2 oxidation of thiolate sulfur to sulfenate takes place via an S_N2 mechanism.[55] Both Λ and Δ forms of the complex exist, and since cysteine contains a chiral carbon, the complex occurs as a mixture of diastereomers. Cation exchange chromatography was used to separate these and also the different oxidation products. The product S-bonded sulfenates could be further oxidized to S-bonded sulfinates by the addition of more H_2O_2. The change of oxidation state was correlated to the wavelength of the LMCT band.

The IR spectra of the three complexes are nearly identical. The major difference is in the 900-1300 cm^{-1} region, where the sulfenate exhibits a strong asymmetric S=O stretch at 953 cm^{-1} while the sulfinate exhibits the asymmetric S=O stretch at 1250 cm^{-1}. These peaks are absent from the thiolato complex. There is also a minor shift in the location of the uncoordinated carboxylate peak with oxidation. The isolation of a stable sulfenate complex is significant, since free sulfenic acids are theorized as metabolic intermediates, but are too reactive to be isolated.

Bonding of sulfenate sulfur to cobalt makes the sulfur chiral, creating the possibility of two diastereomers for both the Λ and Δ forms of the complex. These were separated on a cation exchange column. Both the S and R sulfenate isomers of the Λ complex were found in a 2.9:1 ratio.[69] The R sulfenate is converted to the S isomer in dilute solution by exposure to light, without any loss of intensity in the 371 nm absorption band.

Deutsch's group used the $(en)_2Co(SCH_2CH_2NH_2)^{2+}$ ion to demonstrate that bound thiolate sulfur will cause a kinetic trans effect (KTE).[60] The ligand opposite the sulfur is labilized toward substitution, increasing the rate of the reaction. Similarly, a ground state weakening, termed the structural trans effect (STE), was shown to exist in the crystal structure of the molecule. The amine trans to sulfur has a longer bond to cobalt than do any of the cis nitrogens. Both trans effects are caused by the formal negative charged sulfur atom being bound to the positive metal ion, enhancing the σ-donating properties of the ligand, resulting in the weakening

of the cobalt-nitrogen bond directly opposite to the bound sulfur which requires the same metal orbital for bonding. A bound sulfito complex $[(NH_3)_5Co(SO_3)]^+$ has also been studied for trans effects. The sulfur lone pair causes a shortening of the amine trans to the sulfur by increasing the S=O π-bond order.[70] The trans effects may be a function of the ligand field strength, since weaker field ligands, thioether and sulfenamide, both form complexes which do not show trans effects.[63,66]

The product of CH_3I methylation of $(en)_2Co(S(O)CH_2CH_2NH_2)^{2+}$ is an O-bonded sulfoxide.[71] Methyl addition occurs with retention of configuration at the sulfur. The mechanism involves the migration of the methyl group from the O-methyl ester to form a bound S-methyl sulfoxide which subsequently rearranges to the less hindered O-bound form. This causes an increase in ring size from 5 to 6 members. The analogous mercaptoacetate sulfenate gives the coordinated thioether as the major product under similar reaction conditions. The latter mechanism occurs because the mercaptoacetate complex has acidic hydrogen atoms on the alpha carbon which contribute to the formation of methanol at the coordinated sulfur during the initial CH_3I reaction. This allows the attack of a second CH_3I molecule on the freshly generated thiolate.

Kojima and Fujita prepared p and t isomers of N,S-bound $S(O)CH_2CH_2NH_2$ with the tris(2-aminoethyl)amine (tren) ligand, a symmetrical tetradentate N_4 chelate.[72] This allowed the sulfenate function to be the only source of optical activity in the molecule. By using column chromatography with a solution of a d-tartrate salt

as the eluent, one isomer of each complex was isolated. The complexes were assigned the S configuration by comparison of their circular dichroism spectra with those of the bis(ethylenediamine) complexes.

Adamson, et al., have explored the photochemistry of sulfenato and sulfinato cobalt(III) complexes and found that aquation and decomposition were the primary reactions.[73] The π-donor ability of the sulfur containing ligand affects the distribution of products; the more active π-donors cause aquation, while less effective π-donors cause decomposition. The sulfinato complex of cysteamine undergoes molecular rearrangement from the S-bonded to the O-bonded linkage isomer.[74] A loss of the 280 nm S-->Co LMCT band is accompanied by formation of a less intense O-->Co LMCT band at 326 nm. The mechanism involves a homolytic bond fission followed by rapid cage recoordination after rotation about the sulfur-carbon bond.

Our interests turned to the effect of oxidation upon a metal complex that has a cis-thiolate ligand geometry. Compounds of this type should provide insight concerning the mechanism of dioxygenase enzyme active sites which contain multiple cysteine residues. Herting studied a bis(cysteinato)cobalt(III) anionic complex, first reported by Neville and Gorin, which failed to oxidize when treated with H_2O_2.[1,75] He proposed a trinuclear structure, where all of the thiolate ligands are bridged between cobalt(III) ions.

Suades and coworkers reported the crystal structure for a 1:2 cobalt complex of 1,3-aminopropanethiol.[76] The structure has two tris-ligand cobalt units bridged to the central cobalt via all six thiolate sulfurs. This compound is also inert to chemical oxidation,

and is similar to the bis(cysteinato)cobalt complex proposed by Herting.

Helis, de Meester, and Hodgson structurally characterized the first mononuclear bisthiolato complex.[77] Following the oxidation of a basic mixture of D,L penicillamine (PenSH) and Co(II), a complex was isolated in which the two PenS ligands have opposite stereochemistries. Okamoto, et al., have reported several multithiolate complexes containing the biologically relevant thiolates, cysteine and penicillamine.[78] They prepared the trans-N and trans-O isomers of the bis(S-penicillaminato) cobaltate(III) ion and reported on the methylation reactions to form the corresponding thioethers.

The tris-cysteaminato cobalt(III) complex has been oxidized with H_2O_2 by Kita, Yamanari and Shimura.[37,79] The oxidation resulted in several mixed sulfenato and sulfinato complexes. Each successive oxidation adds two optically active isomers to the number of products, and thus requires an effective means of separation. Tartrate derivatives were prepared prior to separation by anion exchange chromatography. The change in charge distribution by the addition of a second chiral center allows the effective resolution of similarly structured compounds. Circular dichroism was then used to assign the different optical isomers by analogy to complexes of known structure.

Miller isolated a mononuclear bis-penicillaminato compound, $K[Co(S\text{-}PenS)]_2$, which reacted readily with hydrogen peroxide to give a color change.[1] The shift of the absorption band at 292 nm

demonstrated that the complex retained a S-Co bond during the oxidation of the sulfur atom. Proton NMR showed two methyl resonances, indicating C_2 symmetry for the bis-thiolato complex. The oxidation removed the degeneracy. Molecular models were used to identify three possible complex geometries, and a trans-N geometry was assigned for reasons that will be discussed later.

Tridentate coordination of the penicillamine ligands places the two nucleophilic thiolates cis to each other. Oxidation to monosulfenate introduces a steric restriction upon the opposite thiolate, which governs the stereochemistry of subsequent oxidations. The trans-N K[Co(S-PenS)$_2$] complex provides an opportunity to examine the oxidation of bis-thiolates in adjacent (cis) positions. This may provide insight towards defining the mechanism of oxidation at the dioxygenase enzyme active sites.

Circular Dichroism. Circular dichroism (CD) spectroscopy is a technique employed specifically for the study of chiral molecules. By differentiating between left-handed and right-handed circularly polarized light absorbed by a sample, a characteristic spectrum is produced for any asymmetric compound. When the two opposite waves are combined, an elliptically polarized light beam will result as long as the two components have different amplitudes. As with normal absorption techniques, the spectrum conforms to the Beers law relationship, $\delta A=\delta\varepsilon bc$. The difference $(\varepsilon_L-\varepsilon_R)$ is generally less than 0.3% of the total absorption.[80]

The wavelength region covered in CD spectroscopy is the same as that in UV-Vis and features in the CD spectrum arise from the same transitions. For transition metal complexes, the d-d metal orbital transitions occur at higher wavelength, while the charge transfer bands occur at higher energy. The magnitude, sign and contour of the curves generated depend on structure and, collectively, are known as the Cotton Effect.

There are three major factors that contribute to the Cotton Effect in the CD spectrum of coordination complexes. The configurational effect is caused by the arrangement of the chelate rings about the octahedral metal center. For a system containing three bidentate chelate ligands, this effect correlates to the direction of the overall ring pattern. The two configurations about the metal center are denoted as Δ and Λ. (Figure 18) Each has an opposite Cotton effect.

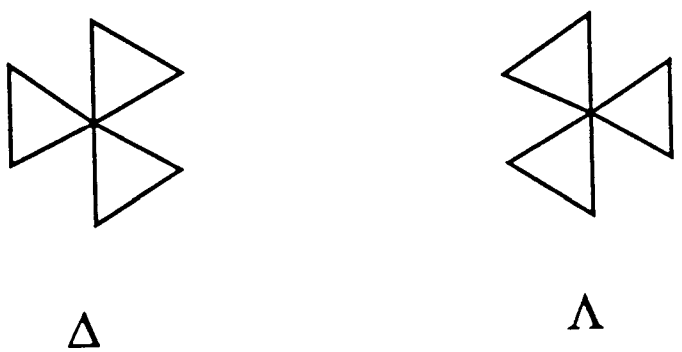

Figure 18. Definition of Optical Terminology : R vs S, Λ vs Δ and λ vs δ.

The second contribution to a CD spectrum is a conformational effect. The contribution arises from the puckering of the five member ring. A planar ring, or one that can be easily transformed between the two states, will not cause a conformational effect. This type of contribution will cause subtle shape changes in the configurational features that are already present and but will not cause a complete inversion of the CD spectrum. It will allow definition of λ vs δ skew.

The third contributing factor is the vicinal effect, which arises from the presence of a chiral atom in a ligand. Each chiral center will produce a contribution to the Cotton effect, since it has a unique arrangement with respect to the other atoms of the molecule. The asymmetric carbon of an amino acid is an example of an atom which contributes a vicinal effect. Enantiomeric molecules will have absorbtions from the same transition that are equal and opposite in magnitude and, thus, no Cotton effect will be observed for a 1:1 mixture of these.

The three factors operate independently of each other and the net effect is the sum of the individual contributions. Spectral assignments of R vs S, λ vs δ, and Λ vs Δ can be made by analogy to the assignments of molecules whose crystal structures have been solved. For $[CoN_5S]$ chromophores, McCaffery and Mason have done the yeoman work in establishing the data base for CD assignments.[81]

Experimental

Materials and Methods. UV-Visible spectra were collected on a Cary 16K Spectrophotometer equipped with matched 1-cm glass stoppered quartz cells. Each spectrum was referenced to a solvent blank, and the absorbance values were corrected by subtracting a baseline of solvent referenced to solvent.

Infrared spectra were taken on either a Perkin-Elmer 727 IR spectrophotometer, or a Mattson Sirius-100 Fourier Transform IR spectrophotometer, using KBr pellets or Nujol mulls.

^{1}H NMR spectra were recorded on a Varian HA-100 spectrometer or a Varian FT-80A Fourier Transform NMR. D_2O (99.8%) was from Stohler Isotope Chemicals. Spectra were recorded using tetramethylsilane as an external standard.

Circular dichroism spectra were run on a Jasco 41A spectropolarimeter in a Hellma round 1-cm Teflon-stoppered cell. The spectra were corrected for baseline drift by subtracting a spectrum of water The spectra were referenced to (+)-10-camphor sulfonic acid (CSA).

Anion, cation, and gel exclusion chromatography columns were prepared by using Bio-Rad AG1-X4, 200-400 mesh, chloride form; Bio-Rad AG50-X4, 200-400 mesh, hydrogen form and Bio-Rad Bio-gel P-2, 200-400 mesh (wet) respectively. The anion and cation columns were cleaned by washing with 3% H_2O_2, followed by 0.1 M NaOH and then finally by gradient elution with NaCl in freshly distilled water (0.1M to 1.0M) prior to the initial use. This left the anion column in chloride ion form and the cation in sodium ion form. KCl was used to wash the column when the potassium ion form was desired. The gel

exclusion column was flushed with deionized water, which was then tested for chloride ion eluent with dilute $AgNO_3$ solution until there was no white precipitate (AgCl) present. A Buchler peristaltic pump was used to feed the solvents into the columns using 1/16th inch plastic Tygon tubing.

Fractions were collected from the columns using a ISCO model 4500 fraction collector, at ten minute intervals. The fraction collector was wrapped in foil to protect the solutions from light. The lead and trail edges of each band were checked by UV-Vis to ensure that fractions containing only one species were combined prior to rotory evaporation to dryness. For the preparatory-scale dark experiments, the columns were also encased in foil, so that the sulfenates were protected during the entire collection and concentration process.

Water was distilled from alkaline permanganate prior to use.

The concentration of the H_2O_2 was determined by iodometry just prior to the use in the synthesis.[82] About 1.0 g KI was dissolved in 20 mL water in a 125 mL Erlenmeyer flask, 5.0 mL 2 M H_2SO_4 was added, and then 5.0 mL of the peroxide solution was pipetted into the flask. 3 drops of 3% $(NH_4)_2MoO_4$ soln were added. This red solution was then titrated with standardized 0.20 M $Na_2S_2O_3$ until the color was light yellow. Two drops of starch were added and the solution swirled, causing a deep blue color. The titration then continued until the blue color disappeared. The process was repeated in triplicate.

The thiosulfate solution was prepared by adding 6.4 g $Na_2S_2O_3$ and 0.1 g Na_2CO_3 to a liter of freshly boiled water. The

thiosulfate molarity was determined with KIO_3. A 0.1500 g KIO_3 sample was placed into a 250 mL volumetric flask and diluted to the mark with H_2O. 25 mL of this solution was pipetted into a 125 mL Erlenmeyer flask. 1.0 g KI and 3.0 mL 2 M H_2SO_4 were added and the solution titrated with the thiosulfate. All measurements were repeated in triplicate.

Cobalt was determined by a modified Kitson procedure.[83] In 100 mL beakers, 25 mg sample were dissolved in 13 mL 7% $HClO_4$ and 2 mg $Mn(ClO_4)_2$ was added. The solution was heated to 75° C and 0.6 g of finely crushed $KMnO_4$ added in three increments over 15 minutes. After 2 hours stirring, 10 mL H_2O was added, followed by small portions of oxalic acid, until the purple permanganate color had disappeared. The solution was quantitatively transfered to a 50 mL volumetric flask and diluted to the mark with water. In a second 50 mL volumetric flask, 25 mL reagent grade acetone was mixed with 5 mL 5 M HCl and allowed to cool. 10 mL Co solution and 5 mL 3 M KSCN solution were pipetted into the flask, causing the system to turn blue-green. The flask was then topped off to the mark with water, shaken, and the absorbance measured at 622 nm, referenced to a solution prepared by the same method using an H_2O blank mixed with the reagents.

Microanalyses were preformed by Galbraith Laboratories, Knoxville TN.

Syntheses: Preparation of Potassium trans-N-Bis(Penicillaminato-N,S,O)cobaltate(III). $K[Co(S\text{-}PenS)]_2$ was synthesized by the method of Miller[1]. Any impurity was removed by anion exchange using either

NaCl or KCl, depending on the cation desired. A small amount of a slow eluting green isomer, possibly the 1⁻ trans-O form described by Okamoto[78] was detected. The brown trans-N solid was recrystallized from a minimum amount of water by slowly adding isopropyl alcohol.

Preparation of Sodium (S-Penicillaminato-N,S,O) (S-Penicillaminesulfenato-N,S,O)-cobaltate(III). The synthesis of the monosulfenate K[Co(PenSO)(PenS)] was carried out on both a preparatory scale, and also a smaller scale. In the typical preparative reaction 250 mg (0.50 mmol) of $K[(CoPenS)_2]\cdot 2H_2O$ was mixed with 15 mL H_2O in a foil wrapped beaker and stirred until it had dissolved. Dilute H_2O_2 (0.1M) was added dropwise via a 5 mL syringe until a 1:1 mole ratio was achieved, plus a 3% excess to ensure complete reaction. In some cases Oxone® ($2KHSO_5\cdot KHSO_4\cdot K_2SO_4$) was used in place of the peroxide. The deep red mixture was stirred in the dark for one half hour and then loaded onto a foil wrapped BioRad AG1-X4 anion exchange column. The column was swept with water and then eluted with 0.05 M NaCl solution.

Four principal bands were found. The details of the separation are given in the discussion of column chromatography in the Results section. The second band "B" (brown; 368, 280 nm) contained the monosulfenate. The absorption spectrum was checked for each fraction and those having $A_{368}/A_{281} > 0.70$ were rejected. When the reaction was carried out with a larger amount of material, a grey-green material was found to adhere to the column top. When this occurred, the top of the column was removed using a Pasteur pipet.

The Oxone preparations also had a dark, non-mobile band at the top of the column which was presumed to be a small amount of compound trapped in a tightly bound 2- sulfate band.

Pure fractions of band "B" were combined and rotoevaporated to dryness at < 40°C. A minimal amount of water was used to dissolve the solid. The solution was then filtered and adsorbed onto the gel exclusion column. The brown band was eluted through the column with water, collected and reduced in volume. The eluent directly behind the band was tested for chloride presence by the addition of 0.1M $AgNO_3$. Two desaltings were necessary before the band was shown to be Cl^- free by the $AgNO_3$ test. The solution was then evaporated to dryness at low temperature. Miller produced the sodium salt of this compound in a similar manner.[1] Yield: 75 mg (38%)

The material proved to be very hygroscopic, picking up moisture from the air. Tiny elongated brown needle crystals formed in the puddle, but were too few to be recovered. Several attempts were made to recrystallize this material, using both the Na and K salts of the complex. The sodium salt was eventually recrystallized from water/acetone by using a minimum amount of water and carefully layering the acetone onto the top of the water solution.

There was no evidence for a second monosulfenate band. An alternative method to the column chromatography was attempted after the discovery of the R isomer during a CD scale (10^{-4} M) synthesis. The same sequence of preparation was carried out, but instead of placing the solution onto the column, isopropyl alcohol was added slowly to the stirring solution until precipitation was induced. The

solid was collected and redissolved in a minimum of water. This process was repeated several times, but failed to produce a pure compound.

UV-Visible $\lambda_{max}(\varepsilon)$ 281(11300), 368(7220); IR(KBr) (ν_{SO}) 960cm^{-1}, (ν_{CO}) 1625cm^{-1}. Anal. Calcd for Na[Co(PenS)(PenSO)]·4H_2O: C, 25.87; H, 5.64; N, 6.03. Found: C, 26.17; H, 5.18; N, 6.04.

Preparation of Sodium Bis(S-Penicillaminesulfenato-N,S,O)-cobaltate(III). The R,S and S,S disulfenate isomers were prepared by the same method used for the S sulfenate, except that two moles of oxidant were used for every mole of thiolate. K[Co(S-PenS)$_2$·2H_2O (150 mg, 0.35 mmol) was dissolved in 10 mL water in a foil wrapped beaker. Hydrogen peroxide (6.0 mL, 0.1000 M) was added via syringe over 5 min. After 1/2 hr another 0.5 mL peroxide was added. After stirring the solution was loaded onto the AG1-X4 anion column. Two red bands ("A" & "D") were now the major constituents, distinctly separated on the anion column, with only a minor amount of "B" and no appreciable amount of starting material. Both bands showed the same UV-Vis spectrum. The criterion for rejection of these disulfenates was that any fraction with $A_{383}/A_{293} < 1.6$ was discarded. CD was used to confirm the two different isomers based on their different spectra.

The two red bands were evaporated to dryness, then desalted using the Bio-gel column. After three desaltings the pure disulfenato complexes were obtained. The S,S isomer was not completely desalted by the Bio-gel column, but the total amount of residual salt was very

low. Another desalting could not be accomplished due to the small amount of material recovered. Yield R,S 32.6 mg (21.0%); S,S 14.3 mg (9.2%)

Na_2EDTA was added in several trials, to sequester any Co(II) which may have been formed. This did not affect the product distributions. When a solution of the S-monosulfenate was oxidized with one mole of H_2O_2, the product distribution ratio was inverted; the S,S disulfenate was produced in greater amount than the R,S isomer. In some of the synthetic trials, an orange species (356,281) was found to elute over the entire region between the two major bands. A non-mobile polymeric type species was also found to adhere to the column top in some trials, similar to the monosulfenate preparations. It was removed prior to the elution.

UV-Visible $\lambda_{max}(\varepsilon)$ R,S 293(5950), 383(11500), 495(530) : S,S 293(6150), 383(12000), 495(490); IR(KBr) (ν_{so}) 950 cm^{-1} , (ν_{co}) 1630 cm^{-1}. Anal. Calcd for $Na[Co(PenSO)_2] \cdot 2H_2O$: Co, 13.08; S, 14.43; C, 27.03; H, 4.99; N, 6.30. Found: RS Co, 13.20; S, 14.63; C, 26.99; H, 4.99; N, 6.20. Found: SS Co, 13.00; C, 25.07; H, 5.30; Cl, < 2%.

Results and Discussion

Structural Information for Potassium Bis(D-penicillaminato)-cobaltate(III). There are three possibilities for the structure of this complex (Figure 19). Crystals of the brown complex were isolated by Dr. J.H. Krueger and a structural determination of the compound was undertaken by Dr. C.B. Shoemaker. The results strongly indicate that the brown isomer is the trans-N form, although some uncertainty remains due to a very high R factor (0.147), the result of a supercell. This structure is assumed for the rest of the discussion. During the progress of this work, Okamoto reported the synthesis and characterization of two isomers of potassium bis(D-penicillaminato)-cobaltate(III).[78] The brown and green isomers were assigned as the trans-N and trans-O forms, respectively, on the basis of their CD spectra. The trans-S form remains unknown.

The trans-N configuration places the two nucleophilic thiolate centers into close proximity. (Figure 20) Two lone pairs are directed somewhat toward each other above the metal center, creating a nucleophilic pocket which should be the primary site for an oxidation reaction. The spatial arrangement fixes the outward lone pair of each thiolate between a methyl group and the amine group of the opposite ligand. The methyl groups may partially block the approach of an electrophile, whereas the lone pairs in the pocket have no steric hindrance toward approach of the oxidant. This implies that an inner lone pair should be the initial site of oxidation of the thiolate, which is contradictory to the fact that only the S sulfenate is

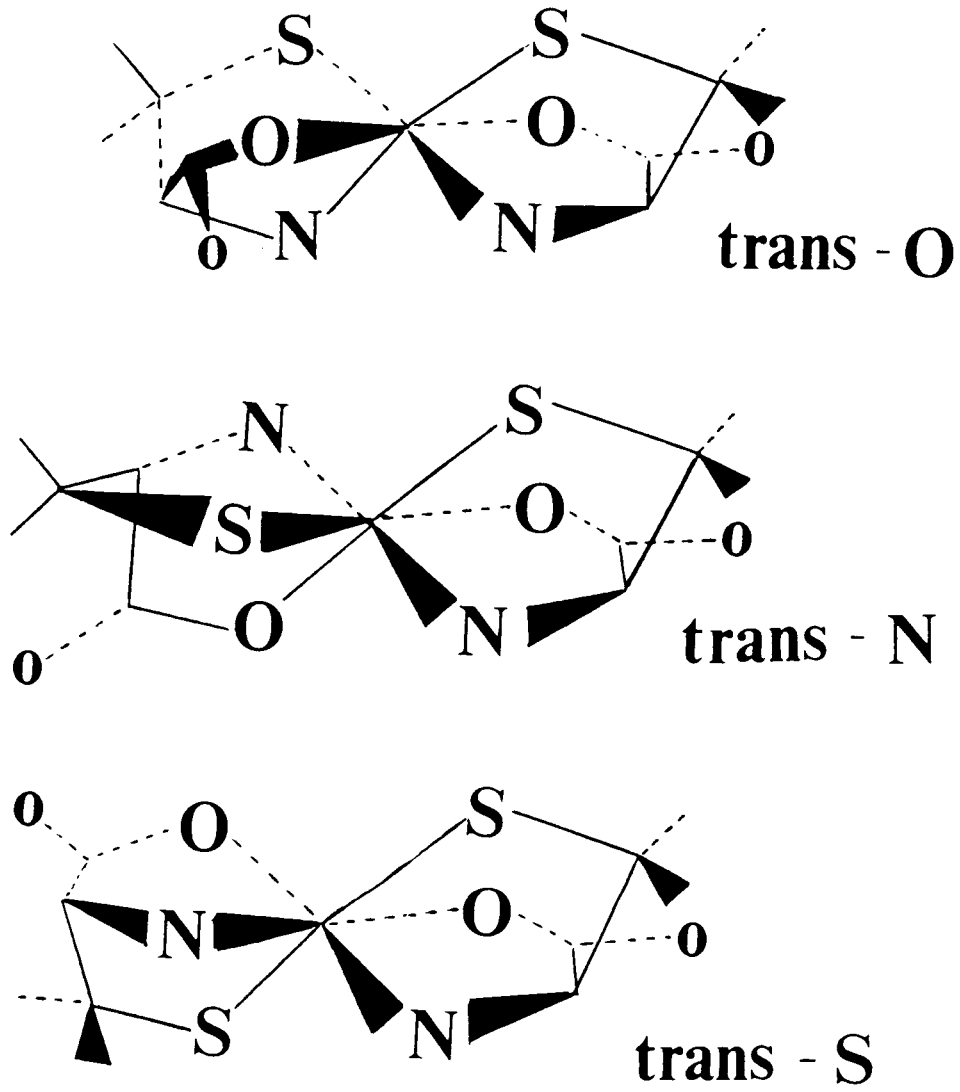

Figure 19. Three Possible Structures for Bis(N,S,O-Penicillaminato)-cobaltate(III) ion. Trans-O, Trans-N, and Trans-S.

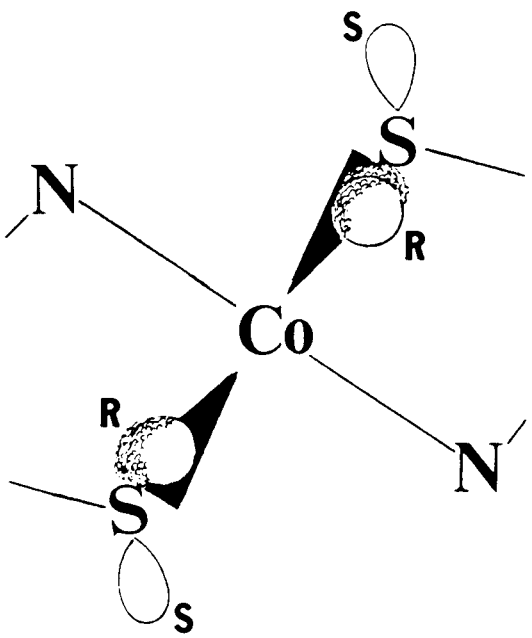

Figure 20. Spatial Orientation of the Lone Pairs at the Electron Rich Thiolate Pocket of the Trans-N Bis(N,S,O-Penicillaminato)-cobaltate(III) Ion.

isolated by anion chromatography.

Column Chromatography of Sulfenato Complexes. The column separation of sulfenates within this system is more complex than expected. There are at least seven distinct species resolved from the synthesis. Assignments of these species are from UV-Vis, NMR and CD spectroscopies.

For the monosulfenate syntheses, the lead band "A" (minor, orange; 385,293) corresponds to a small amount of the R,S disulfenate produced by the oxidation of both penicillamine thiolates. The second band "B" (major, brown; 368,280) contained the desired monosulfenate compound, and was collected in eight fractions over 40 minutes. The third band "C" (major, purple-brown; 284) was unreacted bis(thiolato) starting material. The trail band "D" (minor, orange; 382,293) was shown to be the S,S disulfenate isomer. The relative proportions of these bands varied with the conditions employed (light, temperature, stoichiometry, etc.).

There were also three minor constituents. The lead band is preceded by the elution of a small amount of yellow material (383,300) with a very weak absorbance spectrum. Another impurity was lighter, almost peach in color, and appeared to elute continuously following behind the R,S throughout the rest of the separation. This peach complex never appeared as a distinct band on the column. It could be a slow moving product of a rearrangement process of the R,S disulfenate isomer. All attempts to isolate this species have proved fruitless, since only a small amount of material was ever generated. The seventh and final species, purple in color, remained adhered to

the resin top and is likely polymeric in nature.

The Bio-gel column was able to remove the peach species from the main bands during the desalting process. The impurity was retained for a slightly longer time than the main band. When used first, prior to the cation column, the Bio-gel eluted two broad bands, one red, the other brown, but did not resolve them completely. Both bands underwent severe spreading. When the columns were run in a cold room (3°C), the resolution of the bands was more efficient, but the elution rate was much lower. The peach interferent was still present.

Product separations in the disulfenate syntheses had the same order of elution as for the monosulfenate systems. The differences between the systems result from the amount of materials produced. Bands "A" and "D" were red rather than orange, and contained a much greater amount of the total material. Band "B" was a faint yellow band, while band "C" was negligible. The impurities were still present, but to a similar extent as in the monosulfenate separations.

NMR. The ^{1}H NMR assignments for the sequence of oxidation products exhibit the expected chemical shift changes due to a redistribution of electron density.

In free penicillamine there is an asymmetric carbon center (D≡S) which makes the two methyl groups inequivalent. One of the groups is located closer to the lone pair electrons on the oxygen atom of the carboxylate function, causing a minor shielding effect. Upon tridentate binding to a metal center, a rigid geometry is enforced upon the ligand. The difference in shifts is now greater. The

Table 10: ^{1}H NMR Chemical Shifts for Bis(N,S,O-Penicillaminato)-cobaltate(III) Ion and its Oxidation Products.

PenSH	$(en)_2CoPenS^+$	$Co(PenS)_2^-$	$Co(PenS)(PenSO)^-$		$Co(PenSO)_2^-$
			S	S,S	R,S
Methine					
4.11	3.59	3.85	4.06	4.40	4.28
			3.98		4.25
Methyl					
2.00	1.96	1.75	1.90	1.91	1.94
1.92	1.62	1.62	1.85	1.74	1.76
			1.80		1.63
			1.50		1.55

bis(thiolato) complex has C_2 symmetry, so the spectrum is very similar to that of the free ligand. The flow of electron density from the heteroatoms of the ligand to the cobalt causes the entire spectrum to be shifted away from the external reference peak (TMS).

Oxidation of the bis(thiolate) to a monosulfenate breaks the C_2 symmetry. Since the two tridentate ligands are inequivalent, all four methyl groups have distinct chemical shifts. The methyl group that is closest to the sulfenate oxygen has a greater amount of shielding than the other three methyl groups and will appear closer to the reference peak. Therefore, the R and S sulfenates are expected to have different NMR spectra. The thiolate ligand methyl groups should have equivalent shifts upon oxidation, since both have similar inductive effects through the ligand chain. These methyl groups are far away from the oxidation site, so "through space" interactions should be negligible.

For the S sulfenate, the methyl opposite to the sulfenate oxygen is only slightly shifted from its bis(thiolate) position. This methyl sits outside the five-member chelate ring, causing a deshielding effect counter to the inductive effect. The net result is a slight upfield shift, which is lower in magnitude than either thiolate shifts.

The disulfenates also have different NMR spectra since the S,S disulfenate has C_2 symmetry. Both oxygen atoms point outward, shielding one methyl group more than the other. For the R,S isomer, in which the R oxygen lies above the sulfur pocket, the chemical shifts for the methyls fall into two groupings. The R oxygen interacts with the inward facing methyl apparently causing it to behave similar to the S-monosulfenate, as far as shielding is concerned.

Circular Dichroism. When a two-electron oxidation transforms a thiolate to a monosulfenate, the conformation and configuration of the complex remain essentially unchanged. The major changes in the CD spectrum are caused by the vicinal effect of adding an oxygen atom, which creates a chiral sulfur center, and the consequent relocation of electron density. The former gives rise to a completely new transition, while the latter modifies the energies of the remaining affected transitions and also the magnitude of their Cotton effects.

Miller has assigned the CD spectrum of trans-N-Bis (S-penicillaminato)cobaltate ion.[1] The negative band at 505 nm is assigned to an $^1A_1 \rightarrow {}^1E_A$ ligand field band. The positive band located at 430 nm corresponds to an $^1A_2 \rightarrow {}^1T_1$ d-d transition.

The lower wavelength bands found about 280 nm and 260 nm are due to S-->Co (LMCT) absorptions.

Before discussion of the assignments of the individual optical isomers, the general changes observed in the CD spectrum upon oxidation to the mono- and di- sulfenates are described. The lowest energy band (@ 520 nm) arises from the overall conformation of the chelate rings. As shown in Table 11, its sign remains unchanged by the oxidations, but its energy and magnitude shift. The dissymmetric environment causes an increase in the wavelength, due to a change in the dipole moment of the cobalt-sulfur bond.

The d-d transition (@ 430 nm) can be used to estimate the extent to which the oxidation has proceeded. This band shifts to higher energy upon oxidation: 430 nm for the bis(thiolate), 418 nm

Table 11: CD Spectral Features of Bis(Penicillaminato)cobaltate(III) Ion and its Oxidation Products. (λ nm, $\Delta\varepsilon$ $\underline{M}^{-1}$ cm^{-1})

$K[Co(PenS)_2]$	$K[Co(PenS)(PenSO)]$		$K[Co(PenSO)_2]$	
	$\underline{R}$[a]	$\underline{S}$	$\underline{R},\underline{S}$	$\underline{S},\underline{S}$
505 -11.53	523 -11.2	529 - 7.5	505 - 7.8	521 - 4.6
435 + 5.44	414 +16.8	417 +11.6	395 +31.1	389 +27.9
		375 + 8.3		
348 - 9.77	348 - 6.7		345 -10.6	
			307 -17.2	306 -16.2
293 +49.5	290 + 9.1	287 - 9.1	280 + 3.0	272 - 9.0
261 -26.6	264 - 5.5		260 + 4.8	
	252 - 2.1	253 + 1.5		245 + 1.0

[a]Based upon initial spectra of a reacting mixture (10^{-4} $\underline{M}$) of $[Co(PenS)_2]^-$ and H_2O_2.

for the monosulfenate, and 390 nm for the disulfenate. The stereochemistry of the sulfur does not affect the sign of the Cotton Effect for this band. The transition is metal-based in origin, but is strongly modified by the nature of the ligands. The increase in oxidation state of the sulfur atom causes a contraction of the d orbitals of the metal, which manifests itself by the shift to shorter wavelengths.

The sulfur-to-cobalt charge transfer (LMCT) bands (≃ 290, 260 nm) exhibit a large decrease in magnitude, along with a slight increase in energy. They are sensitive to the stereochemistry at the sulfur, which determines the direction of the Cotton Effect. Part of the decrease in magnitude may arise from the lone pair perturbation effect, which is known to cause a new transition in the absorption spectrum.[64] The orbitals of the oxygen mix with the orbitals of the sulfur of similar symmetry to form new hybridized orbitals. This prevents the sulfur orbitals from achieving full overlap with metal orbitals of the same symmetry, resulting in a decrease of the LMCT bands. Electron density is transferred away from the metal into the new sulfur-oxygen bond.

As mentioned previously, only the S-monosulfenate was found after separation of the oxidation products by anion exchange chromatography. Evidence for the R-monosulfenate isomer was obtained by following the oxidation of the bis(thiolate) with the CD at a very low concentration (10^{-4} M). By running repetitive CD spectra of the 260-420 nm region at five-minute intervals, it was shown that the initial oxidation results in formation of the R sulfenate. (Figure

21) The new peak at 348 nm is negative in sign, while the 292 nm LMCT peak remains positive. This observation is in agreement with Herting's assignment of the negative 370 nm band for $[(en)_2CoCySO]^+$ ion as being the R isomer.[1] Kita, et al., also demonstrated that the negative 370 nm band for tris(cysteamine-sulfenato)cobalt(III) corresponds to the R configuration by solving the crystal structure of the tris-(R) complex.[79,82]

The measurement of the oxidation at CD concentrations is expected to produce a mixture of the R and S isomers, rather than a single pure species. However, the reaction at precisely 1:1 stoichiometry clearly shows two isosbestic points, at 330 nm and 275 nm, indicating that only one species is initially produced. There is no positive intensity at 380 nm, which would be indicative of the S isomer. The negative peak at 350 nm suggests that only the R isomer is produced.

Complete stoichiometric oxidation of the (bis)thiolate to the disulfenate introduces another transition into the CD spectrum. Both the R,S and S,S isomers have a negative Cotton Effect at 307 nm. The sign and magnitude of the Cotton Effect for the 285 nm transition is also significantly affected by this oxidation. The R,R disulfenate is not found because it would require the sulfenate oxygen to be located at a distance shorter than the sum of the van der Waals radii of two oxygens.

When the reaction conditions were varied to determine the effects of light, different product distributions were found. The extent of disulfenate formation and the stereochemistry of the

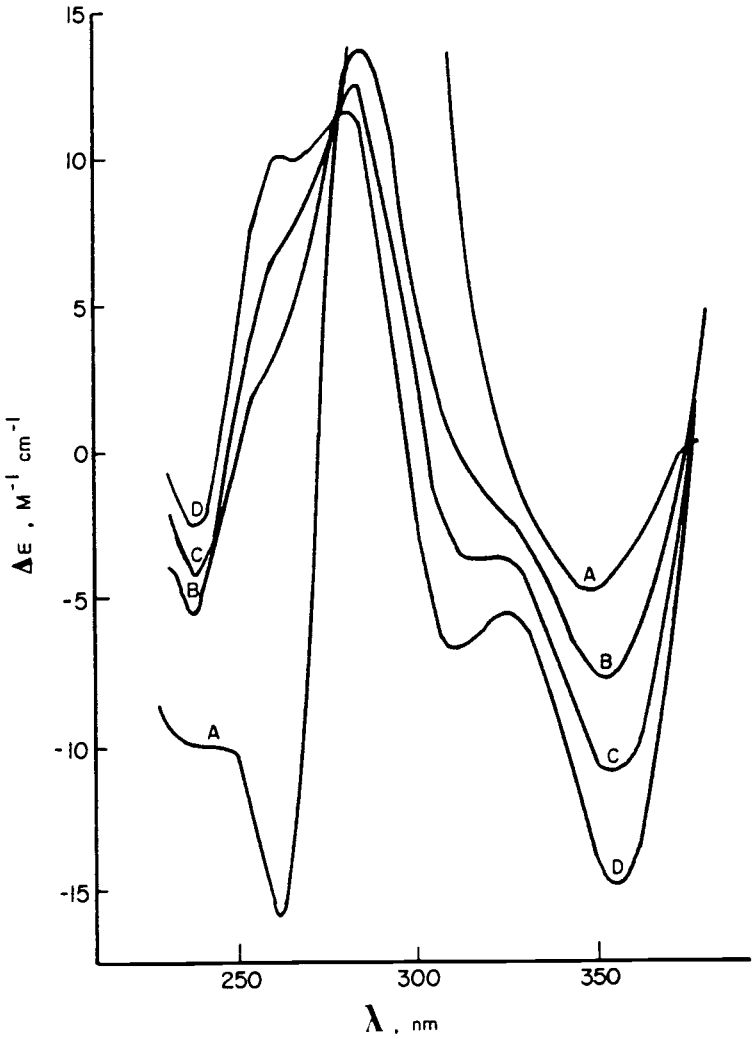

Figure 21. CD Spectra of a Reacting Mixture of $[Co(PenS)_2]^-$ and H_2O_2 (1:1.1 mole ratio). Time Sequence: (A) 0 min, (B) 25 min, (C) 45 min, (D) 70 min.

sulfenate oxygens is influenced by exposure to light.

With a 1:1 mole ratio of $[Co(PenS)_2]^-$ to H_2O_2, the formation of R sulfenate is essentially complete after two hours, based on the development of the negative 350 nm peak. The magnitude of the positive 288 nm peak is less in the light than in the dark, but the direction of the Cotton Effect and peak location are similar in both reactions. After 24 hours, the light reaction has proceeded to the S,S disulfenate, even though the reaction was stoichiometric in peroxide for the monosulfenate. The negative minimum at 350 nm of the R isomer is absent from the spectrum. The d-d band is located at 390 nm, while the characteristic high energy bands are negative at 302 nm and positive at 255 nm.

The dark reaction, on the other hand, gives a product which has the d-d transition at 410 nm, implying only a small amount of further oxidation. There are four higher energy bands (-348 nm, -308 nm, +283 nm, and +255 nm) suggesting that both R and S configurations are present. After 24 hours, the spectrum of the dark reaction product showed little evidence for R to S isomerization, based on the lack of both positive intensity at 375 nm, and negative intensity at 287 nm. The slight increase of intensity for the negative 308 nm peak suggests some further oxidation rather than isomerization.

With a 1:2 stoichiometry, similar light/dark conditions cause different product distributions. The light reaction favors the S,S disulfenate; the spectrum shows a negative shoulder at 340 nm and a nearly zero 280 nm band. A small amount of R,S isomer is formed under these conditions, since there is more positive character at 272 nm

than expected for a pure S,S isomer. Under dark conditions, the R,S isomer is produced in greater yield. The strong negative 350 nm peak demonstrates the presence of the R configuration, while the negative 307 nm peak indicates that further oxidation takes place in the S configuration. The extent of oxidation is less in the dark, based on the d-d band peak location at 402 nm.

Under reaction conditions using a 10% excess of peroxide over complex without light protection, the R peak at 350 nm grows in first, followed by the growth of an S peak at 310 nm. There are subtle changes in the 530, 410 and 280 peaks, implying that a subsequent oxidation is taking place at the opposite thiolate. Since the amount of H_2O_2 was well under that necessary for disulfenate production, an oxidant other than H_2O_2 must be causing the subsequent oxidation in the light reaction. The possibilities are the R sulfenate and molecular oxygen. If the sulfenate causes the oxidation, then an increase of the 280 nm peak for the thiolate moiety ($\Delta\varepsilon$ = 43 M^{-1} cm^{-1}) would be expected as the sulfenate disproportionates to disulfenate and thiolate. There is no evidence of any increase in this region, which strongly implies that O_2 is the oxidation source. Oxidation with molecular oxygen for these types of models is unprecedented in the literature, but has been suggested as the mechanism for the thiolate dioxygenase enzymes.[6]

Conclusion

This cobalt work has been an extension of thesis work done by Krys Miller.[1] The details of the stereochemistry upon oxidation of the thiolate ligand have been brought forward. It appears that steric requirements govern the initial reaction while thermodynamic effects are the dominant factor in the ultimate preference for one stereoisomer over the other.

The thiolate dioxygenase enzymes incorporate O_2 into the substrate thiolate to produce sulfinate products. It seems very likely that this mechanism involves a sulfenate intermediate. Another alternative is a three-center bond from sulfur to dioxygen, where both atoms of oxygen are bound simultaneously to the thiolate. This concerted reaction seems less likely since there is little evidence in the literature for RSOO species.

That the sulfenate species produced are photoactive is not unusual. Herting has previously described a similar isomerization for the $(en)_2Co(S(O)CH_2CH(COO)NH_2)^+$ ion, and Adamson has done much work on homolytic bond fission under UV light.[69,73,74] The demonstration that the R isomer is produced initially is significant. The isolation of 100% S isomer from the column implies that some form of chemical rearrangement takes place during the elution. The R --> S interconversion by the resin is unusual. This may be a light-induced change to a thermodynamically more stable molecular form, although the columns were protected from light during elution. More study should be able to reveal the reason for this isomerization.

The difficulty in collecting a significant amount of material has

made the complete characterization of the mono- and disulfenates difficult. Both oxidation products have formed small amounts of needle crystals on a microscope slide, but these crystals were not large enough for an attempt at x-ray structural determination. Improvement of the yield and better handling technique (i.e., an easier method of removing the KCl or NaCl) should allow collection of better quality of crystals necessary to perform this task.

This work as a whole represents an advance in the proper direction toward understanding the mechanism of these enzymatic reactions. Both the iron and cobalt complexes demonstrate the key role played by the transition metal ion in modifying the reactivity of the organic ligand. By binding the substrate to a metal center, the collection of Fe-SR in the cluster could perhaps mediate the electron transfer necessary for complete reduction of the O_2. This could be through the attainment of a transition state which would not be available in the absence of the metal ion.

Even though there are many inherent difficulties associated with this work, the study of the role of transition metal ions in biological systems is of fundamental importance. The electronic and magnetic properties of the ions can be determined by several instrumental techniques which are not currently available in typical biochemistry laboratories. As the power of these techniques is increased by the interface of spectrometers with computers, the study of metalloenzymes and metalloproteins will advance to center stage. Scientists soon will be able to understand biochemical mechanisms on a molecular level.

Bibliography

(1)(a) Sloan, C.P., M.S. Thesis (1975), (b) Herting, D.L., Ph.D. Thesis (1980), (c) Miller, K.J., Ph.D. Thesis (1981), Oregon State University, Corvallis OR.

(2) Holm, R.H. Acc. Chem. Res. 1977, 10, 427.

(3) Hughes, M.N. The Inorganic Chemistry of Biological Processes, 2nd ed. John Wiley & Sons, New York 1981, Ch. 10, p. 310.

(4) Lippard, S.J. Acc. Chem. Res. 1977, 6, 282.

(5) Hayaishi, O. ; Nozaki, M. ; Abbott, M.T. in "The Enzymes" (Boyer, P.D. ,ed.), 3rd ed., Vol XII, part B, 148. Academic Press, New York, 1975.

(6) Cavallini, D. ; Fiori, A. ; Costa, M. ; Federici, G. ; Marcucci, M. Physiol. Chem. & Phys. 1971, 3, 175.

(7) Cavallini, D. ; De Marco, C. ; Scandurra, R. ; Dupre, S. ; Graziani, M.T. J. Biol. Chem. 1966, 241, 3189.

(8) Drago, R.S. Physical Methods in Chemistry. W.B. Saunders Company, Philadelphia, 1977.

(9) Rotilio, G. ; Federici, G. ; Calabrese, L. ; Costa, M. ; Cavallini, D. J. Biol. Chem. 1970, 245, 6235.

(10) Federici, G. ; Barboni, E. ; Costa, M. ; Fiori, A. ; Arduini, E. ; Cavallini, D. Physiol. Chem. & Phys. 1972, 4, 553.

(11) Cavallini, D. ; Cannella, C. ; Barboni, E. ; Fiori, A. ; Marcucci, M. Eur. J. Biochem. 1969, 11, 360.

(12) Lombardini, J.B. ; Singer, T.P. ; Boyer, P.D. J. Biol. Chem. 1969, 244, 1172.

(13) Hayaishi, O. ; Nozaki, M. Science 1969, 164, 389.

(14) Malmstrom, B.G. Ann. Rev. Biochem. 1982, 51, 21.

(15) Mukerji, S.K. ; Pimstone, N.R. ; Burns M. Gastroenterology 1984, 87, 1248.

(16) Holm, R.H. Endeavour 1975, 34, 38.

(17) Murray, K.S. ; Newman, P.J. Aust. J. Chem. 1975, 773.

(18) Panossian, R. ; Terzian, G. ; Guiliano, M. Spect. Letters 1979, 12, 715.

(19) Bell, C.M. ; MacKenzie, E.D. ; Orton, J. Inorg. Chim. Acta 1971, 5, 109.

(20)(a) Herskovitz, T. ; DePamphilis, B.V. ; Gillum, W.O. ; Holm, R.H. Inorg. Chem. 1975, 14, 1426. (b) Mukherjee, R.N. ; Rao, C.P. ; Holm R.H. Inorg. Chem. 1986, 25, 2979.

(21) Snow, M.R. ; Ibers, J.A. Inorg. Chem. 1973, 12, 249.

(22) Hu, W.J. ; Barton, D. ; Lippard, S.J. J. Am. Chem. Soc. 1973, 95, 1170.

(23) Hu, W.J. ; Lippard, S.J J. Am. Chem. Soc. 1974, 96, 2366.

(24) Karlin, K.D. ; Lippard, S.J. J. Am. Chem. Soc. 1976, 98, 6951.

(25) Hagen, K.S. ; Holm, R.H. Inorg. Chem. 1984, 23, 418.

(26) Lane, R.W. ; Ibers, J.A. ; Frankel, R.B. ; Papaefthymiou, G.C. ; Holm, R.H. J. Am. Chem. Soc. 1977, 99, 84

(27) Coucouvanis, D. ; Swenson, D. ; Baenziger, N.C. ; Murphy, C. ; Holah, D.G. ; Sfarnas, N. ; Simopoulis, A. ; Kostikas, A. J. Am. Chem. Soc. 1981, 103, 3350.

(28) Koch, S.A. ; Maelia, L.E. ; Millar M. J. Am. Chem. Soc. 1983, 105, 5944.

(29) Millar, M. ; Lee, J.F. ; Koch, S.A. ; Fikar, R. Inorg. Chem. 1982, 21, 4105.

(30) Collman, J.P. ; Sorrell, T.N. ; Hodgson, K.O. ; Kulshrestha, A.K. ; Strouse, C.E. J. Am. Chem. Soc. 1977, 99, 5180.

(31) Collman, J.P. ; Sorrell, T.N. ; Hoffman, B.M. J. Am. Chem. Soc. 1975, 97, 913.

(32) Koch, S. ; Tang, S.C. ; Holm, R.H. ; Frankel, R.B. J. Am. Chem. Soc. 1975, 97, 914.

(33) Koch, S. ; Tang, S.C. ; Holm, R.H. ; Frankel, R.B. ; Ibers, J.A. J. Am. Chem. Soc. 1975, 97, 916.

(34) Walters, M.A. ; Dewan, J.C. Inorg. Chem. 1986, 25, 4889.

(35)(a) Jicha, D.C. ; Busch, D.H. Inorg. Chem. 1962, 1, 872. (b) Jicha, D.C. ; Busch, D.H. Inorg. Chem. 1962, 1, 878. (c) Busch, D.H. ; Jicha, D.C. Inorg. Chem. 1962, 1, 884.

(36) Butler, P.R. ; Blinn, E.L. Inorg. Chem. 1978, 17, 2037.

(37) Blinn, E.L. ; Butler, P.R. ; Chapman, K.M. ; Harris, S. Inorg. Chim. Acta 1977, 24, 139.

(38) Schlapfer, C.W. ; Nakamoto, K. Inorg. Chim. Acta 1972, 6, 177.

(39) DiSimone, R.E. ; Ontko, T. ; Wardman, L. ; Blinn, E.L. Inorg. Chem. 1975, 14, 1313.

(40) Heeg, M.J. ; Blinn, E.L. ; Deutsch, E. Inorg. Chem. 1985, 24, 1118.

(41) Willis, L.J. ; Loehr, T.M. ; Miller, K.F. ; Bruce, A.E. ; Stiefel, E.I. Inorg. Chem. 1986, 25, 4289.

(42) Kolthoff, I.M. ; Sandell, E.B. ; Meehan, E.J. ; Bruckenstein, S. Quantitative Chemical Analysis 4th ed. Collier-Macmillan Ltd.: London 1969 Ch. 40, p. 798.

(43) Marczenko, Spectrophotometric Determination of Elements 1976 Ch. 27, 305.

(44) Werth, M.T. ; Kurtz, D.M. ; Moura, I. ; LeGall, J. J. Am. Chem. Soc. 1987, 109, 273.

(45) Lewis, J. and Wilkins, R.G. Modern Coordination Chemistry: Principles and Methods, Interscience Publishers Inc.: New York 1960, p. 403.

(46) CRC Handbook of Chemistry and Physics 59th ed. The Chemical Rubber Co. : Cleveland 1978.

(47) Livingstone, S.E. ; Nolan, J.D. Aust. J. Chem 1970, 23, 1553.

(48) Goodwin, H.A. ; Lyons, F. J. Am. Chem. Soc. 1960, 82, 5013.

(49) Mayerle, J.J.; Denmark, S.E.; DePamphilis, B.V.; Ibers, J.A.; Holm, R.H. J. Am. Chem. Soc. 1975, 97, 1032.

(50) Nakamoto, K. Infrared and Raman Spectra of Inorganic and Coordination Compounds 3rd ed. Wiley-Interscience : New York 1978 , p. 339

(51) Murad, E. ; Schwertmann, U. American Minerologist 1980, 65, 1044.

(52) Tao, X. ; Stephan, D.W. ; Mascharak, P.K. Inorg. Chem. 1987, 26, 754.

(53) Eley, R.R. ; Duffy, N.V. ; Uhrich, D.L. J. Inorg. Nucl. Chem. 1972, 34, 3681.

(54) Carlin, R.L. Magnetochemistry Springer-Verlag: New York 1986.

(55) Krueger, J.H.; Sloan, C.P. Inorg. Chem. 1975, 14, 1481.

(56)(a) Jackson, W.G. ; Sargeson, A.M. ; Whimp, P.O. J. Chem. Soc. Chem. Com. 1976, 934. (b) Freeman, H.C. ; Moore, C.J. ; Jackson, W.G. ; Sargeson, A.M. Inorg. Chem. 1978, 17, 3513.

(57) Adzamli, I.K. ; Lisbon, K. ; Lydon, J.D. ; Elder, R.C. ; Deutsch, E. Inorg. Chem. 1979, 18, 303.

(58) Herting, D.L. ; Miller, K.J. ; Schussel, L.J. ; Shoemaker, C.B. ; Krueger, J.H. unpublished results.

(59) Lydon, J.D. ; Deutsch, E. Inorg. Chem. 1982, 21, 3180.

(60)(a) Lange, B.A. ; Lisbon, K. ; Deutsch, E. ; Elder, R.C. Inorg. Chem. 1976, 15, 2985. (b) Elder, R.C. ; Florian, L.R. ; Lake, R.E. ; Yacynych, A.M. Inorg. Chem. 1973, 12, 2690.

(61) Gainsford, G.J. ; Jackson, W.G. ; Sargeson, A.M. J. Chem. Soc. Chem. Com. 1979, 802.

(62) Root, M.J. ; Deutsch, E. Inorg. Chem. 1981, 20, 4376.

(63) Elder, R.C. ; Kennard, G.J. ; Payne, M.D. ; Deutsch, E. Inorg. Chem. 1978, 17, 1296.

(64) Lane, R.H. ; Sedor, F.A. ; Gilroy, M.J. ; Eisenhardt, P.F. ; Bennett, J.P.,Jr. ; Ewall, R.X. ; Bennett, L.E. Inorg. Chem. 1977, 16, 93.

(65) Lydon, J.D. ; Elder, R.C. ; Deutsch, E. Inorg. Chem. 1982, 21, 3186.

(66) Reynolds, M.S. ; Oliver, J.D. ; Cassel, J.M. ; Nosco, D.L. ; Noon, M. ; Deutsch, E. Inorg. Chem. 1983, 22, 3632.

(67) Sanguanruang, O. ; Krueger, J.H. unpublished results.

(68) Adzamli, I.K.; Deutsch, E. Inorg. Chem. 1980, 19, 1366.

(69) Herting, D.L. ; Sloan, C.P. ; Cabral, A.W. ; Krueger, J.H. Inorg. Chem. 1978, 17, 1649.

(70) Elder, R.C. ; Heeg, M.J. ; Payne, D.M. ; Trkula, M. ; Deutsch, E. Inorg. Chem. 1978, 17, 431.

(71) Gainsford, G.J. ; Jackson, W.G. ; Sargeson, A.M. J. Am. Chem. Soc. 1982, 104, 137.

(72) Kojima, M. ; Fujita, J. Bull. Chem. Soc. Jpn. 1983, 56, 139.

(73) Houlding, V.H. ; Macke, H. ; Adamson, A.W. Inorg. Chem. 1981, 20, 4279.

(74) Macke, H. ; Houlding, V.H. ; Adamson, A.W. J. Am. Chem. Soc. 1980, 102, 6889.

(75) Neville, R.G. ; Gorin, G. J. Am. Chem. Soc. 1956, 78, 4893.

(76) Suades, J. ; Solans, X. ; Font-Altaba, M. ; Aguilo, M. Inorg. Chim. Acta 1985, 99, 1.

(77) Helis, H.M. ; de Meester, P. ; Hodgson, D.J. J. Am. Chem. Soc. 1977, 99, 3309.

(78) Okamoto, K-i. ; Wakayama, K. ; Einaga, H. ; Yamada, S. ; Hidaka, J. Bull. Chem. Soc. Jpn. 1983, 56, 165.

(79) Kita, M. ; Yamanari, K. ; Shimura, Y. Bull. Chem. Soc. Jpn. 1982, 55, 2873.

(80) Cantor, C.R. and Schimmel, P.R. Biophysical Chemistry Part II: Techniques for the Study of Biological Structure and Function. W.H. Freeman and Co.: San Francisco 1980.

(81)(a) McCaffery, A.J. ; Mason, S.F. ; Norman, B.J. J. Am. Chem. Soc., 1964, 86, 5094. (b) McCaffery, A.J. ; Mason, S.F. ; Ballard, R.E. Mol. Phys. 1965, 2883. (c) Mason, S.F. Quart. Rev. (London) 1963, 17, 20.

(82) Reference 42. Ch. 44, p. 842.

(83) Kitson, R.E. Anal. Chem. 1950, 22, 664.

(84) Kita, M. ; Yamanari, K. ; Kitahama, K. ; Shimura, Y. Bull. Chem. Soc. Jpn. 1981, 54, 2995.